(NASA-CR-143258) MELTING BEHAVIOR AND PHASE RELATIONS OF LUNAR SAMPLES Semiannual Progress Report, 1 Feb. 1975 - 31 Jul. 1976 (Harvard Univ.) 67 p HC $4.25 CSCL 03B

N75-28992

Unclas
G3/91 31357

Progress Report to

NATIONAL AERONAUTICS AND SPACE ADMINISTRATION

Summarizing progress of research on

MELTING BEHAVIOR AND PHASE RELATIONS OF LUNAR SAMPLES

carried out under

NGL 22-007-247

Principal Investigator: James Fred Hays
Professor of Geology
Hoffman Laboratory
Harvard University
Cambridge MA 02138

~~Semiannual Progress Report, 1 August 1974-31 January 1975~~
~~and~~
Semiannual Progress Report, 1 February 1975-31 July 1976

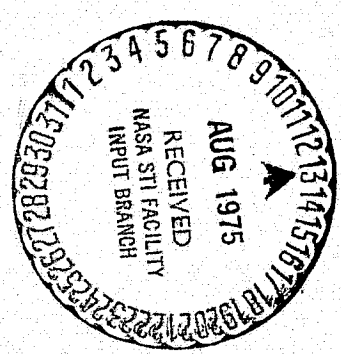

PERSONNEL

James Fred Hays Professor of Geology	Principal Investigator
David Walker Research Fellow	Co-Investigator
John Longhi Graduate Student	Research Assistant
Mark L. Rivers Undergraduate	Research Assistant
Anthony Anastasio	Machinist
Nancy Jackson	Secretary and Bookkeeper
Sarah Adams	Secretary

PROGRESS REPORT

This report summarizes research carried out at Harvard University under NASA grant NGL 22-007-247, during the report periods 1 August 1975-31 January 1975 and 1 February 1975-31 July 1975. Four papers and abstracts have been published since the last such report (1 August 1974) and five other papers have been accepted for publication and are now in press. These publications are listed here and copies of some of them are appended.

Research during the report year has followed a number of different lines. Our cooling-rate studies of 12002 have now been completed and our results have been interpreted in terms of the crystallization history of this rock and certain other picritic Apollo 12 samples. This work was reported at the Sixth Lunar Science Conference and a paper on the experimental portion of the study has been accepted for publication in the Geological Society of America Bulletin. Calculations of liquid densities and viscosities during crystallization, crystal settling velocities, and heat-loss by the parent rock body are in progress, as are petrographic studies of other Apollo 12 samples with the aim of generalizing and extending the results of the experimental study.

We have given some thought to the process of magmatic differentiation that must have accompanied the early melting and chemical fractionation of the moon's outer layers. The effects of the pressure differential in such an immense magma body introduce some

novel features into the crystallization process that seem not to have been previously considered. The chemical and petrological nature of the outer few hundred kilometers of the moon and its potential as a source region for mare basalts cannot properly be understood without taking these features into account. This work was also reported at the Sixth Lunar Science Conference and a paper has been accepted for publication in the Proceedings volumes.

Our interest in the source regions of both high- and low-titanium mare basalts continues. The work on high-Ti basalts reported last year has been widely cited and used as a basis for geochemical calculations by a number of authors, but it has also been criticized and challenged, particularly by the group at Canberra. We have had many discussions on this problem and expect to conduct further experiments on a critical sample, 74275, in an attempt to resolve the points of controversy. We are also preparing a manuscript on the nature and origin of the low-titanium mare basalts.

Finally, we are attempting to analyze a very large body of chemical data on our experimental run products and to summarize this data in forms useful to terrestrial petrologists and geochemists as well as to other lunar scientists. A first report on this work was given at the annual meeting of the American Geophysical Union.

PUBLICATIONS

(1 August 1974 - 31 July 1975)

1. The petrology of the Apollo 17 mare basalts. J. Longhi, D. Walker, T. L. Grove, E. M. Stolper, and J. F. Hays. Proc. Fifth Lunar Sci. Conf., Geochim. Cosmochim. Acta, Suppl. 5, 1, 447-469, Pergamon Press, 1974.

2. Differentiation of a very thick magma body. D. Walker, J. Longhi, and J. F. Hays. Lunar Science VI, 838-840, The Lunar Science Institute, 1975.

3. 12002 Revisited. D. Walker, R. J. Kirkpatrick, J. Longhi, and J. F. Hays. Lunar Science VI, 841-843, The Lunar Science Institute, 1975.

4. Fe-Mg distribution between olivine and lunar basaltic liquids. J. Longhi, D. Walker, and J. F. Hays. Trans. Am. Geophys. Un. (EOS) 56, 471, 1975.

PAPERS IN PRESS

1. Lunar igneous rocks and the nature of the lunar interior. J. F. Hays and D. Walker. Proc. Soviet-American Conf. on Cosmochemistry of the Moon and Planets, Moscow. The Lunar Science Institute (in press).

2. Origin of titaniferous lunar basalts. D. Walker, J. Longhi, T. L. Grove, E. M. Stolper, and J. F. Hays. Geochim. Cosmochim. Acta (in press).

3. Differentiation of a very thick magma body with implications for the source regions of mare basalts. D. Walker, J. Longhi, and J. F. Hays. Proc. Sixth Lunar Sci. Conf., Geochim. Cosmochim. Acta, Suppl. 6, Pergamon Press (in press).

4. Crystallization history of lunar picritic basalt 12002: phase equilibrium and cooling-rate studies. D. Walker, R. J. Kirkpatrick, J. Longhi, and J. F. Hays. Geol. Soc. Amer. Bull. (in press).

5. Direct determination of the quartz-coesite transition by in-situ x-ray measurements: a discussion. J. F. Hays. Contrib. Min. Petr. (in press).

REPRINTS AND PREPRINTS

1. Origin of titaniferous lunar basalts

2. Differentiation of a very thick magma body with implications for the source regions of mare basalts

3. Crystallization history of lunar picritic basalt 12002: phase equilibrium and cooling-rate studies

MS 556

GEOCHIMICA ET COSMOCHIMICA ACTA, 1975, Vol. 39, pp. 000 to 000. Pergamon Press. Printed in Great Britain

Origin of titaniferous lunar basalts

DAVID WALKER, JOHN LONGHI, EDWARD M. STOLPER,
TIMOTHY L. GROVE and JAMES F. HAYS

Center for Earth and Planetary Physics, Hoffman Laboratory, Harvard University, Cambridge, MA 02138, U.S.A.

(*Received* 13 *August* 1974; *accepted in revised form* 31 *December* 1974)

Abstract Delineation of low pressure phase equilibria in the composition space relevant to titaniferous lunar basalts demonstrates a significant degree of control by those equilibria on the compositions of the basalts. The existence of two distinct chemical groups of basalts (high and low-K) which cannot be related one to the other by fractional crystallization at any pressure, suggests that melting is responsible for the two groups. Consideration of the pressure shift required to produce the differences between groups constrains magma segregation to have occurred in the outer 150 km of the Moon. It is difficult to relate low-Ti and high-Ti basalts to the same source region. The preferred source region of high-Ti basalts, based on phase equilibrium considerations, is a late ilmenite-rich cumulate produced from the residual liquid of the primordial differentiation of the outer portions of the Moon. This ilmenite-rich layer is sandwiched between the lunar feldspathic crust and a complementary mafic cumulate.

INTRODUCTION

THE FIRST Apollo mission to the Sea of Tranquillity returned a suite of highly titaniferous basaltic rocks and mechanical degradation products of such rocks. Within six months a number of conflicting hypotheses for the origin and significance of these rocks had appeared in print. After four other Apollo missions had revealed a rich variety of lunar rock types and established a framework of geochemical and geophysical constraints on lunar structure and history, the Apollo 17 mission again returned titanium-rich lunar basalts resembling those of Apollo 11, but more mafic in character and texturally more diverse. In view of the wealth of new information now available and our improved understanding of lunar structure and history, it seems useful to re-examine the questions posed by lunar titaniferous basalts and to attempt to resolve some of the points of controversy that have surrounded these intriguing rocks.

These rocks have been universally recognized as volcanic igneous rocks that flooded low-lying portions of the lunar surface about 3·7 gy ago. Leading hypotheses for the origin of the magmas that produced the rocks are:

(1) direct partial melts of the primitive lunar interior at depths of 200–400 km, and, as such, capable of revealing the mineralogy and chemistry of their source region (RINGWOOD and ESSENE, 1970).

(2) residual liquids of advanced stages of fractional crystallization near the lunar surface, probably in gigantic lava lakes (O'HARA *et al.*, 1970).

(3) partial melts of evolved regions of the lunar interior modified to greater or lesser degrees by near-surface fractional crystallization and/or volatile losses.

Various depths of origin and a variety of constraints on the source materials have been proposed (PHILPOTTS and SCHNETZLER, 1970; SMITH *et al.*, 1970; WOOD *et al.*, 1970; BRETT, 1973; PRINZ *et al.*, 1973; TAYLOR and JAKES, 1974*a*, 1974*b*; WAKITA *et al.*, 1974; WALKER *et al.*, 1973).

We will attempt to show here that hypotheses (1) and (2) are extremely unlikely to be correct and that one or more variants of hypothesis (3) are consistent with known facts.

CHEMISTRY AND PHASE EQUILIBRIA

The titaniferous basalts form a distinctive lunar type easily distinguished from other lunar magmatic types on the basis of TiO_2 in excess of 6 wt % and abundant (10–20 per cent) modal ilmenite (PAPIKE and BENCE, 1973). Several subdivisions are recognizable on the basis of chemistry and correlative mineralogy. JAMES and JACKSON (1970) have summarized relations from Apollo 11 where two major subgroups were noted: an ophitic-textured group which was chemically richer in Al_2O_3 and poorer in TiO_2, K_2O, and REE than an intersertal-textured group. These are the low-K and high-K groups, respectively, in the present discussion. The Apollo 17 mission sampled more Ti basalts, chemically similar to the Apollo 11 low-K group but with some more mafic members which also had TiO_2 contents approaching the high-K group, although their chemistry did not overlap in other respects (LSPET, 1973). These samples exhibited a wide range of textures in contrast to the Apollo 11 low-K ophitic suite. The Apollo 17 Ti

basalts are considered part of the low-K suite of titaniferous lunar basalts for the present discussion.

Experimental studies of phase-equilibrium at low pressures in Apollo 11 compositions have been reported by several laboratories. These studies established some facts that bear on the origin of the rocks concerned:

(1) the observed mineralogy and texture of the rocks is consistent with crystallization at low pressures and very low fugacities of oxygen and H_2O (MUAN and SCHAIRER, 1971; SMITH *et al.*, 1970; TUTHILL and SATO, 1970; WEILL *et al.*, 1970).

(2) Rocks of the low-potassium or ophitic group were close to multiple saturation with olivine, pyroxene, *plagioclase*, and/or armalcolite at the liquidus (BIGGAR *et al.*, 1971; O'HARA *et al.*, 1970, 1974*a*, 1974*b*).

(3) Rocks of the high-potassium or intersertal group had olivine, pyroxene or armalcolite as a liquidus phase, but plagioclase appeared relatively late in the crystallization sequence (RINGWOOD and ESSENE, 1970; RINGWOOD and GREEN, 1972).

(4) Soil compositions matched neither group of basaltic rocks nor any mixture of them. Soil compositions had plagioclase with or without olivine or pyroxene on the liquidus (O'HARA *et al.*, 1970, 1974*a*).

(5) No simple scheme of low-pressure fractional crystallization could produce high-potassium liquids from a low-potassium parent or vice versa. Complex schemes are possible (O'HARA *et al.*, 1974*a*).

In addition to these experimental constraints, a number of geochemical constraints were established:

(6) high-potassium rocks are enriched in elements such as K, Rb, Cs, REE by factors of 2–5 relative to low-potassium rocks (e.g. TERA *et al.*, 1970; GAST *et al.*, 1970).

(7) Rare earth elements show near-chondritic relative abundance patterns except for pronounced negative europium anomalies with absolute abundances levels 40–100 times chondritic (e.g. PHILPOTTS and SCHNETZLER, 1970; HASKIN *et al.*, 1970).

(8) Rb/Sr model ages are 4·6 gy for low-potassium rocks and 3·7 gy for high-potassium rocks (PAPANASTASSIOU and WASSERBURG, 1971).

While it was clear that the mineralogy of these samples was the result of near-surface crystallization, it was not clear to what extent the chemistry of these rocks was a result of near-surface fractional crystallization. The inability of the above observations to constrain the problem sufficiently was partly a result of the narrow range of major element chemistry in the Apollo 11 suite. The return of the Apollo 17 samples has somewhat extended the compositional range of the high-Ti suite.

In order to document possible near surface fractional crystallization, which might affect the compositions of the titaniferous basalts, we have performed melting experiments in iron capsules in evacuated silica tubes on crystalline powders of Apollo 17 basalts 70017 and 70215 (LONGHI *et al.*, 1974). Microprobe analysis of quenched glasses, coexisting with crystals, allows delineation of saturation curves in the

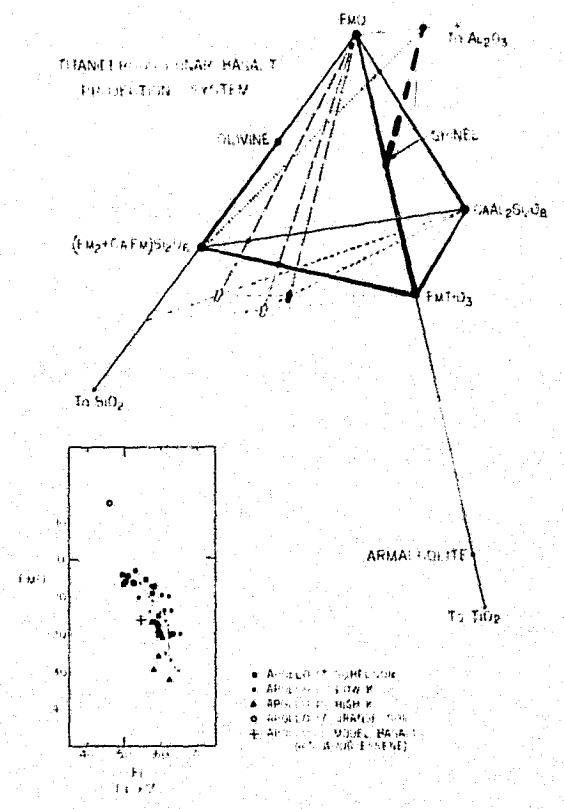

Fig. 1. The tetrahedron FmO 'anorthite' 'ilmenite' 'pyroxene' is used to discuss the titaniferous lunar basalts. Formulae for locating molar oxide analyses in this tetrahedron have been given in LONGHI *et al.* (1974, Fig. 2). Many compositions of interest have negative FmO values. Projection of one such point is illustrated with an arbitrary symbol (an arrow). FmO = (FeO + MgO + CaO + Al_2O_3 SiO_2 TiO_2)/(FeO + MgO + Al_2O_3) in molar units. This differentiation index has been plotted against Fe/Fe + Mg in the lower portion of the figure to allow separate inspection of the variation of this parameter. Experimental liquids from LONGHI *et al.* (1974, Table 2) appear as dots along the dashed curve of this lower inset. The temperature range of these experimental liquids, which are also shown in Figs. 2–4, is 1197–1125 C. Decreasing FmO corresponds to decreasing temperature in all figures.

Compositions of Apollo 11 and 17 materials in this figure and Figs. 2–5 are taken from AGRELL *et al.* (1970), COMPSTON *et al.* (1970), MAXWELL *et al.* (1970), RINGWOOD and ESSENE (1970), WARNER (1971), DUNCAN *et al.* (1974), NAVA (1974), RHODES *et al.* (1974), and LONGHI *et al.* (1974).

portion of composition space relevant to these materials at low pressure. A graphical representation of the results requires projection since there is more compositional variation present than can be completely described by three or four components. A projection scheme which can be used to compare the compositions of the basalts with the curves of multiple saturation has been presented by WALKER *et al.* (1974) and LONGHI *et al.* (1974). It is illustrated in Fig. 1. Details of the experimental methods, the compositions of experimental phases, and an analysis of the strengths and shortcomings of the projection system can be found in LONGHI *et al.* (1974). Molar units are used throughout. FeO and MgO are combined to form FmO, but Fe/Fe + Mg variation is specifically considered in the inset included in Fig. 1. FmO, TiO_2, CaO, Al_2O_3, and SiO_2 are recalculated into 'minerals' FmO, $FmTiO_3$ ('ilmenite'), $CaAl_2Si_2O_8$ ('an'), and $CaFmSi_2O_6$ plus $FmSiO_3$ (combined as 'pyroxene'). These 'minerals' are then used as coordinates described in the captions to the various subprojections. Neglecting K_2O and Na_2O in the projection system has the desirable effect of suppressing compositional variations introduced by alkali volatilization; however, care must be taken to note that all feldspars do not plot at $CaAl_2Si_2O_8$ as a consequence.

Crystallization behavior of 70017 and 70215 as a function of pressure has been presented by LONGHI *et al.* (1974). The results of this work which are relevant to the present discussion are that these compositions are in liquidus equilibrium with olivine, low-Ca clinopyroxene, ilmenite, and spinel in the pressure range 5–7·5 kbar. Less olivine-normative materials such as the Apollo 11 high-K suite are in liquidus equilibrium with this assemblage at pressures less than 5 kbar (O'HARA *et al.*, 1970; WALKER, 1972). These pressures up to 7·5 kbar correspond to depths of up to 150 km in the Moon. Further experimental results confirming the applicability of these diagrams to lunar basalt compositions are presented in the Appendix.

Detailed inspection of the low pressure phase relations for evidence of fractional crystallization control

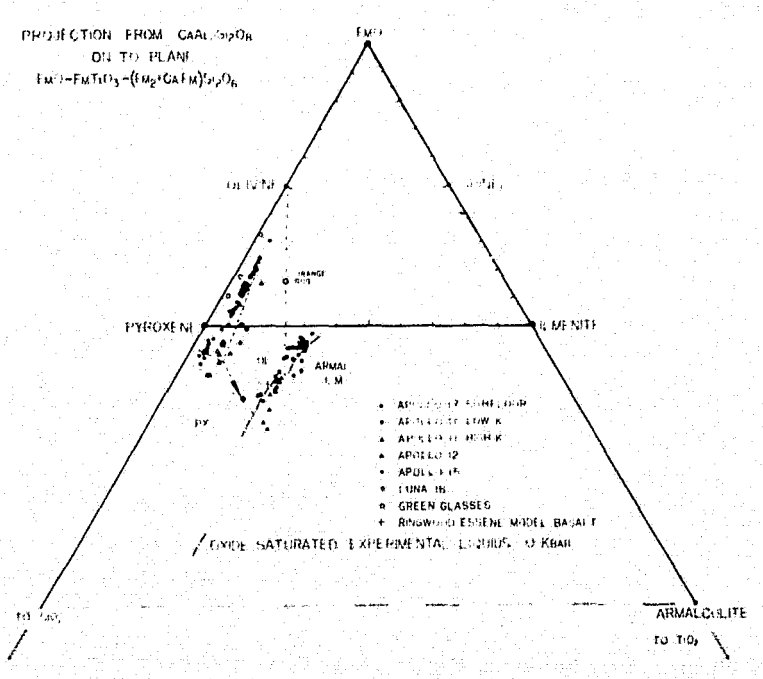

Fig. 2. The image plane of this subprojection is the front face of the tetrahedron of Fig. 1. The points between the heavy dashes are the experimental liquid compositions reported in LONGHI *et al.* (1974, Table 2). The short-dash line between armalcolite and ilmenite indicates the position of this reaction on the trace of the oxide saturation surface and does not represent a line separating those phase volumes in the oxide-oversaturated region of the composition space. The dashed lines separating the olivine and pyroxene volumes are drawn on the basis of experiments on 12002, 15065, and 15555 (GROVE *et al.*, 1973; LONGHI *et al.*, in preparation). Dashed and dotted lines emanating from olivine trace olivine fractionation paths. Low-Ti bulk compositions are taken from CHAPPELL and GREEN (1973), COMPSTON *et al.* (1971), CUTTITTA *et al.* (1971, 1973), KUSHIRO and HARAMURA (1971), RHODES and HUBBARD (1973), STEELE and SMITH (1972), STOLPER (1974), and WILLIS *et al.* (1971).

on the compositional variation of the titaniferous basalts is necessary before a discussion of the high pressure phase relations can assume any genetic significance. Such as inspection follows.

DISCUSSION OF PHASE EQUILIBRIA AND CHEMICAL VARIATION

One possibility to evaluate is that variability is caused by addition or subtraction of a single crystalline species within its liquidus volume. LONGHI *et al.* (1974) considered this problem and concluded that only minor aspects of the compositional variation shown could be described in terms of any single crystalline species. Figures 2 and 3 show olivine fractionation paths through the orange soil composition 74220, and indicate either that equilibrium crystallization of olivine from 74220 or accumulation of $\sim Fo_{<70}$ in olivine-saturated liquids similar to some but not all parts of the Ti basalt suite might have occurred (see Appendix). ROEDDER and WEIBLEN (1973) have presented evidence that the 74220 composition existed

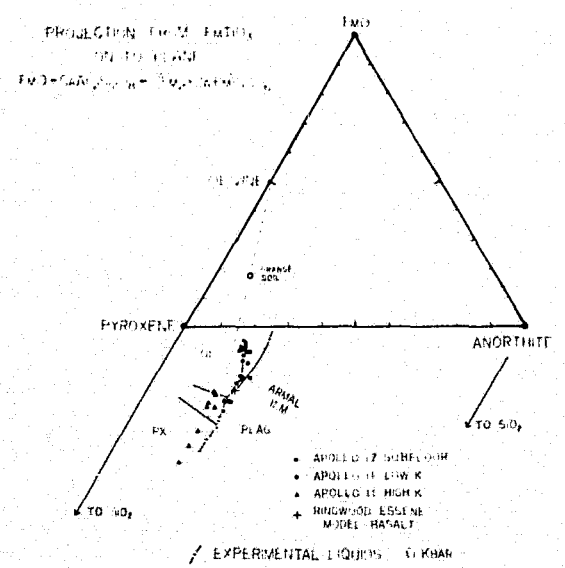

Fig. 3. The image plane of this projection is the rear face of the tetrahedron of Fig. 1. Dots along the saturation boundaries are experimental liquids from LONGHI *et al.* (1974, Table 2). The composition plane can be divided into regions according to the silicate (plagioclase, olivine and/or pyroxene) which coexists with armalcolite and/or ilmenite. The dotted line separating armalcolite from ilmenite saturation regions is largely schematic except in the vicinity of the actual experimental liquids. This projection behaves very much like a pseudoternary liquidus diagram for these materials for the physical conditions of these experiments. It is useful in delineating crystallization sequences and estimating the proximity of saturation boundaries. It should only be applied with caution to other materials.

as a liquid with suspended microphenocrysts of $\sim Fo_{>80}$. This suggests that the former possibility would be the more likely. However, LSPET (1973) on the basis of Rb, Sr, Zn, and Cl abundances have shown that neither process can in fact be responsible, since these elements are noticeably enriched in 74220 relative to the basalts rather than depleted, as would be expected.

On the other hand, LONGHI *et al.* (1974, Fig. 2) have shown that there is continuous compositional trend from Apollo 17 to Apollo 11 low-K basalt which can be described to a very good approximation in terms of the multiply-saturated liquid line of descent observed for Apollo 17 experiments. Since this line-of-descent was produced in a mild vacuum, there appears to be evidence for crystal liquid differentiation processes acting at a similar low pressure, presumably near the lunar surface. It should be noted that this trend does not include the Apollo 11 high-K suite. Projecting from alkali feldspar components instead of Na_2O and K_2O does not substantially affect the relative dispositions of these composition groups.

A subprojection is seen in Fig. 2. The experimental liquids are saturated with armalcolite and/or ilmenite and so this heavy-dash curve represents the Ti-oxide saturation boundary in this portion of composition space. The volumes for olivine and/or pyroxene crystallization are indicated on the Ti-oxide undersaturated side of this curve. The relative positions of these volumes have been determined by work on Apollo 12 and 15 low-Ti basalts (GROVE *et al.*, 1973; LONGHI *et al.*, in preparation). It can be seen to a first approximation that the Apollo 11 and 17 basalt compositions cluster along the curve of Ti-oxide saturation. The most noticeable deviations are seen for the Apollo 11 high-K suite. The deviations are such that these materials are over-saturated with respect to Ti-oxide. This compositional distribution contrasts strongly with that of the low-Ti mare basalts also displayed in Fig. 2, which are undersaturated with respect to Ti oxides. Olivine fractionation paths are indicated with dotted and/or dashed lines. Extreme fractional crystallization of low-Ti liquids involving olivine then pyroxene (and plagioclase) is capable of producing Ti-oxide-saturated liquids. A liquid produced in the experimental crystallization of 12002 (GROVE *et al.*, 1973) is indicated by the diamond at the end of the arrow. These residual liquids become ilmenite-saturated but only at temperatures below 1125°C and below the armalcolite stability field even for the most titaniferous of the low-Ti basalts. The fact that armalcolite- (not ilmenite)-saturated compositions such as 70215 appear to have existed in the liquid state at

~1200°C very strongly suggests that such liquids are not the dregs of fractional crystallization of these or similar low-Ti magmas. Furthermore, fractional crystallization of low-Ti basaltic liquids will produce Ti-oxide-saturated liquids with high Fe/Fe + Mg (~0·8) unless there is simultaneous separation of a metal phase. If metal does not separate, the liquid produced is too iron-rich. If metal does separate, olivine becomes unstable as silica activity increases. The suggestion of O'HARA *et al.* (1970) that titaniferous basalts represent the residual liquids of advanced fractional crystallization cannot be sustained unless the parent is already highly titaniferous so as to produce armalcolite saturation. Low-Ti basalt is not a satisfactory parent.

On the other hand, the hypothetical parent liquid must not be so titaniferous that major precipitation of Fe Ti oxides occurs with consequent depletion in Cr (RINGWOOD, 1970). The range of plausible parent liquid compositions is therefore narrowly restricted. Among the returned lunar samples only the 'orange soil' (74220) falls within this range and it is unsatisfactory on other grounds (Appendix; LSPET, 1973). We conclude that the titaniferous basalts are unlikely to be direct products of extreme fractional crystallization.

The approximation that the titaniferous basalt compositions are saturated or oversaturated with titaniferous oxide makes possible another useful projection. Figure 3 may be separated into silicate satu-

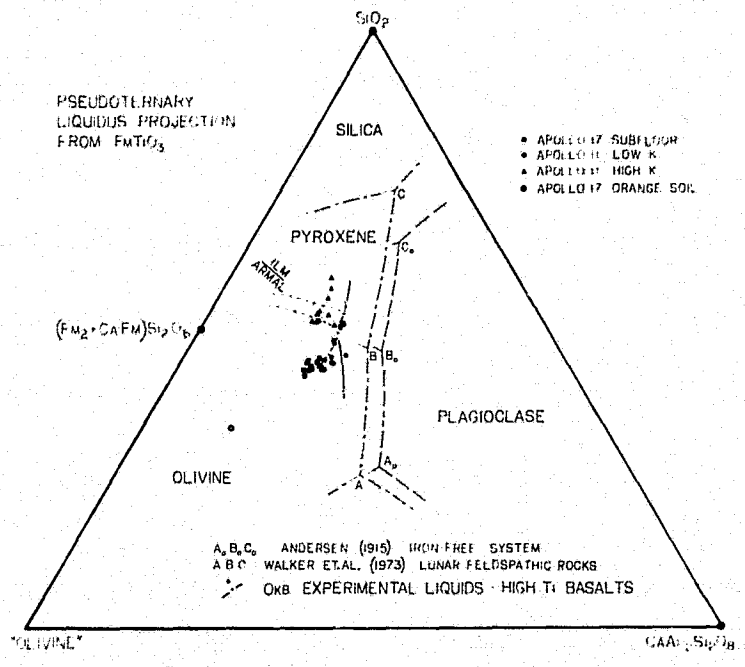

Fig. 4. Projection from $FmTiO_3$ on to plane SiO_2 An Px. This contains the same information as the projection of Fig. 3, but it is recast into a more familiar form. The Px and An molecules are the same but SiO_2 is used instead of FmO; the ternary format uses 'olivine' (not ideal because of $CaFmSi_2O_6$ component in the pyroxene) as a coordinate. Molar oxide analyses may be plotted in this projection according to the following formulae:

$$SiO_2 = \frac{(SiO_2 - CaO - Al_2O_3 + \frac{1}{2}TiO - \frac{1}{2}FeO - \frac{1}{2}MgO)}{SiO_2\text{-}CaO}$$

$$CaAl_2Si_2O_8 = \frac{Al_2O_3}{SiO_2 - CaO}$$

$$\text{'Olivine'} = \frac{FeO + MgO - TiO_2}{2 \times (SiO_2 - CaO)}$$

Note that FmO is now at infinity below 'olivine' on the 'olivine' silica join. For comparison the saturation boundaries for other systems are shown when recalculated in this projection. There is a systematic shift of plagioclase–ferromagnesian silicate saturation curves away from plagioclase with increasing Fe/Fe + Mg of the system.

ration fields which coexist with an oxide (ilmenite and/or armalcolite). The projection is from $FmTiO_3$ on to the FmO–pyroxene $CaAl_2Si_2O_8$ plane and behaves like a ternary liquidus diagram in that crystallization paths and the order of phase appearance may be deduced. New experimental evidence which confirms the applicability of these boundaries to high-K and other materials may be found in the Appendix. (The compositions of the basalts and the saturation boundaries are recast in a slightly more familiar ternary format in Fig. 4.)

Several important conclusions can be drawn from consideration of the positions of the titaniferous basalt compositions relative to the saturation boundaries in Figs. 2–4. The compositions seem to be disposed along the surfaces of multiple saturation. This observation supports the contention of O'HARA *et al.* (1970) that the Apollo 11 basalts were 'near-cotectic' in composition, and indicates that these compositions are controlled to a significant degree by crystal–liquid fractionation at low pressure. Note that 'multiply-'saturated liquids' are not synonymous with 'plagioclase-saturated liquids' although plagioclase-saturated representatives of the titaniferous basalts are found (see Appendix, 75035). Note also that our detailed confirmation of the experimental work of O'HARA *et al.* (1970, 1974) and BIGGAR *et al.* (1971, 1972) is not to be construed as an endorsement of their conclusion that advanced fractional crystallization near the lunar surface is the crystal liquid equilibrium process responsible for the compositions of titaniferous basalts. It has been argued above that an origin by advanced fractional crystallization encounters difficulty in explaining the presence of magmatic armalcolite, high Cr and V (RINGWOOD, 1970) and relatively modest Fe/Fe + Mg, unless rather severe restrictions are placed on the parental liquid. We will argue that melting processes are a more reasonable means of generating the bulk chemistry of two distinct groups of high-Ti basalts. This is to say that the demonstration of low pressure crystal–liquid fractionation control is not sufficient to demonstrate that all the control of chemical variation is by fractional crystallization. We do, however, recognize that these compositions are controlled by low pressure equilibria to a certain extent and that fractional crystallization may interrelate various types within the titaniferous suite, since only relatively minor fractionation is required. For instance, it is possible to consider 70215 a rapidly chilled sample of a sort of magma which may have cooled and differentiated by olivine and armalcolite fractionation to give 75035 (the Apollo 17 basalt poorest in FmO). BROWN *et al.* (1974) have suggested such a petrologic relation may exist between various members of the Apollo 17 suite. A similar case can be made relating the members of the Apo³lo 11 low-K suite except that quickly chilled samples of likely parent liquids were not sampled. Figure 5 shows minor and trace element data compatible with this interpretation. *The compositional variation of Apollo 17 and Apollo 11 low-K titaniferous basalts is continuous, overlapping, and explicable as the result of modest amounts of fractional crystallization of olivine and armalcolite followed by ilmenite then pla-*

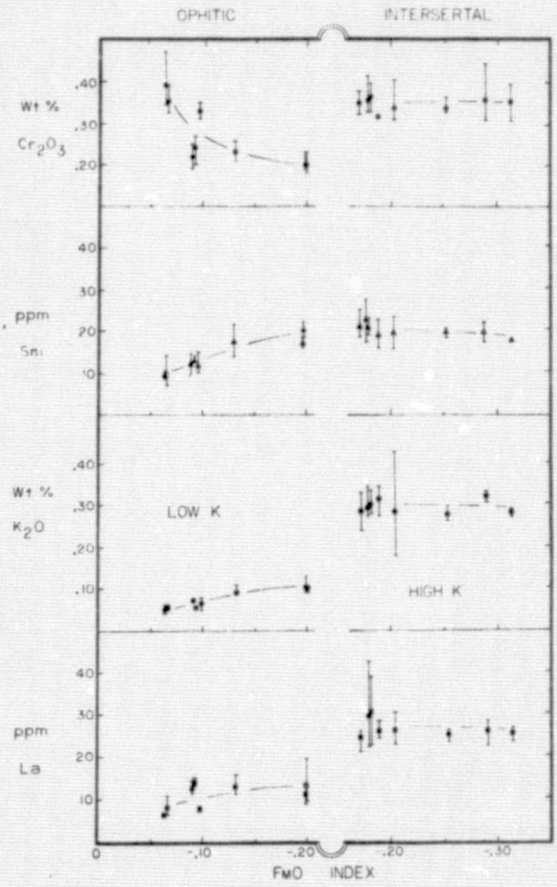

Fig. 5. Minor and trace element data for Apollo 11 basalts are plotted against the FmO value used as ordinate in the inset to Fig. 1. This parameter serves as a differentiation index with increasing differentiation to the right. The ophitic-intersertal classification follows JAMES and JACKSON (1970). Within the ophitic suite there are crude trends toward decreasing Cr_2O_3 and increasing K_2O, La, and Sm with differentiation. These trends are consistent with fractional crystallization of armalcolite, ilmenite, olivine, and plagioclase. No such trends are evident in the intersertal suite, suggesting that SiO_2 analytical problems may be artificially inflating the differentiation index of the three samples to the right (see text). Symbols are average values reported in WARNER (1971). Bars indicate the extreme values reported. Data density is not uniform.

gioclase (so that the derivative members are plagioclase-saturated). However, for the reasons outlined above it is unlikely that the parental liquid is itself the result of extensive fractional crystallization.

It appears unlikely that the Apollo 11 high-K suite can be simply related by low pressure fractional crystallization to either the Apollo 17 or Apollo 11 low-K suite. This point has been made successfully by JAMES and WRIGHT (1972) by consideration of the crystallization sequence within each group and it can be seen in the projections of Fig. 3 and 4 that the high-K suite is not plagioclase-saturated as it should be if it were the fractional crystallization product of plagioclase-saturated Apollo 11 low-K liquids. There is a curious aspect to the compositional variation of the Apollo 11 high-K suite; it appears to parallel the variation of pyroxene–plagioclase–ilmenite-saturated liquids. If this distribution is in fact caused by saturation with these phases, one most postulate some set of conditions where the equilibria (stable or metastable) are shifted in favor of less feldspathic liquids. Pressure increases or hydration would shift the relations the wrong way. Alkali devolatilization would shift the relations the correct way but it will be argued later that the magnitude of the effect is not sufficient and, furthermore, the high-K suite would appear to have sustained less alkali loss than the low-K suite. Alternatively this distribution may be an artifact of SiO_2 analytical uncertainty in the analyses gleaned from several sources. The three low FmO (high SiO_2) points in the distribution are data obtained by activation analysis and spark source mass spectrometry, in contrast to XRF and wet chemical determinations on which the rest of the distribution is based. With reference to Fig. 5, the uniformity of minor and trace element abundances within this group (as opposed to the rudimentary trends within the low-K suite suggestive of crystal fractionation) makes it more likely that this trend is the result of small SiO_2 analytical uncertainties. If this is the case it is not necessary to postulate shifted plagioclase–pyroxene equilibria to explain an artificial distribution, but it is then necessary to postulate a separate parental liquid for the high-K suite. This separate parental liquid cannot itself be the product of advanced low pressure fractional crystallization for the same reasons discussed for the parent to the low-K suite.

Alkali Volatilization, Plagioclase Saturation, and 'Average' Magma Composition

Much has been written concerning the possible role of plagioclase fractionation in the production of the titaniferous basalts, and much of the controversy has been over the location of the plagioclase saturation surface. It can be seen in the projections of Figs. 2 and 4 that the plagioclase saturation surface encroaches upon some of these compositions. This circumstance has been repeatedly emphasized by O'HARA *et al.* (1970, 1974*a*) and BIGGAR *et al.* (1972) and is not open to further question. It can also be seen that parts of the low and high-K distribution are not immediately plagioclase-saturated. These compositions are the ones we consider to be parental to the rest of the low and high-K suites through limited fractional crystallization.

RINGWOOD and GREEN (1972) (and others, including O'HARA *et al.*, 1970) showed that high-K compositions (e.g. 10017, 10072) did not have plagioclase on the liquidus. An extended controversy developed with one group emphasizing the plagioclase-saturated compositions and the other group emphasizing the plagioclase-undersaturated compositions.

O'HARA *et al.* (1970) made the suggestion that the undersaturated materials could be made plagioclase-saturated by restoring alkalies and other volatile constituents presumably lost by volatilization at the lunar surface. RINGWOOD and GREEN (1972) performed experiments to test this contention and found that addition of alkalies suppresses ~~suppresses~~ plagioclase appearance and makes plagioclase saturation more remote. We have performed alkali addition experiments on 70215 and obtained the same result. The pyroxene and plagioclase saturation curve moves closer to plagioclase and hence plagioclase saturation is more remote from the compositions of interest (see Appendix). If addition of alkali makes plagioclase saturation more remote, then loss of alkali should increase the proximity to plagioclase saturation (see Fig. 6).

It is worth pointing out that the two microprobe analyses of BIGGAR *et al.* (1971) for Apollo 11 experimental residual liquids are in exact agreement with the saturation curves presented here. BIGGAR *et al.* (1971) did not perform their experiments in vacuum, as we did, so their liquids have retained roughly three times the alkali content of those reported here. This implies that the magnitude of the alkali-loss effect is not sufficiently large to account for the deviations from cotectic character since experiments in which substantial alkali loss has been sustained, relative to a low starting value, do not move the curves perceptibly. The effect demonstrated by RINGWOOD and GREEN (1972) was only accomplished by substantial addition (2·5 per cent) of alkali.

A related issue has been raised by O'HARA *et al.* (1974*a*). Their contention is that the hand specimen compositions are not truly representative material but

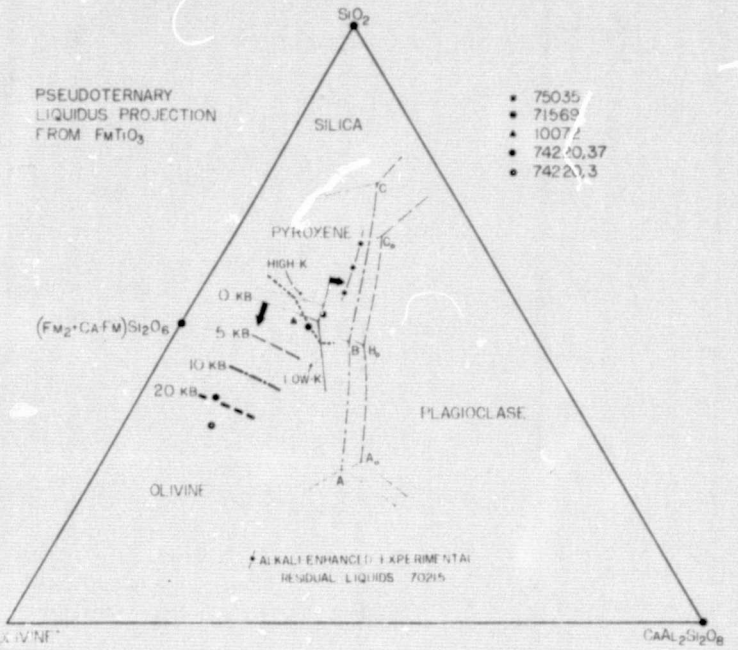

Fig. 6. Experimental results are displayed on the projection of Fig. 4. Bulk compositions of the starting materials and the experimental crystallization sequences may be found in Tables 1 and 2. The shift of the saturation boundaries as a result of changing physical conditions is indicated. Addition of alkalies shifts the pyroxene–plagioclase boundary towards plagioclase. Compositions of alkali-enhanced liquids indicated by diamond symbols are found in Table 1. Increasing pressure shifts the olivine–pyroxene boundary towards more olivine-normative compositions.

rather that statistical studies of lithic fragment compositions in the soils and breccias are more meaningful provided that the effects of contamination with highland debris can be removed. The 'average magma' they obtain is indeed plagioclase-saturated. This approach renders arguments over the hand specimen chemistry, and whether it has been devolatilized, irrelevant, since the shift from plagioclase saturation is not brought about by a change in the saturation boundary but by a change in hand specimen composition, i.e. by partial accumulation of small, petrographically cryptic, amounts of ferromagnesian silicate and oxides. This is to say the hand specimen compositions do not represent liquid compositions.

In contrast to this approach, we and most others have made the tacit or explicit assumption that the hand specimens do represent various *liquid* compositions since there is no obvious petrographic evidence to the contrary. Indeed several Apollo 17 samples (e.g. 70215 and 71569) show quench textures, indicating cooling from a totally liquid state. The inference that the liquid had the same composition as the hand specimen is insecure, however, as has been pointed out by O'Hara (personal communication). Mechanical transfer of cryptophenocrysts or diffusional transfer through the liquid might substantially alter the solid composition if the transfer rate exceeds the cooling rate. If this be the case, it becomes necessary to invoke some special mechanism to explain the compositional trends shown by both high-K and low-K hand-specimen groups and their relationship to the experimentally determined cotectic curves. We prefer to maintain the assumption that compositions of hand-specimens showing glassy or quench textures are the most reliable guide to magma compositions.

If we have correctly identified the low-K parental compositions, limited fractional crystallization of these can potentially produce a large volume of residual cotectic magma. That some has been produced is clear from samples such as 75035 (see Appendix). This derivative, possibly plagioclase-phyric, material could form up to 80 per cent of the cooling unit if differentiation were efficient. (Evidently the differentiation was not completely efficient since most of the range of intermediate compositions between parent and cotectic have been found in the hand specimen suite.) O'Hara's paradoxical discrepancy between hand specimen compositions and compositions of lithic fragments in soils and breccias suggests the existence of some sampling bias. Since the cooling

unit thickness and sampling mechanics are unknown, it appears equally probable to us that the soil could be skewed toward the derivative compositions instead of toward the parental compositions if the cooling unit contains subequal parts of preserved parent and derivative cotectic material.

Origin of Parental Liquids

We have shown here that the titaniferous lunar basalts exhibit compositional variations within the suite that appear to be controlled by low-pressure crystal–liquid equilibria. We have also argued that, although the relationships among the samples in the Apollo 11/17 low-K suite appear to be controlled by modest amounts of fractional crystallization at or near the lunar surface, the parental liquids themselves are not likely to be products of advanced low-pressure fractional crystallization. Furthermore, there appears to be no plausible scheme of fractional crystallization capable of relating the high-K Apollo 11 to the low-K Apollo 11/17 suite.

We are therefore forced to seek an origin for at least two parental magmas by partial melting somewhere within the lunar interior.

Ringwood and Essene (1970) attempted to locate the depth of origin and source material for the Apollo 11 suite by means of high pressure studies of a 'model basalt composition' based on an average of Apollo 11 high-K and low-K rock analyses. Unfortunately, this model composition was prepared at an early date when only preliminary emission spectrographic data on rock compositions were available, and as a consequence its MgO/FeO ratio is higher that that of average Apollo 11 magma, although within the range of values reported (Ringwood, personal communication). In most other respects it lies near the pyroxene–plagioclase–ilmenite-saturated experimental liquids (Figs. 1–3) and far from the compositions that we would regard as possibly parental and least likely to have been affected by low-pressure fractional crystallization. We therefore reject the main conclusion of Ringwood and Essene (1970) and Ringwood (1970), which was based on the study of their model basalt, that titaniferous magmas are produced by partial melting of primitive lunar material at a depth of 200–400 km, even though most of the general arguments presented in these papers are valid.

We have reported elsewhere (Longhi *et al.*, 1974) on high-pressure studies of 70215, a composition which we regard as a possible parent magma for the low-K suite. Such a liquid would be in equilibrium with a crystalline residue of olivine, pyroxene, ilmenite and possibly Ti–Cr spinel at some depth near 120 km. A depth of origin greater than 150 km would suggest unrealistically large degrees of partial melting. A less olivine-rich high-K parental liquid would be in equilibrium with a similar residual assemblage at even shallower depths. Such an episode of magma segregation at modest depth precludes the possibility of deducing the nature of the deep lunar interior on the basis of high pressure study of the titaniferous basalts.

An ilmenite-rich assemblage is unlikely to represent primitive lunar material, and the shallow inferred depth of origin strongly suggests that the source material has been subjected to the early magmatic differentiation that produced the feldspathic lunar crust. A possible primitive liquid such as that suggested by Walker *et al.* (1973; Fig. 3, pt. A) with 0·9 wt % TiO_2 and Fe/(Fe + Mg) = 0·24 (molar) would begin to crystallize ilmenite when approximately 90 per cent crystallized (reversible path). The residual liquid at this stage would have Fe/(Fe + Mg) = 0·45–0·50 and would be in equilibrium with olivine (Fo_{80-77}), pyroxene, ilmenite and plagioclase. (Departure from reversible crystallization would yield more iron-rich residual liquids.) Such a liquid would produce sinking cumulates of olivine, pyroxene, and ilmenite, floating plagioclase, and LIL enriched residuum. Later remelting and mixing of residuum with melted mafic cumulate at variable depths of up to 150 km would yield titaniferous parental basalts capable of further near-surface fractionation to produce the observed Apollo 11 and Apollo 17 rocks. Variable proportions of residuum to cumulate phases in the molten products might explain some of the observed minor element correlations.

Similar models have been proposed by others (e.g. Philpotts and Schnetzler, Smith *et al.*, Wood *et al.*, all 1970; Brett, 1973; Taylor and Jakes, 1974*a*, 1974*b*; Wakita *et al.*, 1974) to explain the Eu-anomaly and other details of minor element geochemistry. A vexing question has been whether or not plagioclase was present in the source material. If plagioclase is not present in the post-melting residue then the source materials must possess a strong intrinsic Eu-anomaly. Such an intrinsic anomaly seems a natural consequence of the prior separation of a feldspathic crust. In the case of the low-K titaniferous rocks (both Apollo 11 and Apollo 17) the existing Rb–Sr data yield model ages near 4·6 gy, requiring that no significant fractionation of Rb and Sr occurred after that date. Hence the proposed partial melting event at 3·7 gy must have quantitatively extracted Rb and Sr from the source material; plagioclase cannot have remained in the residue

(although it may have been present before the melting). This is consistent with the phase equilibrium data for the supposed parental liquids. The high-K titaniferous rocks of Apollo 11 have model-ages near the crystallization ages (PAPANASTASSIOU and WASSERBURG, 1971). This suggests that some strontium-bearing phase, presumably plagioclase or calcic pyroxene, was left in the crystalline residue. Available phase equilibrium data are not adequate to identify this phase conclusively but indications are that it is not plagioclase.

Relationship of Titaniferous Mare Basalts to Low-Ti Mare Basalts

It has been proposed by GREEN *et al.* (1971, 1974) that low-Ti mare basalts represent partial melting products of an olivine pyroxenite source region at depths of 200–400 km in the Moon. This proposal was supported for the case of Apollo 12 by GROVE *et al.* (1973) but the matter is not beyond dispute, as is clearly shown by the arguments of BIGGAR *et al.* (1971, 1974). An important problem in mare basalt petrogenesis is: can the low- and high-Ti varieties be related to a single source by various degrees of partial melting and/or various depths of magma segregation? GREEN *et al.* (1974) have argued that it is possible to relate the two types at a depth of 400–500 km on the basis of studies on Apollo 17 orange soil, a strongly olivine-normative titaniferous composition. We argue (in the Appendix) that such a parent to the high-Ti suite cannot produce both the high- and low-K suites by fractional crystallization at any depth and so we are constrained to accomplish magma segregation from an ilmenite-rich source in the outer 150 km of the Moon. We do not endorse the proposition that both low- and high-Ti basalts can be derived at depth from the same primitive source material. We are arguing for the necessity of a near-surface, *differentiated* source region for the high-Ti basalts. DUNCAN *et al.* (1974) and PHILPOTTS *et al.* (1973) have demonstrated that there is also evidence in the trace element abundance patterns to support the notion of a two-stage model of titaniferous magma production. RINGWOOD (1974*a*, 1974*b*), on the other hand, has surveyed the broader aspects of the trace element abundance patterns in mare basalts and proposed a single-stage model for the production of both low- and high-Ti basalts from the same source material. It seems premature to us to construct elaborate models which attempt to reconcile the trace element abundance patterns of the various basaltic types when the major element relations are in doubt. In this connection it is worth noting that all models proposed have difficulty reconciling the trace element abundance patterns in detail. In a word, complete consistency with regard to major and minor elements has not been achieved by any model.

Objections to Melting of Cumulates

RINGWOOD (1974*b*) has raised four objections to the generic class of models which melt cumulates to produce titaniferous magmas. The most serious of these objections involves the observation that source regions which have had a prior history of crystal liquid fractionation should produce basalts with strong minor element fractionations, for example, fractionation within the REE. The europium anomaly of these basalts fits the model very well, but one might also expect relative depletion in the heavy REE. This objection is not easily met in equilibrium crystal fractionation models and it is just this sort of objection which has forced RINGWOOD (1974*a*, 1974*b*) to abandon the bulk equilibrium boundary condition. If this constraint is removed the objection is less serious. It is possible, however, to construct models in which cumulates depleted in the light REE with an intrinsic europium anomaly might give rise to partial melts with apparently unfractionated REE patterns (except for europium) without abandoning the bulk equilibrium constraint. These models constrain the cumulate REE pattern and the degree of melting required. Much progress has been made in constructing such models by TAYLOR and JAKES (1974*a*, 1974*b*) and WAKITA *et al.* (1974).

Another objection involves the lack of chromium depletion which might be expected if the source region is produced by extensive fractional crystallization. O'HARA *et al.* (1974*a*) have pointed out the weakness of this argument. Chrome depletion by spinel must exceed chrome enrichment by olivine and plagioclase for the argument to work. Modeling chrome depletion by analogy with internal fractionation in crystallization of high-Ti basalt hand specimens (RINGWOOD, 1974*b*) is not relevant since ilmenite is also fractionating there. The only significant Cr depletion envisaged in the fractionation producing the Ti basalt source region results from spinel crystallization which must compete with Cr enrichment caused by subtraction of olivine and plagioclase. The competition will not deplete Cr unless spinel is more than about 1–3 per cent of the total crystal extract. Cr is, of course, depleted, possibly from a high starting value, when the residual liquid begins to crystallize ilmenite. But Cr is recovered in melting that ilmenite to produce the Ti basalts.

A third objection regards the absence of a suitable heat source to melt shallow cumulate layers after the outer parts of the Moon have cooled by conduction. If it is assumed that the radioactivity of the residual liquids from which the cumulates formed was sufficient to remelt the cumulate at 3·7 gy then it is hard to understand how the liquid could have crystallized in the first place. John Wood (personal communication) has suggested that a transition from a convective mode of heat loss through the lunar crust to a conductive mode may have accompanied the decline in impact activity at about 4 gy, and that this transition may have initiated a subsequent rise in temperature in the subcrustal regions.

SMITH (1974) and WONES (1974) have suggested that viscous tidal heating may be an important lunar heat source; and this mechanism is especially useful for heating the postulated source region of the titaniferous basalts. This source region is sandwiched between complementary feldspathic and mafic cumulates of contrasting density and mechanical properties and may have trapped small segregations of uncongealed liquid residue as noted above. Such a layer would be an ideal locus for dissipation of tidal energy. It is not clear, however, that tidal energy available at the time of mare filling would have been adequate.

We consider the heat source problem to be serious and unsolved. It seems clear, however, that the equilibrium chemical relations do not indicate a deep source region where the thermal and rheological problems might be less severe.

A fourth objection concerns the feasibility of producing late stage cumulates *within* the Moon. It is possible that the late liquids will segregate and differentiate at a level *below* the feldspathic crust rather than be extruded? This question is transitional to but clearly distinguishable from the one which asks if feldspar flotation in a global magma ocean can be responsible for the feldspathic crustal rocks and the late residual liquids. An attempt was made to answer the former question by equilibrating a crystalline powder starting material synthesized to have the composition of Apollo 11 soil 10084 (FRONDEL *et al.*, 1970) at 1200°C for 4½ days. This titaniferous composition has plagioclase at the liquidus (WALKER, 1972) and can be used as a rough model for the residual liquids. The quenched product of this experiment (in vacuum in high purity iron container) was >95 per cent glass with plagioclase concentrated at the top of the charge and spinel and iron metal droplets at the bottom. The plagioclase coarsened upwards in the charge, and the clear implication is that plagioclase floats in such a liquid. The density of this liquid can be calculated from the model of BOTTINGA and WEILL (1970) to be 3·25 gm/cm^3 at 1200°C, which is consistent with plagioclase flotation which is observed experimentally. Estimates of average lunar highland composition such as anorthositic norite have low pressure mineral assemblages which give densities ~2·9 gm/cm^3. Late-stage liquids parental to the ilmenite-rich cumulates should therefore remain beneath such a feldspathic crust.

CONCLUSION

We have shown that near-surface fractional crystallization is capable of explaining the compositional variations within the Apollo 11 low-K and Apollo 17 subfloor basalts, but that liquids parental to this suite are unlikely to be the result of advanced fractional crystallization. The Apollo 11 high-K suite can not be related by fractional crystallization to the Apollo 11 low-K and Apollo 17 subfloor basalts. Compositions that are parental to the Apollo 11 and 17 suites can be generated by partial melting of a differentiated source region (ol + px + ilm [redacted]) in the outer 150 km of the Moon. This model is capable of explaining the origin of and differences between the Apollo 11 high-K basalts on one hand and the Apollo 11 low-K and Apollo 17 subfloor basalts on the other hand. The differences arise from varying degrees of melting of the source region and variable depths of magma segregation. In this model the source region does not contain plagioclase (or at least does not retain it in the residue after melting) and the differences result chiefly from different depths of magma segregation. However, if plagioclase is present, an alternate scheme in which the differences result from increasing degrees of melting is possible.

Acknowledgements. We have benefitted from discussions with M. J. O'HARA, J. PHILPOTTS, A. E. RINGWOOD, J. V. SMITH, and D. R. WONES. Our microprobe is ably maintained by M. CAMPOT. S. ADAMS and N. JACKSON assisted in manuscript preparation. We thank R. BRETT, S. HUEBNER, M. J. O'HARA, A. E. RINGWOOD, and R. J. WILLIAMS for helpful reviews. This work was supported by NASA grant NGL 22-007-247 and by the Committee on Experimental Geology and Geophysics, Harvard University.

REFERENCES

AGRELL S. O., SCHOON J. H., MUIR I. D., LONG J. V. P., MCCONNELL J. D. C. and PECKETT A. (1970) Observations on the chemistry, mineralogy and petrology of some Apollo 11 lunar samples. *Proc. Apollo 11 Lunar Sci. Conf., Geochim. Cosmochim. Acta Suppl.* **1**, Vol. 1, pp. 93–128. Pergamon Press.

ANDERSEN O. (1915) The system anorthite–forsterite–silica. *Amer. J. Sci. 4th Ser.* **39**, 407454.

BIGGAR G. M., O'HARA M. J., PECKETT A. and HUMPHRIES D. J. (1971) Lunar lavas and the achondrites: petrogenesis of protohypersthene basalts in the maria lava lakes. *Proc. Second Lunar Sci. Conf., Geochim. Cosmochim. Acta Suppl.* **2**, Vol. 1, pp. 617–643. M.I.T. Press.

BIGGAR G. M., O'HARA M. J., HUMPHRIES D. J. and PECKETT A. (1972) Maria lavas, mascons, layered complexes, achondrites and the lunar mantle. In *The Moon* (editors H. Urey and S. K. Runcorn), pp. 129–164. I.A.U.

BIGGAR G. M., HUMPHRIES D. J. and O'HARA M. J. (1974) Experimental crystallization and geochemical interpretation of low titanium basalts. In *Lunar Science—V*, pp. 60–62. Lunar Science Institute, Houston.

BOTTINGA Y. and WEILL D. F. (1970) Densities of liquid silicate systems calculated from partial molar volumes of oxide components. *Amer. J. Sci.* **269**, 169–182.

BRETT R. (1973) The lunar crust: a product of heterogeneous accretion of differentiation of a homogeneous moon? *Geochim. Cosmochim. Acta* **37**, 2697–2703.

BROWN G. M., PECKETT A., EMELEUS C. H. and PHILLIPS R. (1974) Mineral chemical properties of Apollo 17 mare basalts (abstract). In *Lunar Science—V*, pp. 89–91. The Lunar Science Institute, Houston.

CHAPPELL B. W. and GREEN D. H. (1973) Chemical compositions and petrogenetic relationships in Apollo 15 mare basalts. *Earth planet. Sci. Lett.* **18**, 237–246.

COMPSTON W., CHAPPELL B. W., ARRIENS P. A. and VERNON M. J. (1970) The chemistry and age of Apollo 11 lunar material. *Proc. Apollo 11 Lunar Sci. Conf., Geochim. Cosmochim. Acta Suppl.* **1**, Vol. 2, pp. 1007–1027. Pergamon Press.

COMPSTON W., BERRY H., VERNON M. J., CHAPPELL B. W. and KAYE M. J. (1971) Rubidium–strontium chronology and chemistry of lunar material from the Ocean of Storms. *Proc. Second Lunar Sci. Conf., Geochim. Cosmochim. Acta Suppl.* **2**, Vol. 2, pp. 1471–1485. M.I.T. Press.

CUTTITTA F., ROSE H. J. JR., ANNELL C. S., CARRON M. K., CHRISTIAN R. P., DWORNIK E. J., GREENLAND J. P., HELZ A. W. and LIGON D. T. JR. (1971) Elemental composition of some Apollo 12 lunar rocks and soils. *Proc. Second Lunar Sci. Conf., Geochim. Cosmochim. Acta Suppl.* **2**, Vol. 2, pp. 1217–1229. M.I.T. Press.

CUTTITTA F., ROSE H. J. JR., ANNELL C. S., CARRON M. K., CHRISTIAN R. P., LIGON D. T., DWORNIK E. J., WRIGHT T. L. and GREENLAND L. P. (1973) Chemistry of twenty-one igneous rocks and soils returned by the Apollo 15 mission. *Proc. Fourth Lunar Sci. Conf., Geochim. Cosmochim. Acta Suppl.* **4**, Vol. 2, pp. 1081–1096. Pergamon Press.

DUNCAN A. R., ERLANK A. J., WILLIS J. P., SHER M. K. and AHRENS L. H. (1974) Trace element evidence for a two stage origin of high-titanium mare basalts. In *Lunar Science—V*, pp. 187–189. Lunar Science Institute, Houston.

FRONDEL C., KLEIN C., ITO J. and DRAKE J. C. (1970) Mineralogical and chemical studies of Apollo 11 lunar fines and selected rocks. *Proc. Apollo 11 Lunar Sci. Conf., Geochim. Cosmochim. Acta Suppl.* **1**, Vol. 1, pp. 445–474. Pergamon Press.

GAST P. W., HUBBARD N. J. and WEISMANN H. (1970) Chemical composition and petrogenesis of basalts from Tranquillity Base. *Proc. Apollo 11 Lunar Sci. Conf., Geochim. Cosmochim. Acta Suppl.* **1**, Vol. 2, pp. 1143–1163. Pergamon Press.

GREEN D. H., RINGWOOD A. E., WARE N. G., HIBBERSON W. O., MAJOR A. and KISS E. (1971) Experimental petrology and petrogenesis of Apollo 12 basalts. *Proc. Second Lunar Sci. Conf., Geochim. Cosmochim. Acta Suppl.* **2**, Vol. 1, pp. 601–615. M.I.T. Press.

GREEN D. H., RINGWOOD A. E., WARE N. G. and HIBBERSON W. O. (1974) Petrology and petrogenesis of Apollo 17 basalts and Apollo 17 orange glass. Abstract in *Lunar Science—V*, pp. 287–289. Lunar Science Institute, Houston.

GROVE T. L., WALKER D., LONGHI J., STOLPER E. M. and HAYS J. F. (1973) Petrology of rock 12002 from Oceanus Procellarum. *Proc. Fourth Lunar Sci. Conf., Geochim. Cosmochim. Acta Suppl.* **4**, Vol. 1, pp. 995–1011. Pergamon Press.

HASKIN L. A., ALLEN R. O., HELMKE P. A., PASTER T. P., ANDERSON M. R., KOROTEV R. L. and ZWEIFEL K. A. (1970) Rare earths and other trace elements in Apollo 11 lunar samples. *Proc. Apollo 11 Lunar Sci. Conf., Geochim. Cosmochim. Acta Suppl.* **1**, Vol. 2, pp. 1213–1231. Pergamon Press.

JAMES O. B. and JACKSON E. D. (1970) Petrology of the Apollo 11 ilmenite basalts. *J. Geophys. Res.* **75**, 5793–5824.

JAMES O. B. and WRIGHT T. L. (1972) Apollo 11 and 12 mare basalts and gabbros: classification, compositional variations, and possible petrogenetic relations. *Bull. Geol. Soc. Amer.* **83**, 2357–2382.

KESSON S. E. (1974) Apollo 15 mare basalts: melting experiments in high purity Fe containers at 1 atm and high pressures. *Abstracts with Programs*. Vol. 6 (7), p. 823. Annual Meetings, Geological Society of America.

KRIDELBAUGH S. J. and WEILL D. F. (1973) The mineralogy and petrology of ilmenite basalts 75055. *EOS, Trans. Amer. Geophys. Union* **54**, 597–598.

KUSHIRO I. and MIYAMURA H. (1971) Major element variation and possible source materials of Apollo 12 crystalline rocks. *Science* **171**, 1235–1237.

LINDSLEY D. H., HARTZMAN M. J., KESSON S. E. and CUSHMAN M. K. (1974) Fe–Mg–Ti oxides in lunar mare basalts: chemical evolution interpreted from experiment and theory. In *Lunar Science—V*, pp. 453–455. Lunar Science Institute, Houston.

LONGHI J., WALKER D., GROVE T. L., STOLPER E. M. and HAYS J. F. (1974) The petrology of the Apollo 17 mare basalts. *Proc. Fifth Lunar Sci. Conf., Geochim. Cosmochim. Acta Suppl.* **5**, Vol. 1 (in press). Pergamon Press.

LONGHI J., WALKER D., GROVE T. L., STOLPER E. M. and HAYS J. F. Petrology and origin of Apollo 15 mare basalts. In preparation.

LSPET (LUNAR SAMPLE PRELIMINARY EXAMINATION TEAM) (1973) The Apollo 17 lunar samples: petrographic and chemical description. *Science* **182**, 659–690.

MAXWELL J. A., PECK L. C. and WIIK H. B. (1970) Chemical composition of Apollo 11 lunar samples 10017, 10020, 10072 and 10084. *Proc. Apollo 11 Lunar Sci. Conf., Geochim. Cosmochim. Acta Suppl.* **1**, Vol. 2, pp. 1369–1374. Pergamon Press.

MUAN A. and SCHAIRER J. R. (1971) Melting relations of materials of lunar composition. *Carnegie Inst. Wash. Yearb.* **69**, 243–245.

NAVA D. F. (1974) Chemistry of some rock types and soils from the Apollo 15, 16, and 17 lunar sites. Abstract in *Lunar Science—V*, pp. 547–549. Lunar Science Institute, Houston.

O'HARA M. J., BIGGAR G. M., RICHARDSON S. W., FORD C. E. and JAMIESON B. G. (1970) The nature of seas, mascons and the lunar interior in the light of experimental studies. *Proc. Apollo 11 Lunar Sci. Conf., Geochim.*

Cosmochim. Acta Suppl. **1,** Vol. 1, pp. 695–710. Pergamon Press.

O'HARA M. J., BIGGAR G. M., HILL P. G., JEFFERIES B. and HUMPHRIES D. J. (1974a) Plagioclase saturation in lunar high-titanium basalt. *Earth Planet. Sci. Lett.* **21,** 253–268.

O'HARA M. J., BIGGAR G. M., HUMPHRIES D. J. and SAHA P. (1974b) Experimental petrology of high titanium basalt. Abstract in *Lunar Science—V*, pp. 571–573. Lunar Science Institute, Houston.

PAPANASTASSIOU D. A. and WASSERBURG G. J. (1971) Lunar chronology and evolution from Rb–Sr studies of Apollo 11 and 12 samples. *Earth Planet. Sci. Lett.* **11,** 37–62.

PAPIKE J. J. and BENCE A. E. (1973) Petrology and chemistry of mare rocks. *Abstracts with Programs*, Vol. 5 (7), pp. 762–763. Annual Meetings, Geological Society of America.

PHILPOTTS J. A. and SCHNETZLER C. C. (1970) Apollo 11 lunar samples: K, Rb, Sr, and rare-earth concentrations in some rocks and separated phases. *Proc. Apollo 11 Lunar Sci. Conf., Geochim. Cosmochim. Acta Suppl.* **1,** Vol. 2, pp. 1471–1486. Pergamon Press.

PHILPOTTS J. A., SCHUHMANN S., SCHNETZLER C. C., KOUNS C. W., DOAN A. S., WOOD F. M., BICKEL A. L. and LUM STAAB R. K. L. (1973) Apollo 17: geochemical aspects of some soils, basalts and breccia. *EOS, Trans. Amer. Geophys. Union* **54,** 603–604.

PRINZ M., DOWTY E., KEIL K. and BUNCH T. E. (1973) Mineralogy, petrology, and chemistry of lithic fragments from Luna 20 fines: origin of the cumulate ANT suite and its relation to high alumina and mare basalts. *Geochim. Cosmochim. Acta* **37** (Luna 20 volume), 979–1006.

RHODES J. M. and HUBBARD N. J. (1973) Chemistry, classification, and petrogenesis of Apollo 15 mare basalts. *Proc. Fourth Lunar Sci. Conf., Geochim. Cosmochim. Acta Suppl.* **4,** Vol. 2, pp. 1127–1148. Pergamon Press.

RHODES J. M., RODGERS K. V., SHIH C., BANSAL B. M., NYQUIST L. E. and WEISMAN H. (1974) The relationship between geology and soil chemistry at the Apollo 17 landing site. In *Lunar Science—V*, pp. 630–632. Lunar Science Institute, Houston.

RINGWOOD A. E. (1970) Petrogenesis of Apollo 11 basalts and implications for lunar origin. *J. Geophys. Res.* **75,** 6453–6479.

RINGWOOD A. E. (1974a) Minor element chemistry of maria basalts. In *Lunar Science—V*, pp. 633–635. Lunar Science Institute, Houston.

RINGWOOD A. E. (1974b) Some aspects of the minor element chemistry of mare basalts. *The Moon* in press.

RINGWOOD A. E. and ESSENE E. (1970) Petrogenesis of Apollo 11 basalts, internal constitution and origin of the moon. *Proc. Apollo 11 Lunar Sci. Conf., Geochim. Cosmochim. Acta Suppl.* **1,** Vol. 1, pp. 769–799. Pergamon Press.

RINGWOOD A. E. and GREEN D. H. (1972) Crystallization of plagioclase in lunar basalts and its significance. *Earth Planet. Sci. Lett.* **14,** 14–18.

RINGWOOD A. E. and GREEN D. H. (1974) Maria, basalts and the composition of the lunar interior. In *Lunar Science—V*, pp. 636–638. Lunar Science Institute, Houston.

ROEDDER E. and WEIBLEN P. W. (1973) Origin of orange glass spherules in Apollo 17 sample 74220. *EOS, Trans. Amer. Geophys. Union* **54,** 612–613.

SMITH J. V. (1974) Origin of moon by disintegrative capture with chemical differentiation followed by sequential accretion. In *Lunar Science—V*, pp. 718–720. Lunar Science Institute, Houston.

SMITH J. V., ANDERSON A. T., NEWTON R. C., OLSEN E. J., WYLIE P. J., CREWE A. V., ISAACSON M. S. and JOHNSON D. (1970) Petrologic history of the moon inferred from petrography, mineralogy and petrogenesis of Apollo 11 rocks. *Proc. Apollo 11 Lunar Sci. Conf., Geochim. Cosmochim. Acta Suppl.* **1,** Vol. 1, 897–925. Pergamon Press.

STEELE I. M. and SMITH J. V. (1972) Mineral and bulk compositions of three fragments from Luna 16. *Earth Planet. Sci. Lett.* **13,** 323–327.

STOLPER E. M. (1974) Lunar ultramafic glasses. Unpublished honors thesis, Harvard University.

TAYLOR S. R. and JAKEŠ P. (1974a) Geochemical zoning in the Moon. In *Lunar Science—V*. Lunar Science Institute, Houston.

TAYLOR S. R. and JAKEŠ P. (1974b) Geochemical zoning and early differentiation in the Moon. *Nature*, in press.

TERA F., EUGSTER O., BURNETT D. S. and WASSERBURG G. J. (1970) Comparative study of Li, Na, K, Rb, Cs, Ca, Sr, and Ba abundances in achondrites and in Apollo 11 lunar samples. *Proc. Apollo 11 Lunar Sci. Conf., Geochim. Cosmochim. Acta Suppl.* **1,** Vol. 2, pp. 1637–1657. Pergamon Press.

TUTHILL R. P. and SATO M. (1970) Phase relations of a simulated lunar basalt as a function of oxygen fugacity, and their bearing on the petrogenesis of the Apollo 11 basalts. *Geochim. Cosmochim. Acta* **34,** 1293–1302.

WAKITA H., LAUL J. C. and SCHMITT R. A. (1974) Some thoughts on the origin of lunar ANT–KREEP and mare basalts. *Meteoritics*. In press.

WALKER D. (1972) Experimental petrology of lunar basalts. Ph.D. Thesis, Harvard University.

WALKER D., GROVE T. L., LONGHI J., STOLPER E. M. and HAYS J. F. (1973) Origin of lunar feldspathic rocks. *Earth Planet. Sci. Lett.* **20,** 325–336.

WALKER D., LONGHI J., STOLPER E., GROVE T. and HAYS J. F. (1974) Experimental petrology of titaniferous lunar basalts. Abstract in *Lunar Science—V*, pp. 814–816. Lunar Science Institute, Houston.

WARNER J. (1971) A summary of Apollo 11 chemical, age, and modal data. Compiled from *Geochim. Cosmochim. Acta Suppl.* **1,** Pergamon Press. Curator's Office, Manned Spacecraft Center, Houston.

WEILL D. F., MCCALLUM I. S., BOTTINGA Y., DRAKE M. J. and MCKAY G. A. (1970) Mineralogy and petrology of some Apollo 11 igneous rocks. *Proc. Apollo 11 Lunar Sci. Conf., Geochim. Cosmochim. Acta Suppl.* **1,** Vol. 1, pp. 937–955. Pergamon Press.

WILLIS J. P., AHRENS L. H., DANCHIN R. V., ERLANK A. J., GURNEY J. J., HOFMEYR P. K., MCCARTHY T. S. and ORREN M. J. (1971) Some interelement relationships between lunar rocks and fines, and stony meteorites. *Proc. Second Lunar Sci. Conf., Geochim. Cosmochim. Acta Suppl.* **2,** Vol. 2, pp. 1123–1138. M.I.T. Press.

WONES D. R. (1974) Lunar crustal processes: homogeneous or heterogeneous? Abstract in *EOS, Trans. Amer. Geophys. Union* **55,** 325.

WOOD J. A., DICKEY J. S., MARVIN U. B. and POWELL B. N. (1970) Lunar anorthosites and a geophysical model of the Moon. *Proc. Apollo 11 Lunar Sci. Conf., Geochim. Cosmochim. Acta Suppl.* **1,** Vol. 1, pp. 965–988. Pergamon Press.

APPENDIX

EXPERIMENTAL RESULTS AND DISCUSSION

Titaniferous basalts

We report here further experimental results relevant to the titaniferous basalt problem. Details of the experimental procedures may be found in LONHGI *et al.* (1974). Table 1 contains the bulk compositions of starting materials used in this investigation and the compositions of selected experimentally produced phases. Figure 6 shows these compositions in the same projection as Fig. 4. Table 2 lists the conditions and results of the individual experiments. It can be seen from an inspection of Table 2 and Fig. 6 that the low-pressure saturation curves determined by microprobe analysis of residual glasses in 70017 and 70215 (WALKER *et al.*, 1974; LONGHI *et al.*, 1974) very closely predict the crystallization behavior of the three other titaniferous basalts reported here. This constitutes a confirmation of the utility of this projection.

An important feature of these experiments is that high purity iron capsules are used inside an evacuated silica tube. The use of iron capsules introduces two problems. There is little direct petrographic evidence that these compositions were iron-saturated at the liquidus; hence, they might be expected to react with the capsule and gain iron. This effect was sought and was undetectable in the original work reported by WALKER *et al.* (1974) and detailed in LONGHI *et al.* (1974) on 70017 and 70215. In the present work the effect was undetectable in 74220, 75035, and 71569. For 10072 the effect produced a gain of 7 per cent of the amount of iron present in the bulk composition. With the exception of 10072, then, the compositions must have been effectively iron-saturated to maintain constant bulk composition. This argument has also been made recently by KESSON (1974) with reference to low-Ti basalts from Apollo 15. For 10072 we have reported the mildly iron-enhanced composition in Table 1 and in Fig. 6. The composition still falls in the range of the high-K suite of which it is a member, and as such, its experimental crystallization sequence is instructive.

The second problem introduced by iron capsules has been noted by LINDSLEY *et al.* (1974). Armalcolite will show a larger stability field in iron capsules than in non-iron-saturated conditions. This effect will tend to make armalcolite persist with ilmenite to lower temperatures.

Another feature of our experimental configuration is a large void-space/sample ratio which allows charge extraction with re-use of the capsule. The large evacuated void is presumably influential in the partial loss of alkali experienced by our charges although the final disposition of the alkali is unknown. By comparison with saturation-curve information in BIGGAR *et al.* (1971) the loss of alkali relative to the very low starting level present does not substantially affect the position of the saturation curves. Any effect introduced by the alkali loss would make the plagioclase more calcic and stable at a higher temperature relative to a non-alkali-depleted situation. The coupled effect, then, of our experimental perturbations is to increase armacolite stability to lower temperatures and plagioclase stability to higher temperatures than might be otherwise achieved. As a result our experimental 'gap' between the removal of armalcolite by reaction and the saturation of the liquid with both plagioclase and pyroxene must be a minimum gap. Under other conditions it would be larger. This consideration strengthens the contention in the text that armalcolite-bearing lavas cannot be erupted from plagioclase pyroxene-cotectic magma bodies. Independent indications of the truth of this proposition may be found in the petrography of 75055 (KRIDELBAUGH and WEILL, 1973), 75035 (LONGHI *et al.*, 1974), 10044 and 10047 (JAMES and JACKSON, 1970), which have cotectic bulk compositions. These samples do not contain armalcolite, and 75035 does not crystallize armacolite experimentally as noted below.

We have given a petrographic description of medium-grained ophitic basalt 75035 (LONGHI *et al.*, 1974) in which ilmenite was recognized as the first crystallizing phase, quickly followed by plagioclase and pyroxene. Experimentally, pyroxene and plagioclase crystallize simultaneously immediately after ilmenite saturation. The maximum temperature interval between the liquidus and three-fold saturation (ilmenite, pyroxene, and plagioclase) allowed by the data is 5°C. The amount of crystallization at three-fold saturation is negligible. Graphically it can be seen that 75035 has a composition which is close to olivine saturation. More olivine-normative compositions which crystallize under equilibrium conditions are beginning the reaction olivine + liquid → pyroxene at this temperature and composition of residual liquid. Therefore 75035 is in reaction relation with olivine at its liquidus, and olivine is not observed experimentally or petrographically in the crystallization sequence. It is clear that 75035 is the crystallization product of the celebrated 'cotectic' liquid (more properly a peritectic liquid since olivine is in reaction relationship). For the reasons stated in the text, we feel that this liquid

Table 1. Electron microprobe analyses

	75035,61*	71569,21*	10072,23*	74220,37*
SiO_2	41.6	38.7	38.7	39.2
TiO_2	10.2	13.0	13.0	9.44
Al_2O_3	9.75	8.64	7.56	5.84
Cr_2O_3	.27	.45	.30	.64
FeO	18.5	18.9	21.4	22.2
MgO	6.16	7.87	7.36	14.1
MnO	.30	.34	.32	.34
CaO	11.5	10.3	9.73	7.10
Na_2O	.48	.41	.47	.38
	98.76	98.61	98.84	99.24

	06-16 opx**	215-50 glass**	215-51 glass**	215-52 glass**
SiO_2	52.4	48.7	46.1	44.1
TiO_2	1.10	5.55	6.93	7.96
Al_2O_3	3.53	12.8	12.0	11.4
Cr_2O_3		.05	.05	.07
FeO	13.4	15.5	16.4	16.9
MgO	26.2	3.62	4.35	5.17
MnO		.26	.28	.29
CaO	2.27	8.26	9.63	10.6
Na_2O		5.13	4.51	3.32
	98.90	99.87	100.25	99.81

* Bulk compositions of experiments above the liquidus: 75035,61 – low-K chemistry; 71569,21 intermediate chemistry; 10072,23 high-K chemistry; 74220,37 orange soil.

† See Table 2 for conditions of the experiments.

is derived from fractional crystallization of the parental liquids to the low-K suite.

We have also given a cursory petrographic description of 71569 in LONGHI *et al.* (1974). Sample 71569 texturally resembles 70215, one of the starting materials used to determine the saturation curves. Both rocks appear to have pyroxene before plagioclase in the petrographic crystallization sequence. However, 70215 has a bulk composition and experimental crystallization sequence in which these two minerals crystallize in the opposite order. The petrographic 'anomaly' was interpreted in terms of delayed nucleation and growth of plagioclase as a result of supercooling during the crystallization of 70215. On the other hand, 71569 has a bulk composition and experimental crystallization sequence compatible with a petrographic sequence in which pyroxene crystallizes first. Noting the similarity of texture to 70215 it is probably that 71569 also crystallized under strongly supercooled conditions even though this interpretation is not required by any discrepancy between experimental and petrographic crystallization sequences.

The bulk composition of 71569 is intermediate between the low and high-K suites with respect to major elements. Its composition cannot be parental to, or be derived from, the parental liquids of either the high or low-K suite by fractional crystallization at the lunar surface.

Sample 71569 is also intermediate in crystallization sequence between the high and low-K suite. We have studied a high-K Apollo 11 basalt 10072. From petrographic observations, these intersertal rocks crystallize pyroxene before plagioclase (JAMES and JACKSON, 1970). Experimental crystallization results on 10072 are consistent with this observation. The compositional and thermal interval between pyroxene and plagioclase entry is greater for 10072 (20°C) than for 71569 (< 10°C). Microprobe analysis

Table 2. Titaniferous basalt experiments

TITANIFEROUS BASALT EXPERIMENTS

Run #	T°C	Hours	Products
[75035,61 rock powder starting material]			
035-13	1156	12	glass
034-4	1146	95	glass
035-12	1142	18	glass
035-6	1138	68.5	glass + ilm
035-11	1137	92	glass + ilm + plag + hiCapx
035-10	1127	73	glass + ilm + plag + hiCapx
035-9	1119	73	glass + ilm + plag + hiCapx
[71569,21 rock powder starting material]			
569-3	1192	34.5	glass
569-11	1156	12	glass + ol + armal + Crsp
569-2	1146	95	glass + ol + armal + Crsp
569-10	1142	18	glass + ol + hiCapx + armal + ilm
569-4	1138	68.5	glass + ol + hiCapx + ilm + plag
569-9	1137	92	glass + ol + hiCapx + loCapx + ilm + plag
569-8	1127	73	glass + hiCapx + loCapx + ilm + plag
569-7	1119	73	glass + hiCapx + loCapx + ilm + plag
[10072,23 rock powder starting material]			
172-2	1195	34.5	glass
172-11	1159	12	glass + ol + armal + ilm
172-1	1149	95	glass + ol + ilm
172-10	1145	18	glass + ol + loCapx + ilm
172-9	1140	92	glass + loCapx + ilm
172-7	1130	73	glass + loCapx + hiCapx + ilm
172-6	1122	73	glass + loCapx + hiCapx + ilm + plag

All above experiments in high purity iron capsules within evacuated silica glass tubes.

ALKALI ADDITION EXPERIMENTS ON 70215

P kb	Run #	T°C	Capsule	Hours	Starting Material	Products
*	215-48	1125	Mo	7	70215 rock powder + 4.7% Na_2O by weight as $NaHCO_3$	glass + Fa_{33} + Ilm_{68}(A.33; C.48)
*	215-49	1072	Mo	18.5	70215 rock powder + 2.3% Na_2O by weight as $NaHCO_3$	glass + Fa_{45} + Cpx(Wo45, En37; T3.3; A3.5; C.53) + Ilm_{83}(A.35, C.52) + An_{46}
*	215-50	1094	Mo	19.5	product of 215-49	glass(Table 1) + Fa_{40} + Cpx(Wo47, En36; T3.4; A3.8; C.38) + Ilm_{80}(A.33; C.48) + An_{52}
*	215-51	1110	Mo	6.3	product of 215-50	glass(Table 1) + Fa_{39} + Cpx(Wo46, En37; T3.4; A4.0, C.31) + Ilm_{77}(A.40; C.54) + An_{54}
*	215-52	1121	Mo	20	product of 215-51	glass(Table 1) + Fa_{36} + Cpx(Wo47, En37; T3.1; A3.7; C.41) + Ilm_{74}(A.49; C.89) + An_{71}

* All experiments performed ...

Move this up from next page?

74220,37 EXPERIMENTS*

P kb	Run #	T°C	Capsule	Hours	Products
0	OG-32	1398	Fe	4	glass
0	OG-31	1302	Fe	10.7	glass + Fa_{23}
0	OG-34	1251	Fe	10	glass + Fa_{25}
0	OG-27	1195	Fe	34.5	glass + Fa_{28} + Crsp
0	OG-39	1159	Fe	12	glass + Fa_{31} + Ilm_{73}(A.59; C2.7) + Fpb_{27}(A2.0; C2.2)
0	OG-23	1149	Fe	95	glass + Fa_{33} + Ilm_{73}(A.64;C2.6) + Crsp
0	OG-38	1145	Fe	18	glass + Fa_{33} + Ilm_{73}(A.54;C1.3)
0	OG-37	1140	Fe	92	glass + Fa_{33} + Ilm_{73}(A.79,C2.5) (+Crsp)
0	OG-36**	1130	Fe	73	glass + Fa_{34} + Cpx(Wo_{10},En_{63};A1.1;C.58) + Ilm_{74}(A.49; C2.3)
0	OG-35**	1122	Fe	73	(glass) + ol + cpx + ilm + plag
0	OG-41**	1136	Fe	16	[orange soil starting material seeded for plag with the product of Run #OG-40] glass + ol + px + ilm
0	OG-40**	1123/ 1130	Fe	68/ 23	[grow plag like OG-35, then try to melt it out] glass + Fa_{37} + Cpx(Wo_{12},En_{59};A1.7;C.58) + An_{96} + Ilm_{76}(A.53;C2.2)
5	OG-8	1395	Mo	2	glass
5	OG-6	1385	Mo	2	glass + Fa_{20}
5	OG-5	1375	Mo	2	glass + Fa_{19}
5	OG-4	1325	Mo	2	glass + Fa_{22}
5	OG-3	1300	Mo	2	glass + Fa_{24}
5	OG-2	1275	Mo	2	glass + Fa_{27}
5	OG-1	1250	Mo	2.1	glass + Fa_{27} (+ Crsp)
10	OG-7	1400	Mo	2	glass + qpx
10	OG-9	1390	Mo	2	glass + Fa_{21} + qpx
10	OG-22	1275	Mo	2.2	glass + Fa_{28} + Opx(Wo_5,En_{71};T1.5;A3.4) + qpx
10	OG-25	1250	Mo	2	glass + Fa_{26} + Cpx(Wo_{13},En_{63};T1.4;A2.6) + qpx
15	OG-12	1430	Mo	2	glass + qpx
15	OG-11,20	1420	Mo	2	glass + Fa_{22} + qpx
15	OG-10	1400	Mo	2.2	glass + Fa_{25} + qpx
20	OG-13	1450	Mo	2	glass + qpx
20	OG-14	1440	Mo	2	glass + qpx
20	OG-15	1430	Mo	2	glass + qpx
20	OG-16,19	1420	Mo	2	glass + qpx
20	OG-18	1410	Mo	2	glass + Fa_{25} + opx(Table 1) + qpx
20	OG-17	1400	Mo	2	glass + Fa_{28} + px + qpx
25	OG-21	1450	Mo	2	glass + qpx
25	OG-26	1437	Mo	2	glass + opx + qpx
25	OG-24	1425	Mo	2	glass + opx(Wo_6,En_{75};T1.4;A3.9) + qpx

* All experiments performed in a mixture of H_2 and CO_2 (log H_2/CO_2 = 0·25) at 1 atm total pressure which had a pO_2 slightly more reducing than the Fe/FeO equilibrium. Estimated pO_2 ranged from $10^{-13.0}$ to $10^{-13.6}$ over the temperature range of these experiments.

† Equilibrium plag. entry between 1130 and 1136. Note glassy starting material for OG-36 failed to nucleate plag during heating or even after 3 days at temperature.

‡ Natural orange soil ground to uniform powder used as starting material unless specified otherwise.

Note: Crsp = chrome spinel; qpx = quench crystals, mostly pyroxene; armal = armalcolite; hiCapx, loCapx = high and low calcium pyroxene. Subscripts to Fa_{xx}, Fpb_{xx}, and Ilm_{xx} are (Fe/Fe + Mg) × 100 compositions for olivine, armalcolite, and ilmenite.

A, C, T are wt% Al_2O_3, Cr_2O_3, and TiO_2 numbers.

of residual liquids from these experiments conform to the saturation curves constructed in the earlier companion paper (LONGHI *et al.*, 1974).

Orange soil 74220

Experimental work up to 25 kbar has been performed on a sample of orange soil 74220,37. The composition of this starting material in Table 1 differs slightly from that of 74220,3 (LSPET, 1973) which was discussed in the text and shown in Figs. 1–4. Sample 74220,3 would be capable of yielding the low-K major element cotectic chemistry by equilibrium crystallization of olivine. On the other hand, our sample 74220,37 crystallizes pyroxene slightly before plagioclase in mild vacuum. Olivine crystallization yields

residual liquids similar to the strongly fractionated representatives of the low-K suite, or liquids transitional to the high-K suite, but not like the parental low-K compositions.

Small compositional dispersions in the neighborhood of 74220 may possibly produce parents to both high and low-K type major element chemistry. (It should be noted that this dispersion cannot be introduced by olivine fractionation.) There is evidence that this composition existed at the surface of the Moon as a liquid. (It should, however, be noted that the liquid was not superheated since olivine phenocrysts are present.) This glass composition has a wide lunar distribution.

Given these circumstances, one cannot ignore the possibility that one is dealing with a primary liquid composition. This possibility has been recognized by GREEN *et al.* (1974), who have reported crystallization experiments on synthetic orange soil. We confirm the results of those experiments here and agree that the orange soil makes a better point of departure for chemical and mineralogical exploration of the deep lunar interior than does the Apollo 11 'model basalt' or other representatives of the titaniferous basalts. Assuming the primary nature of 74220, the experiments show olivine and orthopyroxene simultaneously on the liquidus at 20 kbar. This corresponds to a depth to the supposed olivine–pyroxene source region in excess of 400 km. Figure 6 indicates the migration of the olivine–pyroxene cosaturation boundary across this composition space as a function of pressure. It is the strongly olivine normative character of 74220 which dictates such a deep source region.

Increasing degrees of melting of the olivine–pyroxene source region at depth will produce compositional dispersion of the liquids. Subsequent low-pressure fractional crystallization of olivine in the different batches could produce liquids which crystallize pyroxene and plagioclase in either order. In general, the batch produced by the greater degrees of melting at high pressure will have pyroxene crystallize before plagioclase at low pressure. This property of crystallizing pyroxene before plagioclase characterizes the high-K suite and so if it comes from depth it might be expected to be the result of a greater degree of partial melting than the low-K suite on the basis of its major element chemistry. The trace element chemistry suggests the relationship is the reverse. This discrepancy can be removed by dropping the assumption that the two suites originate at the same depth. The model discussed in the text derives the high-K suite from a shallower source with a smaller degree of partial melting. The resolution of *this* problem does not dictate that the different depths both be at relatively modest depths, as was proposed in the text on other grounds.

If 74220 is a suitable parent for one suite, the parent to the other suite is not obvious. It clearly cannot be parental to both suites. If 74220 can produce titaniferous basalt by fractional crystallization, it is not clear why there are no intermediate differentiates. This contrasts with the continuous compositional variation produced by fractional crystallization within the low-K suite of titaniferous basalts. Furthermore, such a proposition is contradicted by the Rb, Sr, Zn, and Cl anomalies noted by LSPET (1973).

Alkalies?

We have investigated the effect of alkali addition on the location of the saturation curves with results discussed in the text. Sample 70215 was used as a starting material to which Na_2O was added as $NaHCO_3$. Experiments were conducted at 1 atm in Mo capsules in a gas mixing furnace (H_2/CO_2) to regulate pO_2. Results of microprobe analyses of the residual glass are in Fig. 6 and Table 1.

Walker

NASA 133(II)

Proc. Lunar Sci. Conf. 6th (1975), p. 000–000.
Printed in the United States of America

Differentiation of a very thick magma body and implications for the source regions of mare basalts

DAVID WALKER, JOHN LONGHI, and JAMES FRED HAYS

Center for Earth and Planetary Physics, Hoffman Laboratory, Harvard University, Cambridge, Mass. 02138

Abstract—Mass-balance calculations indicate that the molten layer originally covering the moon may have been several hundred kilometers deep. The solidification of this magma ocean involved some unusual effects resulting from the large-pressure differential in the thick magma layer. The sunken cumulates from this differentiation would be more iron-rich, less refractory, and would contain more incompatible elements than would be expected in simple isobaric fractional crystallization and crystal sinking models of magma differentiation. These lower cumulates can have the mineralogical and chemical properties of the source regions of the low-Ti mare basalts.

INTRODUCTION

SEVERAL LINES of geochemical and geophysical evidence suggest that wholesale melting of the outer portions of the moon occurred very early in its history, perhaps due to accretional heating. The basaltic samples returned from the lunar missions may be partial melts of source regions which were differentiated during the solidification of that large magma ocean. It is the purpose of this paper to try to estimate the size of this melted zone, to examine its mode of differentiation, and to see if the postulated differentiation products can have the properties of the source regions of lunar basalts.

MAGMA BODY SIZE

Evidence for a global melting event early in lunar history will not be reviewed in detail here but has been deduced from petrologic, trace-element, geophysical, and isotopic considerations. Early identification of this event was made by Wood *et al.* (1970) and Smith *et al.* (1970) on the basis of the complementary nature of mare basalts and anorthositic particles found in the soil at the Apollo 11 landing site. The feldspathic particles were presumed to be characteristic of lunar crustal material exposed in the highlands. The complementary nature of the basalts and crustal materials was further indicated by respective negative and positive europium anomalies documented by many including Philpotts and Schnetzler (1970) and Wakita and Schmitt (1970). Seismic, gravity, and rheological considerations indicated that the lunar crust was not of trivial thickness and must have been produced early to support mascons. Rb–Sr systematics of lunar rocks and soils and widespread occurrence of ancient Rb–Sr model ages suggested that the event responsible for this state of affairs occurred very near to the formation of the

moon at ~4.6 Gy. (Papanastassiou and Wasserburg, 1971). These early deductions have been reinforced by later studies.

The size and initial composition of the magma body are open questions at present. Estimates of the initial composition of the magma body or, alternatively, assuming homogeneous accretion, the bulk composition of the moon have been made by several authors: (1) Anderson (1973), (2) Ganapathy and Anders (1974), (3) Ringwood and Essence (1970), (4) Taylor and Jakeš (1974), and (5) Wänke *et al.* (1974). None of these suggested compositions appears to be capable of satisfying all geochemical, petrologic, and geophysical constraints but some models appear to be much better candidates than others. There is no obvious way to make model (1) consistent with experimental petrology constraints on the source regions of mare basalts. Model (5) is too low in silica to allow much pyroxene in the source regions of mare basalts. Model (3) may satisfy some gross geophysical constraints on the properties of the moon, but it would be difficult to produce the lunar crust by differentiation of this composition. On the other hand, models (2) and (4) appear to be able to generate rocks of the lunar crust by fractional crystallization and give a plausible constitution for the lunar interior. Hodges and Kushiro (1974) have investigated the phase relations of model (2) as a function of temperature and pressure and reached the conclusion that it could give a generally satisfactory account of lunar petrogenesis and lunar geophysical properties with the following exceptions. The Fe/Mg ratio of lunar crustal rocks was higher than might be expected from model (2) and fractional crystallization of model (2) did not produce troctolite as a rock type. Both these difficulties can be overcome by recalculating slightly more of the total Fe in model (2) as oxidized Fe rather than metal. If model (2) is oxidized it is very similar in major-element composition to model (4) except for its lower silica content. This modified model would precipitate spinel during fractional crystallization at low pressure, leading to Cr depletion of the residual liquid. Since as much as 3% of the crystallization product can be spinel without producing marked Cr depletion (Walker *et al.*, 1975a,b) and since the existence of spinel troctolites requires that there have been some spinel accumulation, a successful model will precipitate only a minor amount of spinel during differentiation. Minor oxidation of model (2) or a slight decrease in silica in model (4) would be an acceptable solution. Therefore we have chosen bulk compositions for the large magma system (or for the moon assuming homogeneous accretion) intermediate between the model of Ganapathy and Anders (1974) and Taylor and Jakeš (1974). (SiO_2, 43; Al_2O_3, 8.2; FeO, 10.5; MgO, 31; CaO, 7.0.)

These magma bulk compositions are shown on Fig. 1. Oxygen units are used to facilitate volume estimates. Also shown is an estimated average composition for the lunar crust deduced from a compilation of published surveys of lunar feldspathic rocks (Walker *et al.*, 1973). This composition is roughly equivalent to "anorthositic norite." Clearly for the case where the anorthositic-norite crust is a differentiate of the large magma there must be a considerable volume of complementary material stored somewhere in the system to preserve mass balance. The central problem is to deduce the character and volume of this missing material.

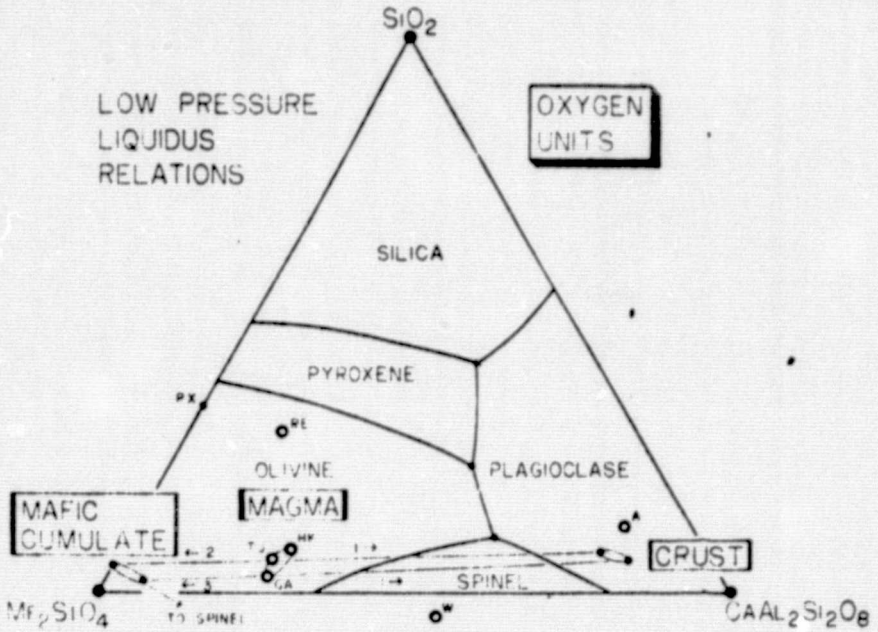

Fig. 1. Estimates of lunar bulk composition are indicated by open symbols. A is from Anderson (1973); GA is from Ganapathy and Anders (1974) calculated with all Fe oxidized; HK is from Hodges and Kushiro (1974) and is based on GA with only part of the Fe oxidized; RE is from Ringwood and Essene (1970); TJ is from Taylor and Jakeš (1974); W is from Wänke *et al.* (1974). Compositions which satisfy petrological and chemical constraints on the lunar bulk composition should lie nearly on a line between Mf_2SiO_4 (Mf = MgO + FeO) and the peritectic involving spinel, olivine, anorthite, and liquid (Walker *et al.*, 1973, 1975a,b). The successful model compositions are labeled MAGMA. The compositions labeled CRUST correspond to anorthositic norite. MAFIC CUMULATE indicates the nature of the material complementary to the crust formed in differentiation of MAGMA. The diagram is plotted in oxygen units to facilitate estimates of the relative volumes of CRUST and MAFIC CUMULATE as indicated on the lines connecting them since oxygen comprises most of the volume of the materials. Oxygen units are calculated by weighting the component formulae by the number of oxygens they contain.

Also shown in Fig. 1 is a set of low-pressure liquidus phase relations which can serve as a rough guide to crystallization behavior (Walker *et al.*, 1973) although the excess high-calcium pyroxene component (Ca : Al > 0.5) is not considered. Crystallization at the upper surface of the magma where heat loss occurs should be controlled by these liquidus boundaries. Olivine should crystallize first (somewhat above 1400°C) followed by co-precipitation of spinel until plagioclase crystallizes at ~ 1275°C. Olivine and plagioclase precipitate until ~ 1225°C when low-calcium pyroxene joins the crystallization. The lunar feldspathic crust is presumably the non-sinking fraction of crystalline material so produced. Differential plagioclase accumulation is responsible for the relative buoyancy of the crust as well as the major component of chemical variation in the crustal rocks. To explain Fe/Fe +

Mg variation in the crustal rocks we need only note that plagioclase fractionation is accompanied by olivine and pyroxene fractionation which can change Fe/Fe + Mg of the evolving liquids. Clearly this ferromagnesian material is not all preserved in the crust and must exist as a complementary cumulate at depth beneath the crust. The volume of this complementary cumulate can be estimated from the bulk composition of the system and the seismically determined volume of the anorthositic-norite crust.

Fig. 1 illustrates how this estimate can be made. It is assumed here that the mafic cumulate is olivine and pyroxene, that it is devoid of plagioclase, and that it has no more than 3% spinel. It is also assumed that the bulk composition is differentiated only into feldspathic crust and complementary mafic cumulate. The residual liquids of the system are lumped with the mafic cumulate for the present. The complementary cumulate must then represent at least $\frac{3}{4}$ or $\frac{4}{5}$ of the material of the whole magma system estimated from the volume proportions shown in Fig. 1. If the complementary mafic cumulate contains plagioclase or other aluminous phases then it will represent even more of the total differentiate. Likewise, since there appears to be little excess high-calcium pyroxene in the anorthositic-norite bulk composition for the crust, the excess high-calcium pyroxene in the bulk composition of the magma system must be incorporated in the complementary mafic cumulate. This consideration would also tend to increase the estimated proportion of material represented in the complementary cumulate. Seismic experiments have been interpreted to show that the lunar crust is about 60 km thick on the moon's nearside (Toksöz *et al.*, 1974). The amount of shattered feldspathic crustal material versus mare basalt in the upper 20 km is uncertain and undoubtedly highly variable. For 60 km of anorthositic norite the whole system must extend to a depth of 200–275 km depending on whether the crust is $\frac{3}{4}$ or $\frac{4}{5}$ of the system. The 200-km figure agrees with the estimate of Hodges and Kushiro (1974) who also noted that this must be a minimum thickness for the whole system.

Wood (1973) has noted that many aspects of lunar asymmetry may be caused by a greater thickness of crust on the moon's farside. If we change the crustal thickness estimate to 100 km, the whole system could be as much as 500 km thick. The presence of plagioclase or other aluminous phases (other than the 3% spinel) and the inclusion of the excess high-calcium pyroxene below the crust will further increase this estimate.

This estimate involves melting of roughly half the volume of the moon. If accretion of cold material is the heating agency to cause the melting, then the magma ocean cannot be very much thicker than this estimate. The total gravitational energy released in accreting the moon is 400 cal/g, which is about sufficient to heat and melt the whole moon, but the accretion process will release heat in a manner dependent on the square of the radius of the growing planet, so the 400 cal/g is not distributed uniformly. Potential energy converted to heat, even with complete efficiency, will be sufficient to melt (and later superheat) subsequent infall only when the moon has reached $\frac{3}{4}$ of its present radius. Appreciable kinetic energy of accreting particles or accretion of hot particles could increase

the depth of the melted zone. Rapid accretion is necessary to prevent escape of the released heat. Mizutani *et al.* (1972) have considered the process of accretion and its implication for lunar thermal history in some detail. They conclude that a satisfactory account of the moon's thermal properties can be given by an accretion model which assembles cold material in about 10^2 yr. The depth of the molten layer is about 400 km, which is compatible with possible estimates of the magma thickness based on chemical and mass-balance arguments above. We must now inquire how such a thick magma will solidify and what will be the character of the differentiation products.

What Rocks are at 200–300 km in the Moon?

Studies of the melting behavior of low-Ti, olivine-rich, mare basalts suggest that they would be in equilibrium with an olivine and low-calcium pyroxene residue at a depth of 200–300 km in the moon (Green *et al.*, 1971; Grove *et al.*, 1973; Kesson, 1974; Longhi *et al.*, 1975; Walker *et al.*, 1975). We have already noted that the complementary mafic cumulate should be composed of those minerals and could easily extend to this depth. An important question in lunar petrogenesis is whether the low-Ti mare basalt source region lies within the complementary mafic cumulates or in undifferentiated material. The former possibility has been considered unlikely by Ringwood (1975) on the grounds that Fe/Fe + Mg and incompatible element abundances attributed to the complementary mafic cumulate are too low to be consistent with the properties of the low-Ti mare basalt source region. For instance, the bulk Fe/Fe + Mg of the model composition we are considering is 0.16; the first olivines to precipitate would have a Fe/Fe + Mg of about 0.06 whereas the source region for the low-Ti basalts must have a Fe/Fe + Mg of 0.24–0.29. The crystallization of the magma at the top of the system where heat loss occurs would precipitate ferromagnesian minerals which sink to form the cumulate. Hodges and Kushiro (1974) quantitatively pursued this approach for a 200-km magma and concluded that about half the system would be composed of dunites and harzburgites. These materials would indeed make poor-mare basalt source regions because of their low Fe/Fe + Mg, low-incompatible element abundance, and refractory nature. This is especially true for a perfect fractionation or totally efficient differentiation model. The very size of the system dictates relatively slow heat loss and hence would promote efficient differentiation by crystal settling. However, for a magma of 400-km depth the very large size also introduces effects which *reduce* the efficiency of the differentiation process. We will now consider these effects.

Effects of Magma Size on Differentiation in the General Case

The principal agent which introduces unusual effects into the differentiation of a very large-magma body is the large-pressure difference between top and bottom (~20 kbar for 400 km on the moon). This pressure differential will change the

crystallization behavior of the magma with depth so that different minerals may crystallize. It will also increase the melting temperature with depth at a rate such that the melting temperature gradient is steeper than an adiabatic temperature gradient. Figure 2 shows a compilation of liquidus curves of various lunar materials which have olivine as the low-pressure liquidus phase. Materials with more normative olivine have higher liquidus temperatures and the change from liquidus olivine to liquidus pyroxene occurs at higher pressure. The temperature

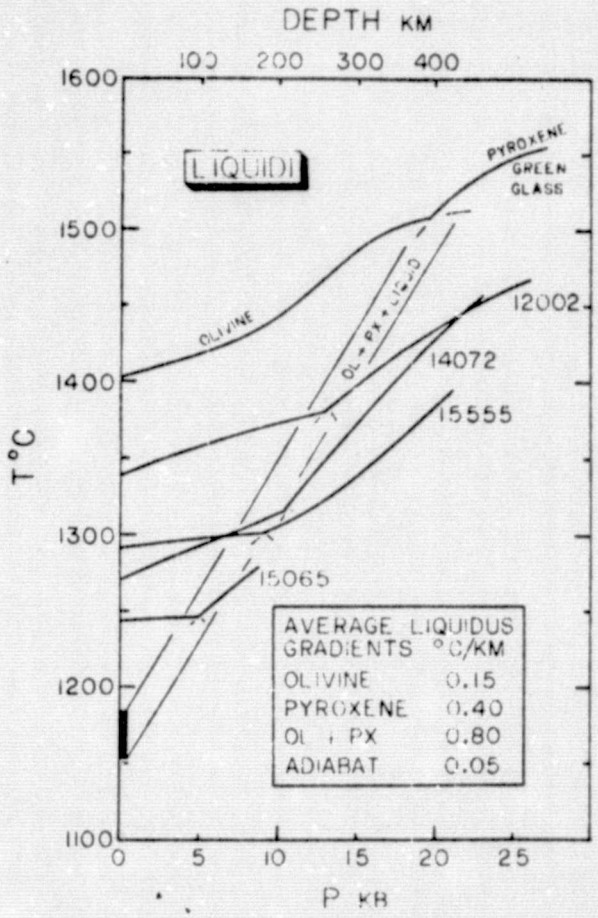

Fig. 2. Liquidus curves as a function of temperature and pressure are plotted for lunar materials having olivine on the liquidus at low pressure (from Longhi *et al.*, 1975; Stolper, 1974; Walker *et al.*, 1972, 1975a,b). The materials with higher temperature liquidus curves have more normative olivine. Note that there is a regular increase of the temperature of pyroxene–olivine co-saturation with increasing pressure. Olivine–pyroxene co-saturated liquids are also increasingly olivine-normative with increasing pressure. Average saturation gradients are indicated. 14072, the most noticeably deviant composition, is distinctly more aluminous than the other compositions. These regularities can be used to roughly extrapolate the liquidus of a composition having olivine as the low-pressure liquidus phase if the low-pressure liquidus temperature is known.

gradient of a magma in liquidus equilibrium with olivine would be ~0.15°C/km; with pyroxene it would be ~0.4°C/km. If a magma were saturated with both olivine and pyroxene throughout its vertical extent the temperature gradient would be ~0.8°C/km. Note that this situation would be accompanied by an appreciable compositional gradient in the liquid since the olivine + pyroxene liquidus boundary curve shifts to more olivine-normative compositions with increasing pressure.

The large-magma system may be expected to crust at the top where rapid heat loss occurs. Growth of the crust by heat loss through it will precipitate olivine, plagioclase, and pyroxene. We have noted above that much of the ferromagnesian material was not retained in the crust but sank due to its high density. Olivine which sinks from the bottom of the solid crust (at ~1200°C) will undergo compression while sinking. An adiabatic temperature rise of about 20°C would be experienced in sinking 400 km. However, the actual temperature rise in the magma must be considerably more than this just for it to be in the liquid state. Furthermore, as we will discuss later, the accretion-produced thermal profile would have a considerable body of superheated magma at depth. Clearly the sinking olivine will not be in thermal equilibrium with the liquid. The olivines will dissolve until the superheated magma is cooled to its liquidus temperature by supplying the heat of fusion. Note also that this process introduced a compositional gradient in the liquid. The magma will have a higher liquidus temperature and become more olivine normative with depth as olivine dissolves. When magma at one depth is cooled to its liquidus temperature, olivine will no longer dissolve but can sink to saturate a deeper level by dissolution there. However, in sinking through the saturated level the cooler olivine must induce extra crystallization of the magma as it approaches thermal equilibrium. Crystal sinking in a large magma may be considered a negative mode of heat transfer which induces crystallization at depth even though heat is lost at the top of the system.

Continued crystal sinking will bring the magma at depth to co-saturation with olivine and pyroxene with a corresponding compositional gradient with depth. The temperature gradient for this situation is seen in Fig. 2 to be ~0.8°C/km. The ability of the system to reach this gradient, rather than "choking" and solidifying at some intermediate depth, depends on the original amount of superheat with depth, the rate of heat loss at the top, and the rate of crystal settling. Rapid crystal addition and small superheat will prevent this gradient from being established over large ranges of depth. To give a feeling of the possible magnitude of the effect for the case where such a situation is reached, we may calculate the amount of heat necessary to bring an olivine sinking from the crust into equilibrium with the magma as it sinks to the bottom of the system. This heat must be supplied by crystallization of the saturated magma through which the cold crystal sinks. In sinking 400 km the olivine experiences a temperature rise of 20°C due to adiabatic compression. At 400-km depth the magma is 300°C (400 × 0.8 − 20) hotter than the olivine. Using representative heat capacity data from Robie and Waldbaum (1968) for olivine, about 14 kcal/gfw is necessary to raise the olivine to the magma temperature. For a heat of fusion of olivine of ~22 kcal/gfw about half as much

olivine as sank into the magma would be required to crystallize in order to keep the olivine in thermal equilibrium with the magma. (These heat capacity values are uncorrected for pressure but serve to give a rough idea of the order of magnitude of the process.) This extra crystallization would, of course, not all take place at 400 km but would happen continuously during sinking.

The pressure gradient also may change the nature of the crystallizing phases with depth. For the case we have just discussed, the composition gradient with depth probably will keep olivine as the liquidus phase with depth. However, if there is appreciable mechanical stirring (e.g. from impacts) or convective stirring (to be considered later) and the compositional gradient is suppressed, the sinking olivine may in some cases become unstable with respect to pyroxene. Should the sinking olivine armor itself with a reaction product of pyroxene, the lesser heat of fusion of pyroxene (15–18 kcal/gfw) would require that a larger number of moles of pyroxene precipitate than was the case of precipitation of olivine to heat the cold sinking olivine. The number of moles of precipitated pyroxene must be comparable to the number of moles of sinking olivine rather than the previous estimate of about half as much for the simple olivine case if olivine precipitation alone is to supply the heat. At depth the reaction relation between olivine, pyroxene, and the liquid becomes a co-precipitation relationship if the liquid composition is allowed to adjust itself according to the pressure constraints. Therefore a combination of olivine and pyroxene precipitation would supply the necessary heat to warm the sinking olivine. In this case the sinking crystal would induce extra crystallization of the liquid by an amount from about a half to a whole of itself, depending on the proportions of olivine and pyroxene precipitated. This is to say that $\frac{1}{3}$ to $\frac{1}{2}$ of the crystal accumulate is material precipitated at depth even though all the heat loss leading to this crystallization occurred at the top of the system.

The result of this process of heat transfer by crystal sinking is not only to accelerate crystallization at the bottom of the system but also to affect the constitution of the cumulate produced. Simple efficient differentiation models not considering this effect give sunken cumulates of dunite then harzburgite which have very high Mg/Mg + Fe at the bottom. The model presented here favors harzburgites over dunites although dunites are still possible. The cumulate will be less refractory as a result of the introduction of pyroxene. Furthermore, the Fe/Fe + Mg of the cumulates will be higher at the bottom of the system. This effect is illustrated schematically in Fig. 3. The upper part of the figure indicates schematic liquid–solid "loops" for phases entertaining Fe–Mg solid solution. At lower pressure (P_a) the solidification curves are at lower temperature (T) than at high pressure (P_{-a}). The lower part of the figure indicates the variation of Fe–Mg in cumulates produced in two different situations. The solid curve is for fractional crystallization at a constant pressure (P_{-a}). The initial phase crystallizing and sinking to the bottom to form the basal layer of the cumulate has a composition appropriate to the liquidus phase for the bulk composition (open symbol) at low pressure. Subsequent fractional crystallization produces extreme iron enrichment. The dashed curve indicates the variation in the resulting cumulate if there is

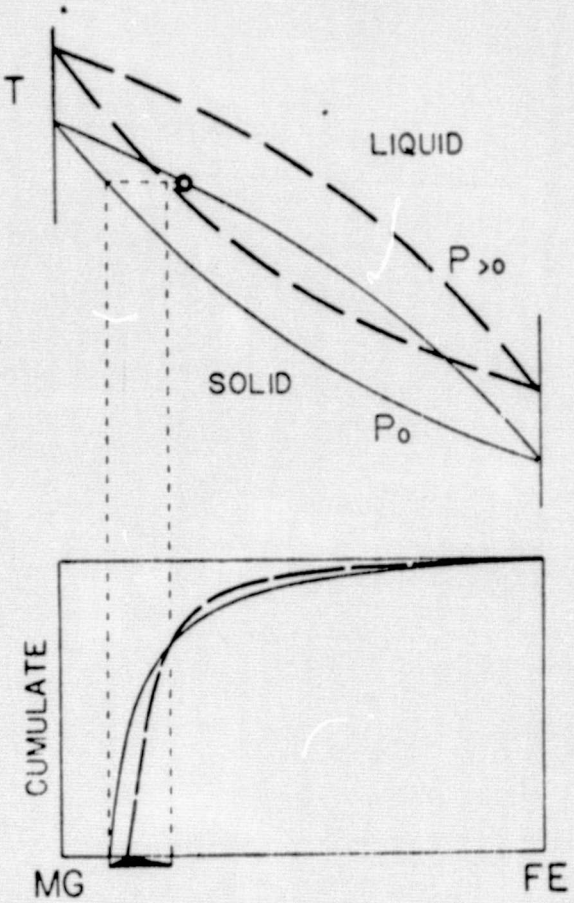

Fig. 3. Schematic illustration of the effect of pressure on the distribution of Fe and Mg in the cumulates produced during differentiation of a large-magma system. See text for discussion.

a substantial pressure gradient between the top and bottom of the melt. Crystals sinking at the top of the system have the liquidus composition as in the first case. However, at deeper levels the shift of the "loop" indicates that the sinking phase becomes more iron-rich as a consequence of the greater degree of crystallization. This is a schematic representation, since the sinking will not be isothermal, but it serves to illustrate that the extra crystallization induced during sinking drives up the Fe/Fe + Mg of the crystalline fraction of sinking material. The composition of the basal cumulate layer will be intermediate between the two vertical dashed lines. The exact composition depends on the degree of Fe exchange with the melt during sinking, the heat capacity, and heat of fusion of the phase. This basal layer will always be more iron-rich than in the first case. As the magma fills up with its settling products the pressure gradient and settling distance decrease, so the "loops" at later stages in the differentiation merge with the P_0 "loop." Extreme

iron-enrichment occurs at the end of the sequence but a smaller volume of iron-rich material is produced since more iron was incorporated in the early cumulate. The solid and dashed curves are shown intersecting at an Fe/Fe + Mg value corresponding to the right vertical dashed line. This situation is possible but need not be the case in general. The composition and depth of this intersection is not uniquely specified by the position of the "loop."

It should be noted this increase in Fe/Fe + Mg of the basal cumulate occurs whether the material transfer is by convection (adiabatic) or crystal sinking (not adiabatic). Either way the increased degree of crystallization induced during sinking increases the Fe/Fe + Mg of the crystalline material deposited at the bottom of the system. The FeO component of the residual liquid is more uniformly distributed in the system than during efficient differentiation.

It is doubtful that the mode of solidification discussed above would ever operate fully for reasons to be discussed below. However, the discussion does show that simple crystal settling models of differentiation are quite inadequate to describe a 400-km magma body and may give incorrect insights into the constitution of the differentiation products. A further factor to be considered is that the increase in the liquidus temperature of the system with pressure is considerably greater (factor of 3–8) than the adiabatic temperature gradient (about 0.05°C/km in the lunar case). The adiabatic gradient should approximate the temperature distribution in a convecting liquid. If our magma system convects then it should solidify chiefly from the bottom up since the adiabat will intersect the steeper liquidus at the bottom of the system first (Fig. 4). This mode of solidification will also subvert the efficiency of differentiation since the opportunity for crystal–liquid separation by crystal settling is diminished when the crystals form at the bottom of the system. The basal members of the solidification product would probably be harzburgite or lherzolite (with garnet or spinel). A complication to be noted is that the model moon composition has an appreciable melting interval so that crystals may precipitate over quite a distance in the column and settle before the bottom is solidified fully. Another complication, to be developed later, involves likely initial temperature distributions which may be gravitationally stable over large parts of the magma. However, neglecting these special initial situations, the magma, when cooled at the top, becomes exceedingly unstable with respect to convection. In the presence of a superadiabatic temperature gradient convection will occur in any magma body deeper than about 10 m for reasonable values of viscosity, thermal expansion, and diffusivity. The Rayleigh number for a 400-km magma with an adiabatic gradient is about 10^{22}. The size outweighs all the other factors. It is clear then that convection should be an important part of any analysis of magma differentiation on this scale. If solidification from the bottom upwards were the only process operating, however, the existence of a thick lunar crust containing material of low Fe/Fe + Mg would be unaccounted for.

It should be noted that once a material becomes partly crystalline it is rather effectively "buffered" against normal convective cycling on an adiabat. Should a parcel of magma with suspended crystals begin to rise, melting of the crystals begins which cools the parcel as the heat of fusion is supplied. The temperature is

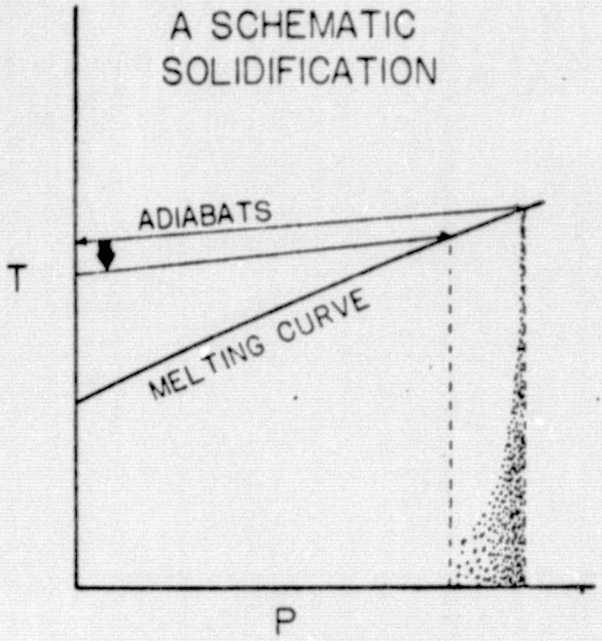

Fig. 4. The effect of having melting curves steeper than adiabats is to induce crystallization at the bottom of the system and during sinking. This effect has been discussed in some detail by Irvine (1970). Ascending convective magma cools at the top of the system and descends, intersecting the melting curve at depth. In actual magma differentiation this effect is complicated by the presence of a melting interval with generally more than one crystallization curve.

buffered on the melting curve which makes the parcel cooler than its surroundings since the melting curve is steeper than the adiabat. Parcels of magma which begin to sink experience extra crystallization. Heat of fusion is liberated, warming the parcel. In general the density contrast produced by melting or solidification is much greater than the density contrast produced by thermal expansion. Therefore sinking parcels continue to sink and rising parcels continue to rise even through they may be respectively warmer and colder than their surroundings. This is the reverse of the temperature relations for normal convective cycling in a homogeneous liquid which has an adiabatic temperature distribution.

We have now considered two "end-member" processes which introduce unusual effects into the solidification of large magmas. Both processes will operate in the solidification of a magma to spread the heat loss sustained through the top crust to the lower parts of the magma and accelerate solidification there. The net result is a reduction in the efficienciency of differentiation by fractional crystallization and crystal settling because crystallization will take place throughout the magma. We now consider a possible outcome of the solidification of the large lunar magma body for plausible initial conditions when these effects are taken into account.

DIFFERENTIATION OF THE LUNAR MAGMA OCEAN

To outline the solidification process of such a large-magma body we must know the phase relations of the material as well as the initial temperature distribution. The phase relations as a function of pressure are deduced in the following way. The solidus is taken from Hodges and Kushiro (1974). The solidus temperatures turn out to be rather insensitive to bulk composition since this solidus is similar to the one proposed by Ringwood and Essence (1970). The low-pressure liquidus temperature (olivine) is taken from putting the bulk FeO and MgO into Roeder and Emslie's (1970) olivine-saturation model. The high-pressure liquidus and olivine + pyroxene saturation curve can then be deduced by extrapolation of the trend shown in Fig. 2. The result is shown in Fig. 5. The principal heat source for the initial melting event is presumed to be accretion. The accretionary temperature profile shown in Fig. 5 is essentially that of Mizutani *et al.* (1972) but has been adjusted for the larger melting interval in the present model composition.

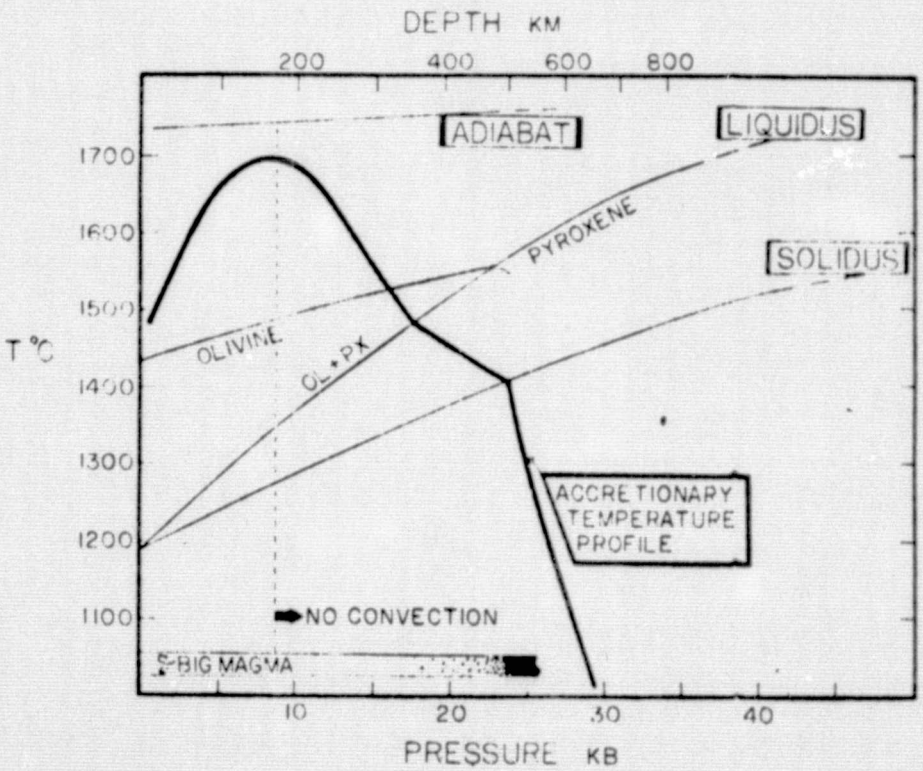

Fig. 5. Possible initial conditions for the primordial lunar magma ocean are illustrated as discussed in the text. Important features include melting to a substantial depth, a large amount of superheated magma, and a gravitationally stable zone deeper than the temperature maximum.

Inspection of the initial conditions postulated in Fig. 5 reveals several points of interest. The material is molten to a depth of ~400 km. (Accretion of hot material would make the molten layer thicker.) Subsequent material infalling after the melting temperature is reached will be superheated. A decline in the accretion rate at the end of the accretional process allows cooling of the surface layer. A maximum in temperature is induced in the system. The temperature profile at depths below the maximum is gravitationally stable and there would be no tendency for convective instabilities to develop. At depths shallower than the temperature maximum, the profile is exceedingly unstable with respect to convection indicating that this initial state of affairs must be very transitory. In actual fact as the rate of infall declines, the subsequent portion of accreting material will probably be falling into a convecting bath. This state of affairs or that which occurs very soon after the decay of the convectively unstable profile is illustrated by profile 1 in Fig. 6. A final feature to be noted in this differentiation

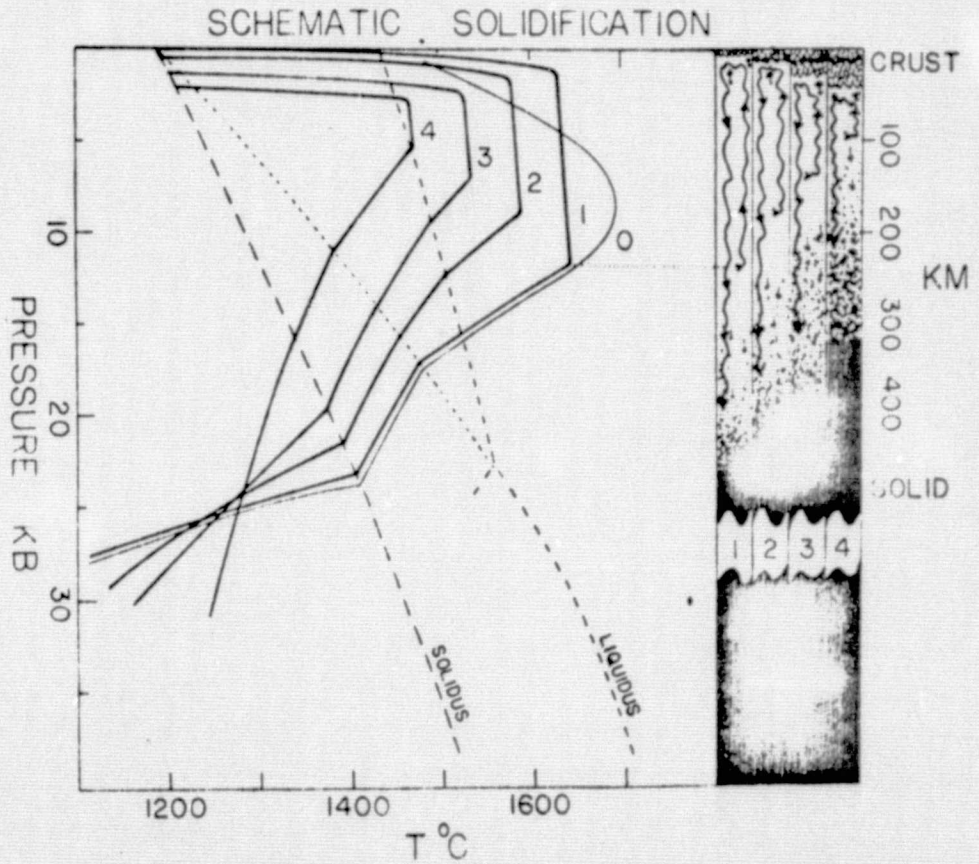

Fig. 6. Illustration of possible mode of solidification of the magma. Initial conditions in Fig. 5 are given by curve 0. Curves and cartoons 1, 2, 3, and 4 are for subsequent stages in the solidification. Temperature profiles are schematic. The gravitationally stable zone which traps residual liquids in the lower cumulates amplifies the normal tendency to trap residual liquids discussed in the text.

model is the presence of a crust at the top of the system. This is imposed as a boundary condition even though there is some tendency for the crust to be disrupted by the convecting layer underneath. This boundary condition is geologically reasonable since large terrestrial lava lakes develop frozen crusts in the presence of convection. Furthermore, the presence of high-Mg/Mg + Fe material in the present lunar crust is most easily explained in this manner (Taylor and Jakeš, 1974). The problem of crust formation is discussed further in a later section.

Material cooled and partially crystallized at the top of the system becomes dense enough to sink due both to thermal contraction and to the presence of suspended solids. It should be noted here that plagioclase (ρ = 2.7) should not sink and would probably float in the fractionated liquids from which plagioclase crystallizes (calculated ρ = 3.0 by the scheme of Bottinga and Weill, 1970). A further argument that plagioclase preferentially remains at the top to be incorporated in the crust is that if more than 15% of the sunken material is plagioclase then the mass-balance calculations presented earlier would require a body of magma larger than the whole moon be melted to extract the crust. The separation of plagioclase from the fractionated liquid and crystals which sink depletes Eu in this descending material.

As the cooled liquid and its mafic minerals begin to descend, further crystallization is induced since the melting curves (e.g. solidus) increase in temperature faster than the liquid adiabat. Even if there is no heat exchange with the surroundings, the sinking material undergoes extra crystallization during sinking. Therefore the actual temperature gradient followed by a descending convective body will be steeper than an adiabat due to release of heat of fusion. The gradient, however, will not exceed the crystallization curve the body follows. It should be noted that there was a "floor" for convective updrafts introduced by the top of the gravitationally stable regime (note dotted line in Fig. 6). This is not a "floor" for downdrafts since they are colder than the surroundings and contain suspended crystals. Sinking material will descend to the bottom of the melted zone. The extra crystallization induced during descent will make the solid material of higher Fe/Fe + Mg than at the beginning of the descent. When the material stops descending there is no incentive for any residual liquid remaining in the batch to rise again for another cycle of convective overturn and further differentiation since the material is now in the gravitionally stable regime. Any further separation of residual liquid occurs only by upward physical displacement of the liquid by denser settled crystals.

The thermal effects of such a cycle can be seen in the sequence of curves 1 through 4 on Fig. 6. Rising of material and cooling at the top of convective curve 1 will lower the maximum temperature of the system from 1 to 2. Sinking of the cool material displaces the remainder of the system upwards. The "floor" of convective updrafts moves up from 1 to 2. To the extent that the sinking material exchanges heat with its surroundings, the temperature slope of the gravitationally stable regime in 2 is less than in 1. The ceiling of the convective zone is lowered as the crust at the top grows. Heat loss out the cold bottom of the system induces

final solidification of sunken material and its trapped juices from the bottom up. Further stages of this process are illustrated by curves 3 and 4 in Fig. 6.

The geochemical novelties introduced in this differentiation scheme are that Fe/Fe + Mg of the sunken crystalline cumulate does not show as wide a variation on a large scale as might be expected during efficient fractionation and that residual liquids on the bottom are not convectively recycled for further enrichments but are trapped with the cumulates. (This material is of course depleted in Eu as a result of plagioclase separation which occurs at the top of the system before this material descends.) The first effect results from the extra crystallization introduced during sinking and operates independently of the second effect. The second effect is a result of the accretionary thermal profile. Inasmuch as this scheme of differentiation overcomes most of the geochemical objections (Ringwood, 1975) to regarding the mafic cumulates as the source material of low-Ti olivine-rich mare basalts, we may conclude that it is still possible to regard the cumulates as a reasonable source region on geochemical grounds.

Discussion

The solidification process outlined in the previous section indicates that the bulk of lower cumulate layers produced in a large-magma body are relatively undifferentiated. If the process operates fully the lower cumulates will differ from the bulk composition of the system only in having lost plagioclase (and Eu, etc.) to the crust. The Fe/Fe + Mg will be roughly the same as the bulk composition and the full complement of Eu-depleted residual liquid is successively incorporated in accumulating layers. This product contrasts with the very magnesian dunite which would be expected in a simple fractional crystallization and crystal sinking model where half the volume of the system crystallizes as magnesian olivine and sinks before plagioclase precipitation initiates crust formation. Instead of a barren, magnesian dunite, a harzburgite forms with some layers enriched in Eu-depleted residual liquid component providing a more attractive source region for low-Ti mare basalts during later remelting.

A more quantitative treatment of the process does not seem possible at this time. Details of the initial temperature distribution, the rates of crust formation and heat loss at the surface, the flow rates and patterns in the magma, and the degree to which chemical equilibration is achieved remain unknown. Further complications which require exact treatment for proper understanding are the effects of compositional gradients introduced by precipitating and dissolving material at intermediate depths. Two features of the model, however, seem to require further discussion. First, how are the trace-element enriched residual liquids produced and where are they to be found at the end of the solidification process? Second, what is the process of crust formation atop a convecting, superheated, magma body?

There is important circumstantial evidence that the trapping of residual liquid in the cumulate has not been complete and uniform. Titaniferous lunar basalts which have strong enrichments in incompatible elements (and Ti) appear to be

derived from source regions in the lunar interior at depths of ~100–150 km, perhaps from a series of ilmenite cumulates derived from late residual liquids (Walker *et al.*, 1975a,b). If this is the correct explanation for the source region of high-Ti basalts then there may have been some recycling of residual liquid during differentiation to achieve the observed trace-element enrichments. In the framework of the proposed differentiation model this could happen in several ways. Crystal sinking may to a certain extent physically displace residual liquid upward from the lower cumulates. Alternatively the solidification by heat loss through the bottom can have an effect analogous to zone refining. As the solidified zone advances upward through the lower cumulates, the incompatible elements may be driven upward if there is good intercumulus plumbing. Either way the Fe/Fe + Mg of the residual liquid is "buffered" by the crystalline phases of the cumulate while the degree of incompatible element enrichment increases. Finally it should be noted that as substantial degrees of solidification of the system are obtained, the pressure differential in the smaller volume of residual magma is less, so that the effects described here become less important. To the extent that the unusual size effects do not totally control the differentiation, the remaining magma fraction will differ from the original bulk composition and later cumulates may increase in Fe/Fe + Mg. Specifically, curve 4 in Fig. 6 probably does not correspond to a real situation because changes in the liquid will have been introduced which modify the phase relations and temperature profiles. The thick magma effects will be most effective in the early stages of differentiation.

The formation of a crust on a large body of superheated magma also requires further inspection. Existence of a crust was assumed as a boundary condition in the discussion above because the moon has a crust and its relatively high-Mg/Fe ratio is most easily explained if it is produced by freezing the top of the magma rather than by later differentiation from material beneath. For crustal formation to occur in this way it is necessary that ascending magma parcels lose enough heat at the top of the system to crystallize at least to the point of plagioclase precipitation. If the feldspar is free to physically separate from the cooled and partly crystallized material which then sinks, this feldspathic segregate becomes the crust. To the extent that feldspar *can* separate, the crustal material will be gravitationally stable against sinking (ρ for anorthositic norite ≈2.9 whereas ρ for the liquid ≈3.0). It remains to be shown that enough cooling of the superheated magma can occur at the top of the convective zone to allow partial crystallization and feldspar separation before the magma has substantially solidified from the bottom upward.

Details of the initiation of crust formation are not clear but may resemble the following. Initially the heat flux cooling the top of the superheated magma is radiation into space and has a magnitude 7 cal/cm^2 · sec for assumed "black-body" behavior. This flux is sufficient to cool and crystallize the magma at the rate of 10 m/day. This rate of crustal growth cannot be maintained after solidification of the top layer limits the heat transfer to the conductive mode. Furthermore this rate of crustal growth is too rapid to allow concentration of plagioclase in the crust by differential buoyancy. Therefore the rapidly frozen crust will sink if disrupted.

as it most certainly would be by continued accretionary bombardment from above and turbulence in the magma below. Crustal fragments would tend to dissolve rather quickly during sinking into the superheated magma beneath. Since the crust at this stage is undifferentiated "chill margin," this dissolution does not introduce compositional gradients but does serve to reduce the temperature of the magma at shallow depths beneath the rapidly reforming crust. As the rate of crust growth decreases during the change to conductive (rather than radiative) heat loss at the top and as the thermal gradient decreases at shallow depths in the magma, it becomes possible to separate plagioclase and olivine. Upward plagioclase concentration leads to the establishment of a crust which no longer sinks when disrupted. This insures that the slow conductive heat loss, conducive to plagioclase separation and further crustal growth, continues. The important feature of this proposed mode of crust formation is that the cooling power of radiative heat loss can be distributed to shallow depths by crustal resorption. A relatively slow-cooling regime which is then established directly beneath the "chill margin" allows olivine–plagioclase separation and formation of a non-sinking crust. This non-sinking crust is then stable against perturbations and grows by differential plagioclase retention from magma crystallizing slowly at its base by conductive heat loss. Ruptures in this crust should heal by a process like that leading to crustal formation when hot magma is again exposed to radiative cooling at the surface.

For the proposed process to be successful, the stable crust must be established before large quantities of the partially cooled layer beneath the crust are subducted by convection. It is possible that the proposed process may succeed. Crystal separation rates leading to crust formation (subtraction of olivine by settling) are driven by liquid–solid density contrasts and may be more rapid than the convection rates driven by thermal contrasts in the liquid alone which act to reduce the opportunity for establishing a zone conductive to plagioclase–olivine separation.

Acknowledgments—We have benefited from discussions with S. E. Kesson, M. J. O'Hara, and A. E. Ringwood, and reviews by R. Brett and J. S. McCallum, but we absolve them of any errors presented here. We thank N. Jackson for assistance in manuscript preparation. This work was supported by NASA grant NGL 22-007-247 and the Committee on Experimental Geology and Geophysics of Harvard University.

REFERENCES

Anderson D. L. (1973) The composition and origin of the moon. *Earth Planet. Sci. Lett.* **18**, 301–316.

Bottinga Y. and Weill D. F. (1970) Densities of liquid silicate systems calculated from partial molar volumes of oxide components. *Amer. J. Sci.* **272**, 438–475.

Ganapathy R. and Anders E. (1974) Bulk compositions of the moon and earth estimated from meteorites (abstract). In *Lunar Science V*, p. 254–256. The Lunar Science Institute, Houston.

Green D. H., Ringwood A. E., Ware N. G., Hibberson W. O., Major A., and Kiss E. (1971) Experimental petrology and petrogenesis of Apollo 12 basalts. *Proc. Lunar Sci. Conf. 2nd*, p. 601–615.

Grove T. L., Walker D., Longhi J., Stolper E. M., and Hays J. F. (1973) Petrology of rock 12002 and origin of picritic basalts at Oceanus Procellarum. *Proc. Lunar Sci. Conf. 4th*, p. 995–1013.

Hodges F. N. and Kushiro I. (1974) Apollo 17 petrology and experimental determination of differentiation sequences in model moon compositions. *Proc. Lunar Sci. Conf. 5th*, p. 505–520.

Irvine T. N. (1970) Heat transfer during solidification of layered intrusions. I. Sheets and sills. *Can. J. Earth Sci.* **7**, 1031–1061.

Kesson S. E. (1974) Apollo 15 mare basalts: Melting experiments in high purity Fe containers at ~1 atm and high pressures. *Abstracts with Programs*, Geol. Soc. Amer. **6**, 823.

Longhi J., Walker D., Grove T. L., Stolper E. M., and Hays J. F. (1975) Petrology and origin of Apollo 15 mare basalts. In preparation.

Mizutani H., Matsui T., and Takeuchi H. (1972) Accretion process of the moon. *The Moon* **4**, 476–489.

Papanastassiou D. A. and Wasserburg G. J. (1971) Lunar chronology and evolution from Rb–Sr studies of Apollo 11 and 12 samples. *Earth Planet. Sci. Lett.* **11**, 37–62.

Philpotts J. A. and Schnetzler C. C. (1970) Apollo 11 lunar samples: K, Rb, Sr and rare-earth concentrations in some rocks and separated phases. *Proc. Apollo 11 Lunar Sci. Conf.*, p. 1471–1486.

Ringwood A. E. (1975) Some aspects of the minor element chemistry of mare basalts. *The Moon*. In press.

Ringwood A. E. and Essene E. (1970) Petrogenesis of Apollo 11 basalts, internal constitution and origin of the moon. *Proc. Apollo 11 Lunar Sci. Conf.*, p. 769–799.

Robie R. A. and Waldbaum D. R. (1968) Thermodynamic properties of minerals and related substances at 298.15°K (25.0°C) and one atmosphere (1.013 bars) pressure and at higher temperatures. U.S. Geological Survey Bull. 1259.

Roeder P. L. and Emslie R. F. (1970) Olivine-liquid equilibrium. *Contrib. Mineral Petrol.* **29**, 275–289.

Smith J. V., Anderson A. T., Newton R. C., Olsen E. J., Wylie P. J., Crewe A. V., Isaacson M. S., and Johnson D. (1970) Petrologic history of the moon inferred from petrography, mineralogy and petrogenesis of Apollo 11 rocks. *Proc. Apollo 11 Lunar Sci. Conf.*, p. 897–925.

Stolper E. (1974) Lunar ultramafic glasses. Unpublished honors thesis, Harvard University.

Taylor S. R. and Jakeš P. (1974) The geochemical evolution of the moon. *Proc. Lunar Sci. Conf. 5th*, p. 1287–1305.

Toksöz M. N., Dainty A. M., Solomon S. C., and Anderson K. R. (1974) Structure of the moon. *Revs. Geophys. Space Phys.* **12**, 539–567.

Wakita H. and Schmitt R. A. (1970) Lunar anorthosites: Rare earth and other elemental abundances. *Science* **170**, 969–974.

Walker D., Longhi J., and Hays J. F. (1972) Experimental petrology and origin of Fra Mauro rocks and soil. *Proc. Lunar Sci. Conf. 3rd*, p. 797–817.

Walker D., Grove T. L., Longhi J., Stolper E. M., and Hays J. F. (1973) Origin of lunar feldspathic rocks. *Earth Planet. Sci. Lett.* **20**, 325–336.

Walker D., Kirkpatrick R. J., Longhi J., and Hays J. F. (1975a) Crystallization history and origin of lunar picritic basalt 12002: Phase equilibria, cooling rate studies, ~~and physical properties of the parent magma~~. Submitted for publication.

Walker D., Longhi J., Stolper E. M., Grove T. L., and Hays J. F. (1975b) origin of titaniferous lunar basalts. *Geochim. Cosmochim. Acta*. In press.

Wänke H., Palme H., Baddenhausen H., Dreibus G., Jagoutz E., Kruse H., Spettel B., Teschke F., and Thacker R. (1974) Chemistry of Apollo 16 and 17 samples: Bulk composition, late stage accumulation and early differentiation of the moon. *Proc. Lunar Sci. Conf. 5th*, p. 1307–1335.

Wood J. A. (1973) Bombardment as a cause of lunar asymmetry. *The Moon* **8**, 73–103.

Wood J. A., Dickey J. S., Marvin U. B., and Powell B. N. (1970) Lunar anorthosites and a geophysical model of the moon. *Proc. Apollo 11 Lunar Sci. Conf.*, p. 965–988.

Crystallization History of Lunar Picritic Basalt 12002: Phase Equilibria and Cooling Rate Studies

D. Walker, R. J. Kirkpatrick,
J. Longhi, and J. F. Hays
Hoffman Laboratory, Harvard University
Cambridge, Massachusetts 02138

ABSTRACT

Experimental crystallization of a lunar picrite composition (12002) at controlled linear cooling rates produces systematic changes in the temperature of appearance of the crystalline phases, the texture, and crystal morphology as a function of cooling rate. Phases crystallize in the order olivine, chrome-spinel, pyroxene, plagioclase, ilmenite during equilibrium crystallization but ilmenite and plagioclase reverse their order of appearance and silica crystallizes in the groundmass during controlled cooling experiments. The partition of iron and magnesium between olivine and liquid (K_D = 0.33) is independent of cooling rate (0.5-2000°C/hour), temperature (1325-600°C), and pressure (0-12 kb). Comparison of the olivine nucleation densities in the lunar sample and in the experiments indicates that the sample began cooling at about 1°C/hour. Pyroxene size, chemistry, and growth instability spacings ("swallowtails") as well as groundmass coarseness all suggest the cooling rate subsequently decreased by as much as a factor of 10 or more. The porphyritic texture of this sample, then, is produced at a decreasing, rather than a discontinuously increasing, cooling rate.

INTRODUCTION

Picritic basalts have been sampled by the Apollo 12 and 15 lunar missions; these rocks show a variety of textures and grain sizes ranging from vitrophyric to porphyritic to gabbroic. Comparison of the compositions of experimental liquidus phases with the most magnesian core compositions of the natural examples of those minerals have shown that some of these porphyries (including those with vitrophyric groundmass) crystallized from a magma batch of composition equivalent to the hand specimen composition (Green and others, 1971; Grove and others, 1973).

Much controversy has surrounded the possible interpretations of magma cooling history deduced from the two-stage crystallization history (phenocrysts then groundmass) implicit in porphyritic textures. Is a two-stage cooling history the proper interpretation of a two-stage crystallization history? It is the purpose of this paper to reconstruct quantitatively the cooling history of 12002, a porphyritic picrite, in an attempt to answer this question.

EXPERIMENTAL METHODS

In our previous studies of 12002 (Grove and others, 1973), molybdenum and ingot-grade iron capsules were used for equilibrium experimental crystallization. These materials interacted with the silicate charges to a certain extent resulting in significant iron

loss. It has since been shown (Kesson, 1974a,b; Walker and others, 1975) that iron loss can be virtually eliminated by use of very high purity iron (<20 ppm total impurities) for lunar high- and low-Ti mare basalts. Presumably the iron loss experienced in the previous work in ingot-grade iron capsules in sealed silica tubes resulted from reduction of some iron in the charge by impurities in the iron of the capsule. Carbon and phosphorous are the most likely agents of this reduction (M. J. O'Hara, personal communication). Samples equilibrated in high purity iron containers will not gain or lose iron if the material is iron-saturated. This appears to be the case for many lunar basalts. Examples of lunar basalts which are not iron-saturated exist (see appendix discussion of Walker and others, 1975) and these materials gain iron when equilibrated in iron capsules. Evidence that rock 12002 was iron-saturated during its crystallization is given by Grove and others (1973) who reported iron spherules included in 12002 olivines. In addition we have observed iron in pyroxenes and in the groundmass of 12002 as well, though it is not abundant (<1%). Therefore use of iron capsules for 12002 should be successful in maintaining constant iron content. Conversely, if constant iron content is maintained, this confirms the inference that 12002 was iron-saturated during crystallization. This appears to have been the case.

The present equilibrium crystallization experiments on 12002 were conducted in high purity iron. The starting material is the

same devitrified glass used by Grove and others (1973). A single capsule was reused within different evacuated silica tubes for experiments in a mild vacuum according to procedures discussed in Longhi and others (1974).* A fresh charge was loaded for each temperature investigated. Capsule recovery was made possible by filling only a small part of the capsule. The evacuated void space apparently caused partial alkali extraction from the charge. High pressure equilibration in iron capsules was done according to the procedures discussed in Walker and others (1972) in a piston-cylinder apparatus. Drying of furnace assemblies and charges was done at 1100°C in H_2 10%-N_2 90% rather than pure N_2, for 15 minutes rather than 30 minutes. Tungsten-rhenium (W3%-W25%) thermocouples were used exclusively in the high pressure experiments with iron capsules.

Experiments were also performed in high purity iron in evacuated silica tubes at programmed cooling rates to study the

---

*The effects of insufficient care to prevent capsule oxidation can be seen in the appendix, Table 1. Runs #188 and #184 were the last experiments performed with the capsule and were done several months after the other runs. The acetone in the storage bottle had nearly evaporated. Although no obvious rusting of the capsules had occurred, microscopic oxidation of the capsule is the most probable explanation for the modest iron gain these runs have experienced.

cooling history of 12002. The capsules were prepared from 5 mm rod stock. All machining was done under heavy oil and capsules were stored in oil or acetone prior to loading and use (Longhi and others, 1975). The O.D. was turned to 4.5 mm and the I.D. drilled to 2.5 mm. Lids were friction fitted plugs. The cylindrical cavity, which was filled with the charge, was 2.5 mm in diameter and 4 mm deep. Capsules in evacuated silica glass tubes were suspended in a Pt-Rh wound resistance furnace. Temperature was monitored and controlled with Pt-Pt10Rh thermocouples which were calibrated against the melting points of gold (1064°C), lithium metasilicate (1203°C), and diopside (1391°C) charges used in the same configuration as the run charges. Two different furnaces were used: a smaller model (1" I.D.) holding a single charge and a larger bore model (2-1/8" I.D.) holding up to 3 charges. Experiments which were cooled at faster than 1°C/hour were first equilibrated at 1350 ± 5°C for 8 hours or more. All cooling experiments were started at 1350 ± 5°C to give a liquid of uniform structure as the starting material for all experiments. Charges were then cooled at a specified rate to a specified temperature and then quenched in water. Examination of the products was made by polishing an axial section through the cylindrical charge for reflected light microscopy and electron probe analysis. Capsules were not reused.

Programming of the temperature drop in these experiments was done two ways. A Eurotherm D120W electronic temperature

program unit was installed between the thermocouple which sensed the furnace temperature and the control/power-supply package which regulated the furnace power in response to the thermocouple signal. The program unit generated a linearly varying potential which caused the regulation system to lower the temperature at a rate corresponding to a linear change in thermocouple EMF. This does not correspond strictly to a linear temperature drop for a Pt-Pt10Rh thermocouple but the deviations are negligible for the resolution of this study. For fast cooling rates (500-2000°C/hour) the program and control system was bypassed and furnace power simply shut off. Cooling proceeded at a rate determined by the thermal properties of the furnace. Two furnaces of different design and insulation were used to allow some variation of cooling rate in this rapid cooling regime. The cooling rates produced are not linear in this situation and decrease with time. Dotted lines on Figure 2 indicate the approximate cooling trajectories. The values quoted for cooling rate are simply the change in temperature divided by the length of time elapsed to produce the temperature drop. Once again the deviations from linearity (a factor of 3) are inconsequential to a study of this resolution covering cooling rates which vary by a factor of 4000 (0.5-2000°C/hour).

Iron metal is present in all experiments as the result of the use of iron capsules. Microprobe analysis of equilibrium run products shows the iron loss or gain is negligibly small. It is, however, quite clear that iron metal is not an inert

container. The silicate charge corrodes the container, eating embayments into the capsule walls and bottom. The iron so dissolved is reprecipitated as prominences on other parts of the capsule or as iron globules in the silicate charge. Iron apparently dissolves and reprecipitates even though the iron content of the silicate charge remains unchanged. The same effects were seen in the controlled cooling runs but the presence of strongly zoned silicates makes it difficult to estimate the amount of iron gain or loss in the system. Consideration of liquidus olivine chemistry (below) suggests that net gain or loss of iron is also small in these experiments. Iron reprecipitated in the controlled cooling experiments does not seem to show much variation in morphology with cooling rate. Experiments cooled to the solidus do not show noticeably more iron transfer than experiments quenched from near the liquidus. The transfer of iron may happen mostly during the initial equilibration above the liquidus at 1350°C.

EXPERIMENTAL RESULTS (EQUILIBRIUM)

The equilibrium phase relations in high purity iron are shown in Figure 1 as a function of temperature and pressure. The difference in phase stabilities from those reported in Grove and others (1973) are small. The principal change at low pressure is that pyroxene crystallization has started at 1175°C rather than 1225°C and the olivine liquidus temperature is about 10° higher. These changes are readily understood as a result of the iron loss

in the earlier experiments. Reduction of the total FeO+MgO available to make ferromagnesian silicates such as olivine depresses the olivine liquidus, even though Mg/Fe+Mg of the silicate increases. Silica activity increases, therefore pyroxene crystallization is enhanced. At high pressures the principal change is that spinel is no longer present at the olivine+ orthopyroxene liquidus pressure. The Mo capsules probably stabilized spinel with a very small addition of oxidized molybdenum which is partitioned exclusively into the spinel. The olivine+ orthopyroxene liquidus pressure is 12-1/2 kb rather than 15 kb.

The most noticeable differences between the previous and present experiments is to be found in the higher Fe/Fe+Mg of the phases in the present experiments. Fo_{78} is the liquidus olivine at pressures up to 12-1/2 kb, whereas iron loss in the earlier experiments produced olivine as magnesian as Fo_{88}. At low pressure, pyroxene crystallization begins with Wo_7En_{66} in high purity iron as opposed to Wo_4En_{82} in the earlier experiments. In general the phases present are unzoned and show only minor heterogeneities.

Details of run products and phase compositions can be found in Tables 1 and 2 and in the appendix.

EXPERIMENTAL RESULTS (CONTROLLED COOLING)

Experimental crystallization of 12002 at controlled cooling rates was performed in order to investigate the variations

observed in changing the cooling rate and the temperature from which the experiment was quenched. The latter parameter was chosen in order to arrest the crystallization process at various stages. Other possible variables which might affect the crystallization behavior (such as large superheating or episodic changes of physical conditions such as pressure) were not investigated.

Figure 2 shows the results of these experiments as a function of these two variables. All experiments were started above the liquidus at 1350 ± 5°C and cooled to the temperature indicated by the circles at the cooling rate corresponding to the value of the abcissa, then quenched. Phases crystallize in the order olivine, spinel, pyroxene, ilmenite, plagioclase (and silica). The equilibrium crystallization sequence of 12002 under the same conditions is included in Figure 2 for comparison. It is to be noted that the order of crystallization of olivine, spinel, and pyroxene is the same but plagioclase and ilmenite have reversed their order relative to one another compared to the equilibrium sequence. The curves labelled "olivine in" etc. indicate that all experiments at temperatures lower than the curve have crystallized olivine, etc. Figure 2 shows that there is a systematic decrease in the temperature at which each phase appears with increase in cooling rate. The extent of this decrease is largest for the late crystallizing phases; i.e., the curvature is greatest for the lowest curves. (The top curves for olivine and spinel may not be observably depressed. The experiments on which this very

slight depression is based report the thermocouple temperature of the most quickly cooled run. While the thermocouple was cooling at ~2000°C/hour it is conceivable that the temperature of the more massive charge in its silica tube did not fall quite this fast.)

The olivines, spinels, and pyroxenes crystallize as zoned microphenocrysts. Changes in morphology and chemistry are discussed below. Ilmenite crystallizes as laths. In all experiments where ilmenite has crystallized, Cr-spinel phenocrysts have developed mantles of Cr-ulvöspinel (see Table 2 of appendix). This may be suggestive of a reaction relation between liquid and Cr-spinel which produced Cr-ulvöspinel and ilmenite; however, no other textural relations observed support this possibility. Ilmenite is not observed in contact with nor in overgrowth relation to the mantled spinels. It may be that the reaction which mantles the Cr spinels with ulvöspinel is independent of ilmenite appearance but coincidentally occurs at about the same temperature at each cooling rate. Nehru and others (1974) have concluded on the basis of similar relations exhibited in Apollo 15 basalts that pyroxene participates in this reaction. In experiments cooled at slower than 50°C/hour a groundmass of plagioclase, pyroxene, and silica crystallizes. At faster cooling rates no groundmass crystallizes above 600°C where our observations end. The grain size of the groundmass increases with decreasing cooling rate.

COMPARISON WITH EQUILIBRIUM CRYSTALLIZATION

The crystallization induced during controlled cooling of 12002 differs in three important ways from the equilibrium crystallization. Temperature of initial phase appearance is depressed, phases produced are chemically zoned, and metastable phases crystallize. These three differences are interrelated. The fact that the temperature at which each phase appears decreases with increasing cooling rate may be partly due to the higher probability of nucleation near the equilibrium temperature at the slower cooling rates. However, this depression of phase-appearance temperature is also undoubtedly aided by growth of zoned phases, which causes substantial departures of the composition of the residual liquid from the equilibrium composition. For example, fractionation of augite (rather than the equilibrium pigeonite) depletes the melt in Ca while surface equilibrium growth of zoned olivine and pyroxene enriches the Fe/Fe+Mg of the residual liquids (to 0.9 vs. 0.6 at bulk equilibrium, see Figure 7). These departures from bulk equilibrium suppress plagioclase and enhance ilmenite growth potentials. Together with the possibility of delayed plagioclase nucleation, they are responsible for the observation that ilmenite and plagioclase have reversed their order of crystallization relative to the equilibrium sequence. It should be noted that the growth of metastable phases is also related to departures of the residual liquid from the equilibrium composition. Silica and ulvöspinel

do not have a stability field between the equilibrium liquidus and solidus although ulvöspinel may have a subsolidus stability field. The growth of silica in the groundmass occurs because the residual liquids are silica enriched and have high Fe/Fe+Mg so that equilibrium of a silica phase with olivine is possible.

It appears that gross errors may result in trying to use equilibrium crystallization data to assign temperatures to petrographically observed crystallization sequences in extrusive rocks or rocks from small intrusive bodies. This can be the case even if the order of phase appearance experimentally matches the petrographically observed sequence. The error is more severe for more quickly cooled rocks.

TEXTURAL VARIATIONS

Systematic variations in crystal morphology with cooling rate are observed. All textures are porphyritic. At cooling rates in excess of 50°C/hour run products consisted of skeletal phenocrysts of olivine, Cr-spinel, pyroxene and ilmenite surrounded by glass. At greater than 500°C/hour olivines have a platy skeletal habit with elaborate and regular cross-ornamentation between the faces of the plates. Maximum dimensions of the plates can be of the order of 1 mm but the thickness of the plates does not exceed 50 µm. Spinels occur as tiny specks or minute dendritic crosses of the order of 5-10 µm. Pyroxenes occur as elaborately ornamented dendritic sprays which form masses as large

as 300 µm although the individual pyroxenes rarely have a thickness greater than 30 µm. Figure 3 shows an experiment cooled at 500°C/hour which exhibits these features. Also shown in Figure 3 at the same scale is a photomicrograph of 12009, a vitrophyre with composition quite similar to 12002. The striking textural similarities suggest that this portion of 12009 may have cooled at about 500°C/hour.

Figure 4 shows representative textures at slower cooling rates. As noted above, and shown in Figure 4A, skeletal olivine, spinel, and pyroxene occur in a glass matrix for experiments cooled at rates greater than 50°C/hour. The skeletal olivines are not as flattened as at 500°C/hour and the dendritic pyroxene is clearly coarser. Figures 4B, C, and D show the products of progressively more slowly cooled runs. In B the phenocrysts are set in a microcrystalline plagioclase-pyroxene groundmass. Silica is probably present. 4C and D show progressive coarsening of this groundmass with silica present. 4B, C, and D also show progressively coarsening olivine and pyroxene phenocrysts which are more equant than at faster cooling rates. Some evidence of skeletal morphology occasionally remains even at the slowest rates.

Cr-spinel also shows systematic morphology changes with cooling rate as seen in Figure 5. At all cooling rates, spinel occurrence strongly suggests nucleation on other preexisting solid phases as does no other phase observed. At faster than 500°C/hour (Figure 5A) minute spinel specks are intimately distributed within the ornamentation of skeletal olivines. At faster than

50 °C/hour spinel occurs as minute dendritic crosses on the edges of olivine phenocrysts (Figure 5B). At slower cooling rates the intimate occurrence of spinel with olivine is replaced by the occurrence of spinel with iron metal (Figure 5C). Equant, euhedral spinel invariably grows on the capsule walls or on iron spherules in the charge. The morphology and occurrence of Cr-spinels with ulvospinel mantles grown at the slower rates observed most nearly correspond to the spinels in 12002 (compare Figures 5C and D).

It should be emphasized that there is a range in morphologies of all phases grown at any particular cooling rate and therefore only a crude estimate of cooling rate can be based on crystal morphology alone. For example, some large equant, faceted olivine phenocrysts in 12002 strongly resemble some olivine phenocrysts grown experimentally at a cooling rate of ~0.6°C/hour. These crystals are of comparable size and morphology so it is tempting to say the olivines in 12002 grew at this rate. This inference is insecure, however, since quite a range of olivine sizes and morphologies are present in both 12002 and experiments at this cooling rate. It would, however, probably be safe to say that 12002 cooled more slowly than 500°C/hour on the basis of olivine morphology since there is no overlap of morphologies in 12002 with those grown so fast.

PORPHYRITIC TEXTURE (I)

We are now in a position to give a partial answer to the question posed in the introduction about the interpretation of

porphyritic texture. These experiments, employing a single cooling rate, produce porphyritic textures. Therefore, two stage crystallization implicit in a porphyritic texture does not necessarily imply a two-stage cooling history. This was clear to Bowen (1914, p. 257). Lofgren and others (1974) have also produced porphyritic textures at single cooling rates in quartz-normative, pyroxene-porphyry compositions under different experimental conditions for containment and p_{O_2} control. Such behavior may be a rather general property of basaltic compositions. This does not negate the possibility that some porphyries do have a two-stage cooling history; however, it cannot be safely inferred that they do on the basis of porphyritic texture alone.

A cooling history commonly inferred from the crystallization history recorded in porphyritic texture is that "slow" cooling is responsible for growth of phenocrysts, after which "fast" cooling is responsible for growth of the groundmass. The two stages of the cooling history may be separated by a discrete event such as eruption of the magma. We previously inferred such a cooling history for 12002 (Grove and others, 1973) on the basis of details of pyroxene chemistry as well as porphyritic texture. Pyroxene is a major phase in both the phenocryst and groundmass population and so its chemical variations record much of the crystallization history of 12002. This general approach has been extensively employed in other investigations by many authors (e.g., Bence and others, 1971; Hollister and others, 1971). Pyroxene phenocrysts in 12002 have Ti/Al of near 1/4 which is the

value observed in equilibrium crystallization of 12002. In contrast pyroxenes of the groundmass have Ti/Al greater than 1/2, values clearly not consistent with the observed equilibrium crystallization. The two stages of crystallization were then seen as quasi-equilibrium crystal growth (phenocrysts) and non-equilibrium crystal growth (groundmass). This is just the sort of behavior to be expected in a two-stage cooling history such as we previously inferred for 12002, if one associates quasi-equilibrium growth with "slow" cooling and non-equilibrium growth with "fast" cooling. We have noted above that this two-stage cooling history is not a mandatory deduction based on porphyritic texture alone. We must now inquire whether the evidence from pyroxene chemistry combined with porphyritic texture is sufficient to make that deduction mandatory.

PYROXENE CHEMISTRY VARIATIONS

Pyroxene compositional variation is shown in Figure 6 for controlled cooling experiments, equilibrium experiments, and 12002 natural pyroxenes. In both natural and controlled cooling experiments, phenocrysts zone from pigeonite cores to augite rims with sectorial complications. In both natural and experimental phenocrysts Ti/Al is close to 1/4; both Ti and Al increase from core to rim, reflecting increasing incorporation of Ti and Al with decreasing temperature, which is also seen in the equilibrium sequence (Table 1). Both natural and controlled

cooling groundmass pyroxenes are of different composition from their respective phenocrysts and are sub-calcic with variable iron-enrichment which can be extreme. Ti/Al can be greater than 1/2 in the groundmass of both natural and controlled cooling crystallization products. In contrast to the pyroxenes grown in controlled cooling experiments, the very limited major element compositional variation, the lack of iron-enriched late pyroxenes, and the lack of Ti/Al > 1/2 in the equilibrium pyroxenes indicate that equilibrium crystallization is not a good model for the natural pyroxene crystallization.

Although the controlled cooling experiments shown in Figure 8 provide a better approximation to the natural pyroxenes, there are still noticeable discrepancies. The experimental pyroxenes show larger amounts of Al and Ti, and, to a modest extent, Fe, than the natural counterparts. The experimental phenocrysts have maximum Ti+Al a factor of $\sim$2 greater than the maximum seen in the natural pyroxenes. Experimental augite margins are slightly iron-enriched and experimental groundmass pyroxenes are markedly iron-enriched compared to the natural counterparts.

The highly skeletal pyroxenes grown at faster than 25°C/hour have the highest Ti+Al observed. The equilibrium pyroxenes have the lowest Ti+Al observed. If equilibrium crystallization occurs at an infinitely slow cooling rate then the amount of Ti+Al incorporated in the pyroxenes would appear to correlate crudely with cooling rate since pyroxenes grown at intermediate rates have maximum Ti+Al intermediate between the equilibrium and most

rapid cooling values. The reason for the lesser amount of Ti+Al in 12002 pyroxenes is probably that pyroxene in rock 12002 grew at a rate slower than our controlled cooling experiments. The Ti+Al enrichment is thought to result in part from the delay in growth of phases which deplete Ti and Al from the melt. We noted above that the delay in ilmenite (with ulvöspinel) and plagioclase appearance increases with cooling rate as seen in Figure 2. Furthermore, during rapid cooling Ti and Al may not have sufficient opportunity to diffuse away from the growth surface and may become incorporated into the growing pyroxene. These two processes produce the same qualitative result; more rapid cooling leads to greater Ti+Al enrichment. The relative importance of the two effects is not known.

The lesser amount of iron enrichment in the natural 12002 pyroxene may also be explained as a result of somewhat slower cooling rate. Fractionation of Fe/Mg by surface equilibrium growth of zoned phenocrysts will be less extreme at slower cooling rates as diffusional exchange with phenocryst cores is more effective. The limit of this process is seen in the trivial iron-enrichment of the pyroxenes grown under bulk equilibrium conditions.

The final feature of the pyroxene compositional variation remaining to be accounted for is the change in Ti/Al from 1/4 in the phenocrysts to $>1/2$ in the groundmass. This phenomenon is basically a depletion of Al at relatively static Ti content. We have already noted that plagioclase entry is likely to put a "lid" on the Al content of the liquid and hence of the pyroxene. If plagioclase is supersaturated with respect to the non-equilibrium

residual liquid a large amount of plagioclase may crystallize all at once upon nucleation. This would cause an essentially discontinuous subtraction of Al from the melt which is reflected in the abrupt drop in Al content of the pyroxenes. Since the groundmass pyroxenes seem to crystallize penecontemporaneously with the plagioclase, some local areas of the melt may not be depleted by prior plagioclase crystallization whereas others are depleted when the pyroxene grows there. This accounts for the fact that some of the groundmass pyroxenes in the experimental case still have Ti/Al of 1/4 while some have >1/2. In the natural case we infer that the residual liquid was already uniformly depleted by plagioclase crystallization before the growth of groundmass pyroxene since the 1/4 trend was not observed.

PORPHYRITIC TEXTURE (II)

We have now considered pyroxene compositional variation produced in one stage cooling experiments. The production of phenocrysts with Ti/Al the "quasi-equilibrium" value of 1/4 and groundmass pyroxenes with the "non-equilibrium" value of >1/2 has been accomplished at constant cooling rate. Clearly then the evidence of Ti/Al variation, even coupled with the evidence of porphyritic texture, is insufficient to make a two stage (slow then fast) cooling history a mandatory deduction from a two-stage crystallization history. Supersaturated crystallization, which can be deduced from the Ti/Al of the pyroxenes cannot be safely equated with fast or slow cooling. It appears

that texture and pyroxene composition cannot be used to translate unambiguously crystallization history into cooling history.

OLIVINE CHEMISTRY VARIATIONS

The variation in olivine chemistry is considerably less than that shown by the pyroxenes. This is a result not only of the more limited solid solution possible in olivine but also of the fact that olivine is the liquidus phase and hence there is no fractionation of solid phases prior to olivine which might affect the composition of the liquid at the start of olivine crystallization. Olivines crystallized in controlled cooling experiments are extensively zoned at all cooling rates. Zoning is not necessarily regular or concentric, especially in the skeletal morphologies grown at high cooling rates. Figure 7 shows the range of olivine compositions seen in controlled cooling experiments as a function of temperature. Only the Fe/Fe+Mg variable is considered since any variability in Ca, Al, Ti or Cr was small or below the observable limit of detection. Experiments for all cooling rates are included in Figure 9 along with the compositions of the equilibrium olivines as a function of temperature. The olivines grown in controlled cooling experiments have their most fayalitic olivines (rims) limited by the equilibrium value for the composition of the residual liquid, regardless of cooling rate, at temperatures between the equilibrium liquidus and solidus. At temperatures at least 100°C below the equilibrium solidus the olivines continue to maintain surface equilibrium in

terms of Fe/Mg distribution with the residual liquid. This is seen in Figure 8 where the most fayalitic olivine found in an experiment is plotted against the Fe/Fe+Mg of the adjacent residual liquid from that experiment. There is very little deviation from a K_D value (Roeder and Emslie, 1970; Longhi and others, 1975) of 0.30-0.33. The same values are also found for the equilibrium experiments. At lower temperatures this comparison is obscured when the olivine becomes largely overgrown with pyroxene and/or groundmass.

A remarkable feature of the ability of olivine to maintain surface equilibrium with the residual liquid, is the constancy of the liquidus olivine composition, irrespective of the cooling rate. The most magnesian olivines observed are about Fo_{78}. (Sometimes slightly less magnesian olivines are found, presumably because of failure to section the olivine core.) This composition is observed irrespective of the cooling rate and can be seen in Figure 7 to be the equilibrium liquidus olivine. Obviously the Roeder-Emslie K_D formulation of Fe/Mg distribution between olivine and liquid is quite general and independent of cooling rate over this range of cooling rates.

This tendency of olivine to maintain surface Fe/Mg equilibrium with the liquid even at very high cooling rates is remarkable and was not expected. A growing olivine crystal must preferentially incorporate Mg, and to a lesser extent Fe, while rejecting the other constituents of the liquid. Diffusive transport of material must then occur near the surface of the growing crystal, and at

fast cooling rates composition gradients in the liquid might be expected to preclude equilibrium partitioning of Fe and Mg. A clue to the mechanism for achieving such equilibrium may lie in the skeletal nature of the olivines formed at high cooling rates. Under these conditions any protrusions out from the olivine growth surface may penetrate the depleted liquid zone and thus sample fresh liquid without the need for long-range diffusion. Such protrusions will therefore propagate rapidly yielding a skeletal crystal with near-equilibrium Fe/Mg ratio.

COOLING HISTORY

We have seen that texture and crystal morphology change as a function of a sample's cooling rate. Likewise pyroxene chemistry shows some variation with cooling rate. We have already noted the qualitative nature of these variations and the crudeness of estimates of cooling rate based solely on such criteria. Clearly these criteria are not sufficient for constructing a quantitative cooling history. They may be used to check for consistency but they cannot point unambiguously to some particular cooling history. To interpret a cooling history quantitatively requires the ability to specify cooling rate for as many stages in the crystallization history as possible.

Since we do not know the possible effects of large superheating, the earliest stage of the cooling history we can hope to reconstruct is the crystallization of olivine, the liquidus phase. Crystal morphology is a rough guide but not really

quantitative. The chemistry of olivine appears to be insensitive to cooling rate and so is no help in this undertaking.

We have noted that the composition of the residual liquid at any temperature appears to be roughly independent of the cooling rate by which that temperature is reached. For this to be true, the total amount of olivine crystallized prior to reaching a given temperature must also be independent of cooling rate. This appears to be true in our experimental runs; however, at slow cooling rates olivine occurs as relatively sparse equant crystals of relatively large volume, while at fast cooling rates olivine occurs as abundant thin plates of small individual volume. These observations suggest that the processes of crystal nucleation and crystal growth may play reciprocal roles as the cooling rate is varied. In order to evaluate this possibility we counted the number of olivine crystals per unit area (a measure of nucleation density) in our experimental products. The results are shown as a function of cooling rate in Figure 9. In spite of some scatter, a regular pattern is obvious; slow cooling produces a small number of relatively large equant crystals, faster cooling produces many skeletal plates of small volume. Increasing the cooling rate for 30°/hour to ≈1000°/hour does not result in further increase in nucleation density. Presumably, still faster cooling rates would result in reduced numbers of crystals and more quenched liquid. Cooling rates faster than 10^5°C/hour are sufficiently rapid to produce glasses with no olivine crystals. The nucleation density, therefore, is at a maximum at cooling rates of a few hundred degrees per hour. Each block on Figure 9 includes runs

quenched from many different temperatures at the indicated cooling rate; the number of crystals does not vary systematically with temperature from which the run was quenched, implying that most of the nuclei are formed early in the cooling process and that the observed scatter is largely due to other factors. One such factor is the small sample size; another may be non-random distribution of olivine crystals with respect to the plane of the section. Some minor effect of continued nucleation of olivine with falling temperature is also possible. In view of the large range of nucleation densities observed (1 crystal/surface to 200 crystals/surface), the scatter does not preclude use of this parameter as an estimator of cooling rates.

The number of olivine crystals per unit area in thin-section 12002,9 is also shown in Figure 9; a cooling rate of 1°/hour, or a little less, is indicated for the beginning of olivine crystallization in 12002. This estimate is compatible with our earlier estimate based on olivine crystal morphology.

This approach cannot be applied directly to estimate the cooling rate at the time of pyroxene crystallization. Since the beginning of pyroxene crystallization, unlike olivine crystallization, occurs at progressively lower temperatures as cooling rate is increased, the liquid from which pyroxene begins to crystallize varies in composition at different cooling rates. If 12002, as we believe, did not cool at a uniform rate, estimates based on nucleation densities in our experimental runs might be misleading. As we have noted, the low Ti+Al content of the 12002

pyroxene phenocrysts compared to our experimental products (Figure 6) suggests that during this stage of its cooling history, 12002 was cooling at a rate slower than any we observed experimentally. A similar conclusion is implied by the large size (up to 3 mm) of the natural pyroxene phenocrysts compared to those grown in our experiments (less than 0.5 mm).

This conclusion can be made roughly quantitative by observation of one aspect of pyroxene crystal morphology. The prominent "swallowtail" growth instabilities seen on the pyroxene phenocrysts in 12002 and in our experiments appear to have a characteristic linear spacing (D_{IS}). In our experiments this spacing is a function of cooling rate. Figure 10 is a plot of $\ln(D_{IS})$ versus cooling rate. The largest spacing shown by a symmetrical "swallowtail" in each section is plotted. The scatter is attributed to slight variations in position and orientation of the crystals relative to the polished section. The range of "swallowtail" dimensions seen in 12002,9 is also shown. Extrapolation of the experimental values suggests that the natural phenocrysts grew at a rate of 0.1 or 0.2°/hour, consistent with the qualitative estimates and several times slower than the cooling rate inferred for the beginning of olivine crystallization.

The crystallization of 12002 ends with groundmass growth and this event is also dependent upon the previous cooling history. Again nucleation density estimates from our experiments at linear cooling rates cannot be rigorously applied since it appears that the rock did not cool at a constant rate. Furthermore

the groundmass is not a single mineral but several minerals which grow penecontemporaneously. An additional complication is that nucleation density (or its equivalent here, grain size) is not constant even at a single cooling rate. For example, Figure 4C shows two regions of groundmass with different degrees of coarseness. Likewise there is quite a variation in the grain size within the 12002 groundmass; a few patches have a coarseness equivalent to the coarsest seen in our experiments even though the bulk of the 12002 groundmass is much coarser (see Figure 11). While a quantitative estimate of the cooling rate of the 12002 groundmass is not possible, it is quite easy to tell that the average groundmass of 12002 is very much coarser than any of our experimental products (as much as a factor of 10 or more in crystal size). Since we have observed experimentally a coarsening of grain size in the groundmass with decreasing cooling rate, the obvious conclusion is that the 12002 groundmass records a slower cooling rate than any of our experiments.

12002 started crystallization with olivine, at an experimentally observed rate and concluded crystallization with groundmass at a rate slower than any observed. Hence this porphyry solidified at a cooling rate that decreased with time. This contrasts with the cooling history we had originally inferred from the crystallization history recorded by porphyritic texture and Ti/Al variation in pyroxenes (Grove and others, 1973). These considerations are illustrated in Figure 12. The time scale on the dashed curve is arbitrary; however, the solid curve of the

present interpretation makes as much use of the quantitative deductions as possible. The slope (cooling rate) at the start is the result of the estimate from olivine nucleation density. The control on the slope is less firm at the temperatures corresponding to pyroxene and groundmass entry, but has been drawn to be roughly commensurate with possible estimates based on pyroxene instability spacing and on the coarseness of the groundmass. Since the lower slopes are not well known the estimates of the time for the completion of solidification are somewhat elastic, although much of the temperature drop leading to solidification must take place in the first 20 days. The estimate for solidification time shown here is on the order of a month or two, but it should be noted that it really is pointless to try to specify this number more precisely since 12002 obviously never completely crystallized (there is mesostasis glass) and the termination of the solidification was not a discrete event. What might be useful to attempt, though, would be refinements of the estimate of the cooling rate in the temperature interval below the appearance of the groundmass. This might be attempted through cation ordering studies although it is doubtful that sufficient calibration exists to substantially improve the quantitative resolution of the present conclusions. These conclusions are that 12002 began cooling at $\sim$1°C/hour and that this cooling rate subsequently decreased.

The form of the cooling history curve shown in Figure 12 is not consistent with the alternate interpretation shown in which

phenocrysts grow during slow cooling (perhaps at depth) and groundmass grows during rapid quenching (perhaps after eruption). The deduced cooling history curve corresponds to that expected for simple conductive cooling of magma solidifying under the influence of heat loss through neighboring margins of a magma body. The general cooling regime observed in solidifying terrestrial Hawaiian lava lakes (Peck and others, 1966; Richter and Moore, 1966), is also for a decreasing cooling rate as indicated by the square root of time dependence of the thickening of the upper crust. However, in cooling through the melting interval in these lava lakes the cooling rate may initially increase before decreasing (T.L. Wright, data on Makaopuhi lava lake, in press). Such effects are probably related to specific boundary conditions such as crust formation which do not seem to have influenced the cooling history of 12002.

Conclusions

We have shown here that finite cooling rates can radically alter the temperature and order of appearance of the crystallization phases from a silicate liquid. Using the results of experiments we have shown that the porphyritic texture of 12002 could have formed in a single continuous cooling event. Nucleation density, swallowtail spacings, and groundmass grain size show that crystallization occurredat a decreasing cooling rate in a period of one or two months.

ACKNOWLEDGEMENTS

T. L. Grove and E. M. Stolper assisted with the experiments. We thank them as well as D. R. Uhlmann, G. Lofgren, C. Donaldson and T. Usselman for many helpful discussions in the course of this work. The manuscript has benefited from reviews of an earlier version of this paper by T. L. Wright, P. L. Roeder, and R. Helz. This work was supported by NASA grant NGL 22-007-247, NSF grant GA 44002, and the Committee on Experimental Geology and Geophysics of Harvard University.

TABLE 1

RUN PRODUCTS FOR 12002 EQUILIBRATED IN HIGH PURITY IRON IN EVACUATED SILICA TUBES

	#180 LIQUID	#179 LIQUID	#188 LIQUID	#184 LIQUID	#176 LIQUID	#175 LIQUID	#177 LIQUID	#178 LIQUID	#168 LIQUID
SiO_2	43.8	43.7	43.1	44.0	46.0	46.0	45.6	45.6	44.9
TiO_2	2.80	2.88	2.43	3.33	3.53	3.79	3.76	4.38	4.74
Al_2O_3	7.95	8.22	8.78	9.63	10.2	11.1	11.4	11.1	10.8
Cr_2O_3	0.65	0.83			0.57	0.45	0.38	0.36	0.36
FeO	22.0	21.8	22.6	21.3	19.5	18.8	19.3	19.6	19.8
MgO	13.5	12.5	9.93	8.69	7.73	7.00	6.41	6.26	6.03
MnO	0.29	0.35			0.32	0.32	0.31	0.32	0.36
CaO	8.18	8.39	9.31	9.95	10.4	11.2	11.2	11.6	11.5
Na_2O	0.22	0.07			0.16	0.04	0.14	0.14	0.23
	99.39	98.74	96.15	96.90	98.41	98.70	98.50	99.36	98.72
		OLI-VINE	OLI-VINE	OLI-VINE	OLI-VINE	OLI-VINE	OLI-VINE	OLI-VINE	OLI-VINE
SiO_2		38.0	35.9	35.9	36.8	36.4	35.9	36.1	35.8
TiO_2		0.14	0.11	0.09	0.17	0.15	0.19	0.20	0.22
Cr_2O_3		0.78			0.66		0.74	0.56	0.49
FeO		21.6	25.8	26.4	27.8	29.2	30.8	31.4	32.0
MgO		38.5	35.5	34.0	33.6	32.2	31.0	30.6	30.3
MnO		0.29			0.36		0.40	0.38	0.40
CaO		0.34	0.40	0.39	0.41	0.41	0.42	0.45	0.47
		99.65	97.71	96.78	99.80	98.36	99.45	99.69	99.68
						6PYRO-XENES	4PYRO-XENES	6PYRO-XENES	9PYRO-XENES
SiO_2						51.7	51.1	52.5	51.7
TiO_2						0.56	0.62	0.70	1.05
Al_2O_3						1.15	1.25	1.55	2.21
Cr_2O_3						0.79	0.73	0.78	0.81
FeO						17.3	17.6	17.7	18.1
MgO						22.9	21.8	21.6	20.7
MnO							0.38	0.39	0.35
CaO						3.60	4.29	4.52	5.59
Na_2O						0.01	0.02	0.05	0.02
						98.01	97.79	100.19	100.53
Other Phases Present				Crsp	Crsp	Crsp	Crsp	Crsp Plag	Crsp Plag
Hrs Run Duration	27	28.1	19.1	18.7	47	72.7	45.8	98.7	75
T°C	1350	1328	1266	1232	1201	1176	1164	1156	1150
Notes			Minor Fe gain	Minor Fe gain					

Run #171 at 1104°C for 163.4 hours had assemblage olivine, pyroxene, plag, sp, ilmenite.

TABLE 2

SELECTED REPRESENTATIVE EXPERIMENTAL PRODUCTS

	Pyro-xene(1)	Pyro-xene(2)	Pyro-xene(3)	Pyro-xene(4)	Crsp (5)	Ulvo (6)	Liquid (7)	Oli-vine(8)	Pyro-xene(9)
SiO_2	50.5	46.1	45.2	44.9	0.07	0.16	43.5	36.1	52.6
TiO_2	0.86	2.85	2.08	3.88	5.47	27.1	2.94	0.09	0.30
Al_2O_3	1.87	6.24	1.98	8.11	13.1	9.38	8.51		1.42
Cr_2O_3	0.98	0.66	0.13	1.30	44.2	6.83	0.91	0.60	0.87
FeO	19.7	16.4	34.0	13.8	31.3	56.1	20.6	22.0	13.8
MgO	20.8	10.9	7.37	10.0	4.42	0.91	12.7	38.4	26.8
MnO	0.38	0.32		0.28	0.38	0.39	0.31	0.25	0.26
CaO	4.30	16.8	6.63	18.0	0.04	0.23	8.78	0.27	2.43
Na_2O	0.01	0.05	0.03	0.08	0.07	0.06	0.19		
	99.40	100.32	97.42	100.35	99.05	101.16	98.44	97.71	98.48

(1) Pyroxene core #172-5 grown at 0.9°C/hour, quenched at 1033°C
(2) Pyroxene rim #172-1 grown at 0.9°C/hour, quenched at 1033°C
(3) Pyroxene in groundmass #146-1 grown at 2.1°C/hour, quenched at 834°C
(4) High Ca-Al pyroxene #170-2 grown at 27°C/hour, quenched at 807°C
(5) Chrome spinel core #191-14 grown at 0.5°C/hour, quenched at 944°C
(6) Ulvö-spinel rim #191-15 grown at 0.5°C/hour, quenched at 944°C
(7), (8), (9) Liquid, olivine, pyroxene in #199, equilibrated 3 hours at 1375°C and 12.5 kb. Olivine and pyroxene model proposed source region at 250 km.

REFERENCES

Bence, A.E., Papike, J.J., and Lindsley, D.H., 1971, Crystallization histories of clinopyroxenes in two porphyritic rocks from Oceanus Procellarum: Proc. 2nd Lunar Sci. Conf., Geochim. Cosmochim. Acta, Suppl. 2, v. 1, p. 559-574.

Bowen, N.L., 1914, The ternary system: diopside-forsterite-silica: Amer. Jour. Sci., 4th series, v. 38, p. 207-264.

Green D.H., Ware, N.G., Hibberson, W.O., and Major, A., 1971, Experimental petrology of Apollo 12 basalts: Part 1, Sample 12009: Earth Planet. Sci. Lett., v. 13, p. 85-96.

Grove, T.L., Walker, D., Longhi, J., Stolper, E., and Hays, J.F., 1973, Petrology of rock 12002 and origin of picritic basalts at Oceanus Procellarum: Proc. 4th Lunar Sci. Conf., Geochim. Cosmochim. Acta, Suppl. 4, v. 1, p. 995-1011.

Hollister, L.S., Trzcienski, W.E., Jr., Hargraves, R.B., and Kulick, C.G., 1971, Petrogenetic significance of pyroxenes in two Apollo 12 samples: Proc. 2nd Lunar Sci. Conf., Geochim. Cosmochim. Acta, Suppl. 2, v. 1, p. 529-557.

Kesson, S.E., 1974a, Petrogenesis of high-Ti mare basalts: melting of 70215 in vacuum and at high pressures: EΦS, Trans. Amer. Geophys. Union, v. 56, p. 1200.

Kesson, S.E., 1974b, Apollo 15 mare basalts: melting experiments in high purity Fe containers at 1 atm and high pressures: Abstracts with Programs, Geol. Soc. Amer., v. 6, p. 823.

Lofgren, G. Donaldson, C.H., Williams, R.J., Mullins, O., Jr., and Usselman, T.M., 1974, Experimentally reproduced textures

and mineral chemistry of Apollo 15 quartz normative basalts: Proc. 5th Lunar Sci. Conf., Geochim. Cosmochim. Acta, Suppl. 5, v. 1, p. 549-567.

Longhi, J., Walker, D., Grove, T.L., Stolper, E.M., and Hays, J.F., 1974, The petrology of the Apollo 17 mare basalts: Proc. 5th Lunar Sci. Conf., Geochim. Cosmochim. Acta, Suppl. 5, v. 1, p. 447-469, Pergamon.

Longhi, J., Walker, D., and Hays, J.F., 1975, Fe-Mg distribution between olivine and lunar basaltic liquids: EΦS, v. 56, p. 471.

Longhi, J., Walker, D., Grove, T.L., Stolper, E.M., and Hays, J.F., 1975, Petrology and origin of Apollo 15 mare basalts: in preparation.

Nehru, C.E., Prinz, M. Dowty, E., and Keil, K., 1974, Spinel group minerals and ilmenite in Apollo 15 rake samples: Amer. Min., v. 59, p. 1220-1235.

Peck, D.L., Wright, T.L., and Moore, J.G., 1966, Crystallization of tholeiitic basalt in Alae lava lake, Hawaii, Bull. Vol., v. 29, p. 629-656.

Richter, D.H., and Moore, J.G., 1966, Petrology of the Kilauea Iki lava lake, Hawaii, U.S.G.S. Prof. Paper 537B.

Roeder, P.L., and Emslie, R.F., 1970, Olivine-liquid equilibrium: Contr. Mineral. and Petrol., v. 29, p. 275-289.

Walker, D., Longhi, J., and Hays, J.F., 1972, Experimental petrology and origin of Fra Mauro rocks and soil: Proc. 3rd Lunar Sci. Conf., Geochim. Cosmochim. Acta, Suppl. 3, v. 1, p. 797-817, MIT Press.

Walker, D., Longhi, J. Stolper, E.M., Grove, T.L., and Hays, J.F., 1975, Origin of titaniferous lunar basalts: Geochim. Cosmochim. Acta, in press.

FIGURE CAPTIONS

Figure 1

Phase relations for 12002 bulk composition determined by synthesis experiments on devitrified glass starting material.

Figure 2

Results of controlled cooling experiments as a function of the cooling rate and temperature of quenching. Dotted lines indicate cooling trajectories from 1350±5°C, where all experiments start, to the quenching temperature. All experiments below a particular curve, such as "olivine in", have olivine present in the product. These phase appearance curves may be compared to the equilibrium crystallization of 12002 shown in the upper right portion of the figure.

Figure 3

Products of rapid cooling. Both photomicrographs to same scale. Bar is 100 μm. Upper photo is a transmitted light view of thin section 12009 seen with crossed nicols. Olivine forms long skeletal blades with elaborate cross-ornamentation. In the center of the picture is a cluster of dendritic pyroxene. Black areas are glass and some submicroscopic devitrification products. The lower photograph is a reflected light view of an experiment on 12002 composition cooled at ~500°C/hour. Note the similarities to the upper photo: barred olivine blades, a cluster of dendritic pyroxene in the left-center, and glass matrix. Bubbles on bottom and top-left are in the epoxy mounting medium.

Figure 4

Experimental textures seen in reflected light photomicrographs. Scale the same on each photo; bar is 100 μm. Cooling

rate decreases from A(57°C/hour), B(11°C/hour), C(3°C/hour), to D(2°C/hour). A. Skeletal olivine with spinel specks around edges. Skeletal high-Ca,Al pyroxenes. Ilmenite fibers resolvable in glass groundmass. B. Principle change from A is that pyroxenes are more euhedral and groundmass is microcrystalline plag+px (+?silica). Olivine is overgrown by pyroxene. Ilmenite is easily observable. C. Pyroxenes and olivines similar to B. Groundmass is coarser and in right center individual crystals are resolvable. Note that the groundmass is not this coarse in all portions of the surface. D. Olivine and pyroxene somewhat coarser than C but groundmass is much coarser than in C.

Figure 5

Spinel relations--a study in heterogeneous nucleation. Reflected light photomicrographs of experimental and natural spinels. Scale bar is 30 μm in each photo. A. Minute spinel specks ornamenting the interior trellis of a skeletal olivine. Glass forms the background. Grown at 1200°C/hour. B. Dendritic spinel cross growth on the margin of an olivine phenocryst (lower portion of photo). Skeletal high-Ca,Al pyroxenes and glass fill upper portion of photo. Grown at 57°C/hour. C. Mantled spinel phenocryst. Cr-spinel interior and ulvospinel rim have grown around an iron globule. A bubble appears to have been trapped. Coarse groundmass with ilmenite laths is seen to the left between olivine and pyroxene phenocrysts. Grown at 3°C/hour. D. Natural mantled spinels in 12002,9. Note similarities to C of the association with iron.

Figure 6

Compositional distribution of pyroxenes observed in 12002, controlled cooling experiments, and equilibrium crystallization of

12002. Data for 12002 are from Grove and others (1973). Experimental pyroxenes are all produced in iron capsules in sealed silica tubes.

Figure 7

Fe/Fe+Mg of 12002 experimental olivines and liquids is shown as a function of temperature for experiments in iron capsules in sealed silica tubes. Solid circles and triangles are for olivines and liquids in equilibrium experiments. Bars indicate the range in olivine composition observed in controlled cooling runs. Bars are shown at the quenching temperature of the experiment, but the range to higher Fo contents indicates that the olivines record the high temperature parts of the cooling experiment. Open triangles are liquid compositions in controlled cooling runs. Compositional gradients are observed in the liquid at high cooling rates and at low temperatures. For inhomogeneous liquids, the open triangles record the liquid composition adjacent to the olivine rims of highest Fe/Fe+Mg. Maximum Fe/Fe+Mg in olivines and liquids in the controlled cooling runs approximate the equilibrium values as a function of temperature above the equilibrium solidus. Deviations do not correlate with cooling rate. Minimum Fe/Fe+Mg values observed in the olivines are shown on a histogram in the lower left. Fo_{78}, the equilibrium liquidus olivine, is most often observed. Fo_{78} is observed at all cooling rates and the deviations are not correlated with cooling rate. Low Fe/Fe+Mg deviations are thought to be the result of iron capsule impurities. High Fe/Fe+Mg deviations may result from oxidation of the capsule during preparation or from failure to section or observe the most forsteritic olivine core.

Figure 8

Olivine-liquid partitioning of Fe and Mg. Data from Figure 7 for olivines (maximum Fe/Fe+Mg observed) and liquids are compared to curves for distribution coefficients (K_D of Roeder and Emslie, 1970). Equilibrium experiments show very little scatter about the curve $K_D = 0.33$, whereas controlled cooling experiments show some scatter. This scatter is not great and does not correlate with cooling rate.

Figure 9

Nucleation density of olivine vs cooling rate in experimental charges. The natural logarithm of the number of olivine crystals observed per mm^2 of section surface is used as a measure of nucleation density. This parameter has been measured in thin section 12002,9 and yields an estimate slightly less than 1°C/hour for the cooling rate at the beginning of 12002 crystallization.

Figure 10

The natural logarithm of the spacing of growth instabilities (D_{IS}) in pyroxene is plotted versus the natural logarithm of the cooling rate at which the pyroxenes grew. D_{IS} is the half width of "swallow tails." The range in this parameter for 12002,9 pyroxene phenocrysts is shown and an extrapolation indicates that they may have grown at a cooling rate of 0.1-0.2°C/hour.

Figure 11

Groundmass relations shown in section 12002,9. Scale bar is 100 μm in all pictures. A and A' (reflected and transmitted light) show a fine-grained fascicle of pyroxene and plagioclase. The pyroxene is the more highly reflective. The grain size in this fascicle is comparable to the coarsest seen in our experiments

(see Figure 4D) but is atypical of the major portion of the 12002 groundmass which is coarser. Note coarser texture surrounding this fascicle. B and B' show a coarser fascicle than A and A', but again notice a small, fine-grained fascicle in the upper right. Also seen are a variety of ilmenite habits. C and D illustrate the difficulties in determining the place of ilmenite in the crystallization sequence on the basis of textural relations. This is also illustrated in B. Ilmenite precedes groundmass crystallization in linear cooling experiments and may do so in 12002 also but the textural evidence is ambiguous.

Figure 12

Summary of present results compared to our previous interpretation (Grove and others, 1973). Present conclusions are based on comparison of 12002 with controlled cooling experiments. Our previous conclusions were based on a comparison of 12002 with equilibrium experiments. (Time scale on this dashed curve is arbitrary.)

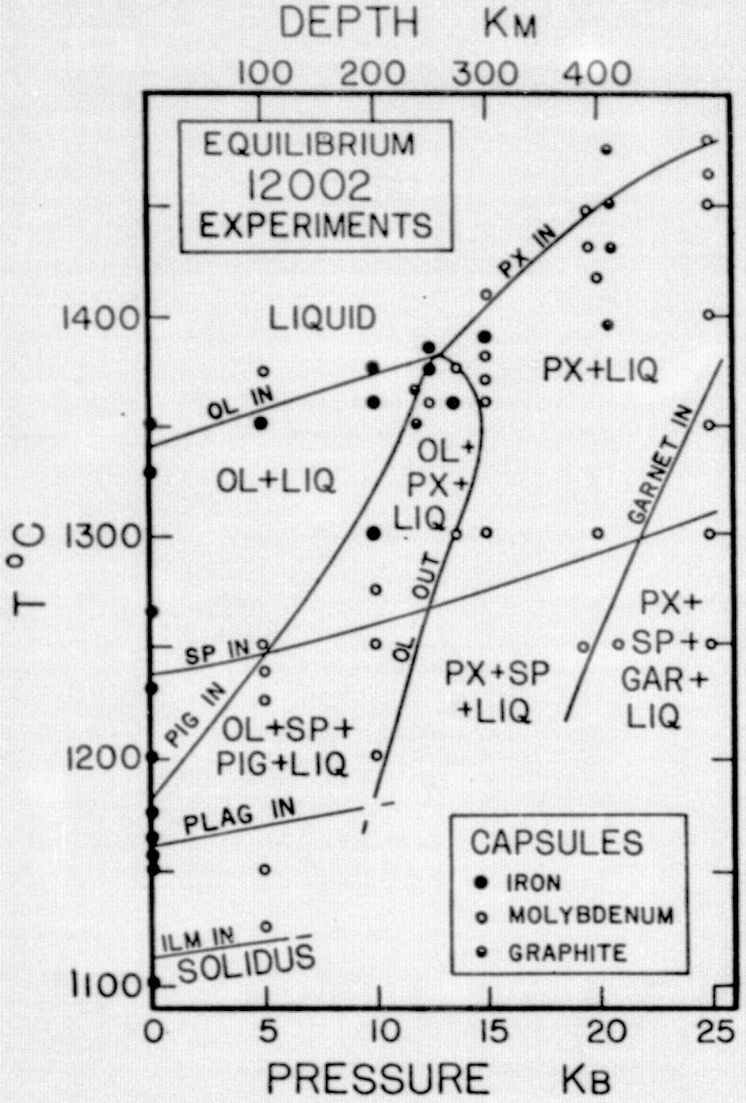

Walker et al. 12002
FIGURE 1 REVISED VERSION

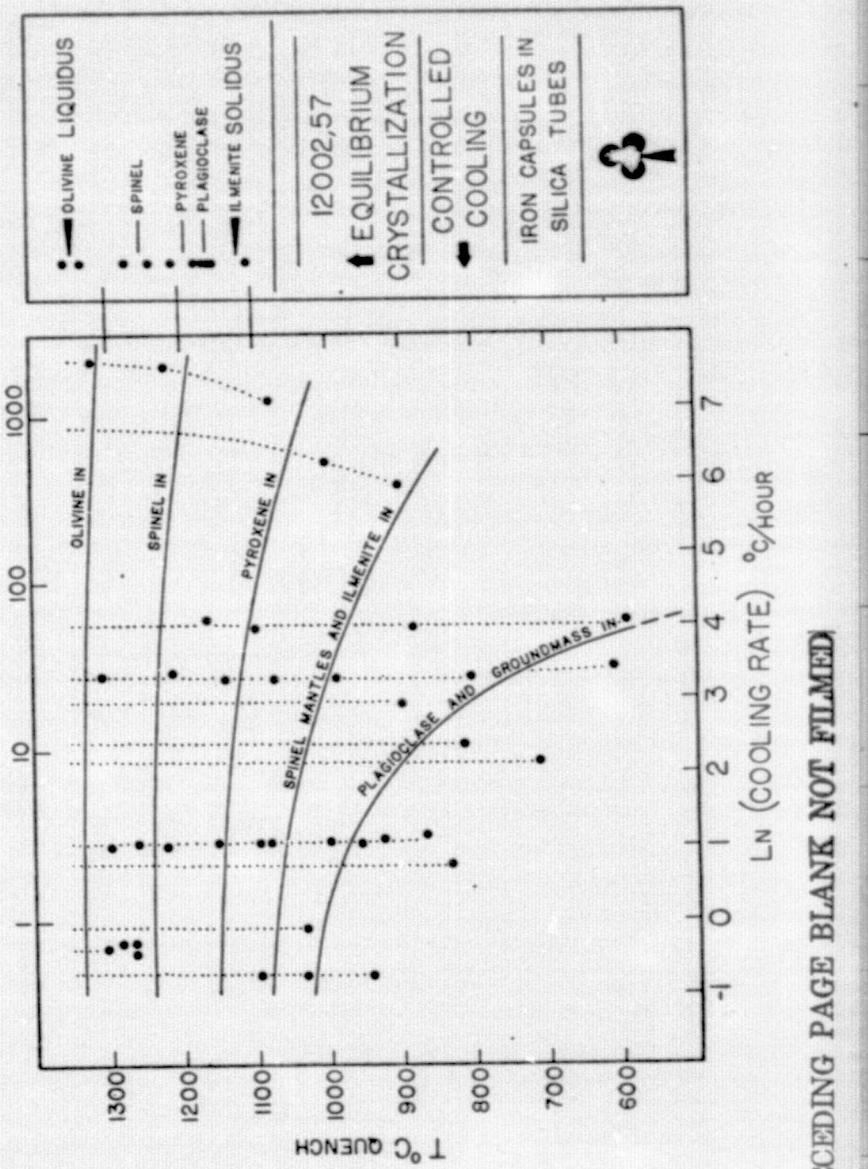

Walker et al. 12002
FIGURE 2 REVISED VERSION

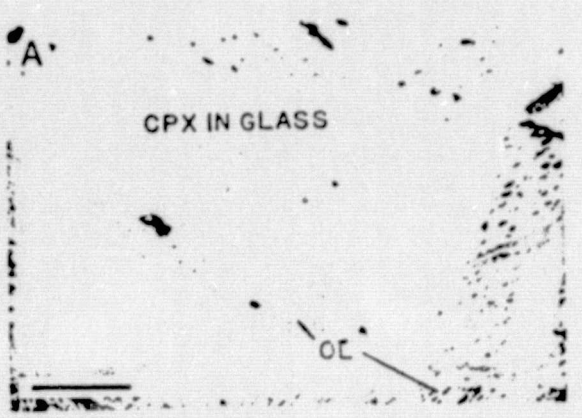

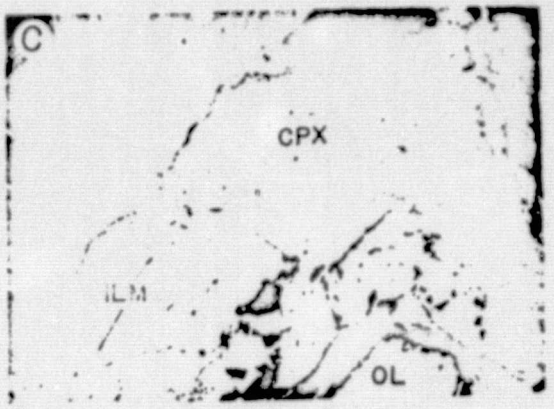

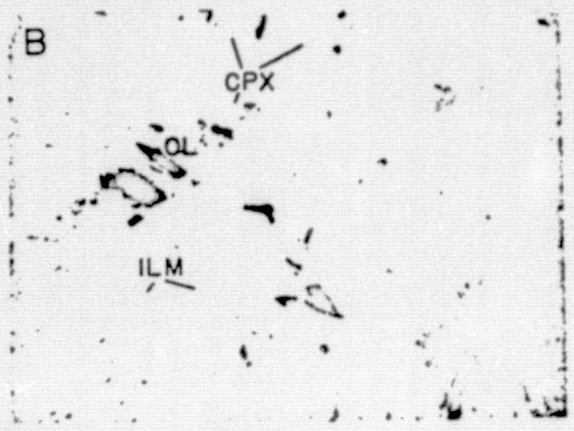

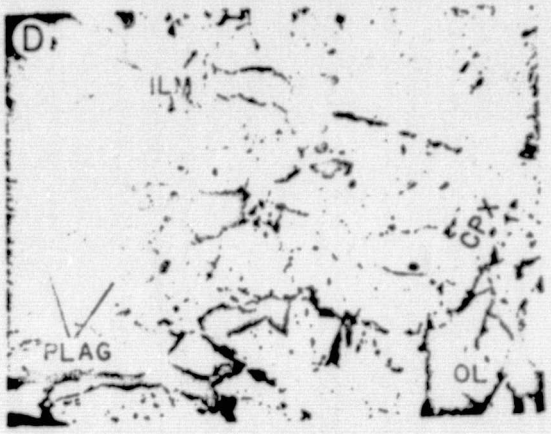

Walker et al. 12002
FIGURE 4 REVISED VERSION

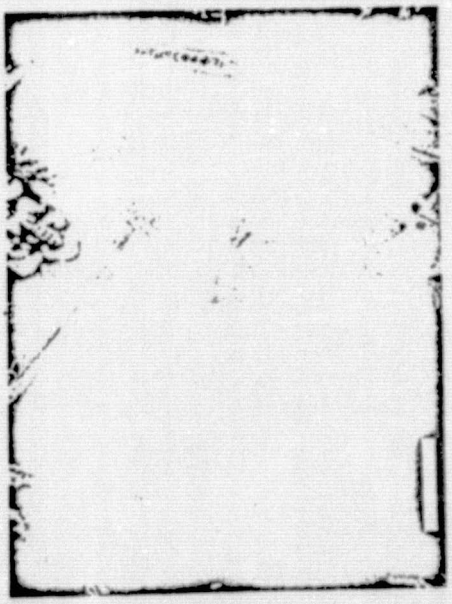

Walker et al. 12002
FIGURE 3 REVISED VERSION

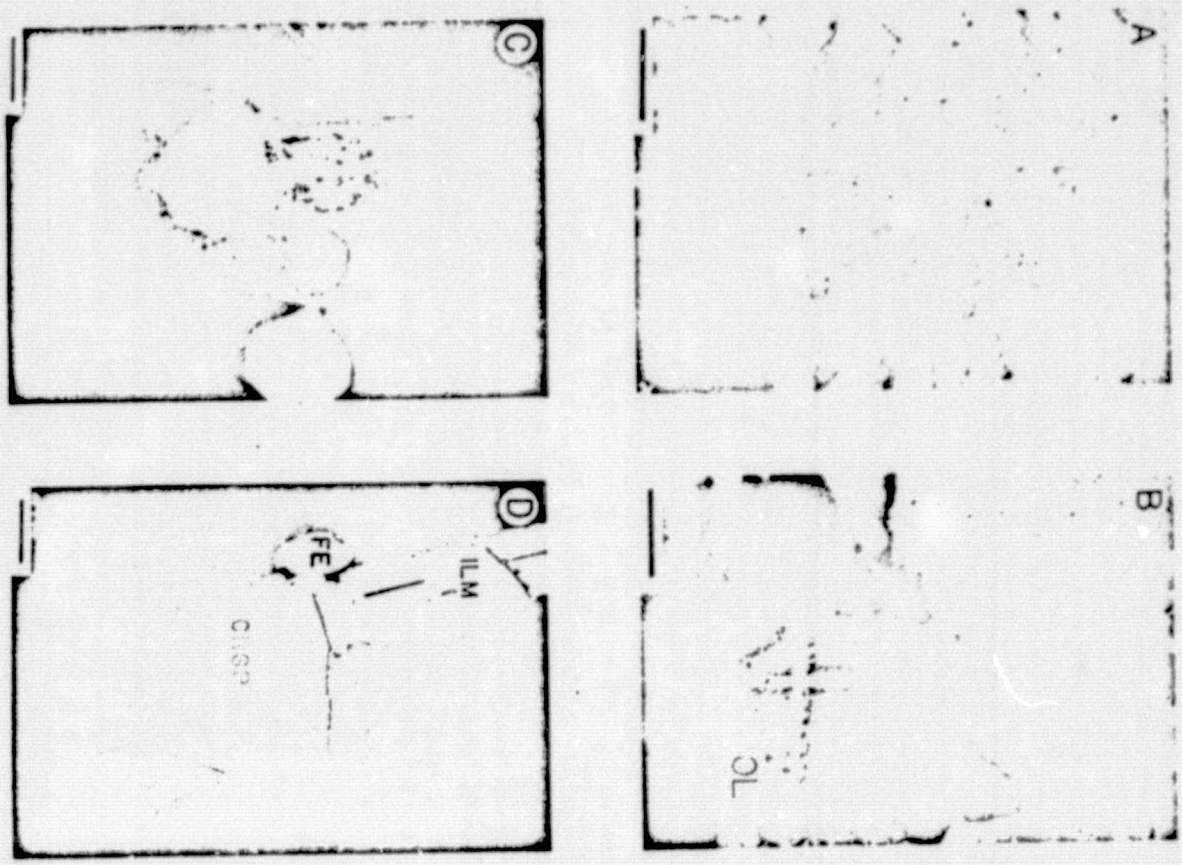

Walker et al. 12002
FIGURE 5 REVISED VERSION

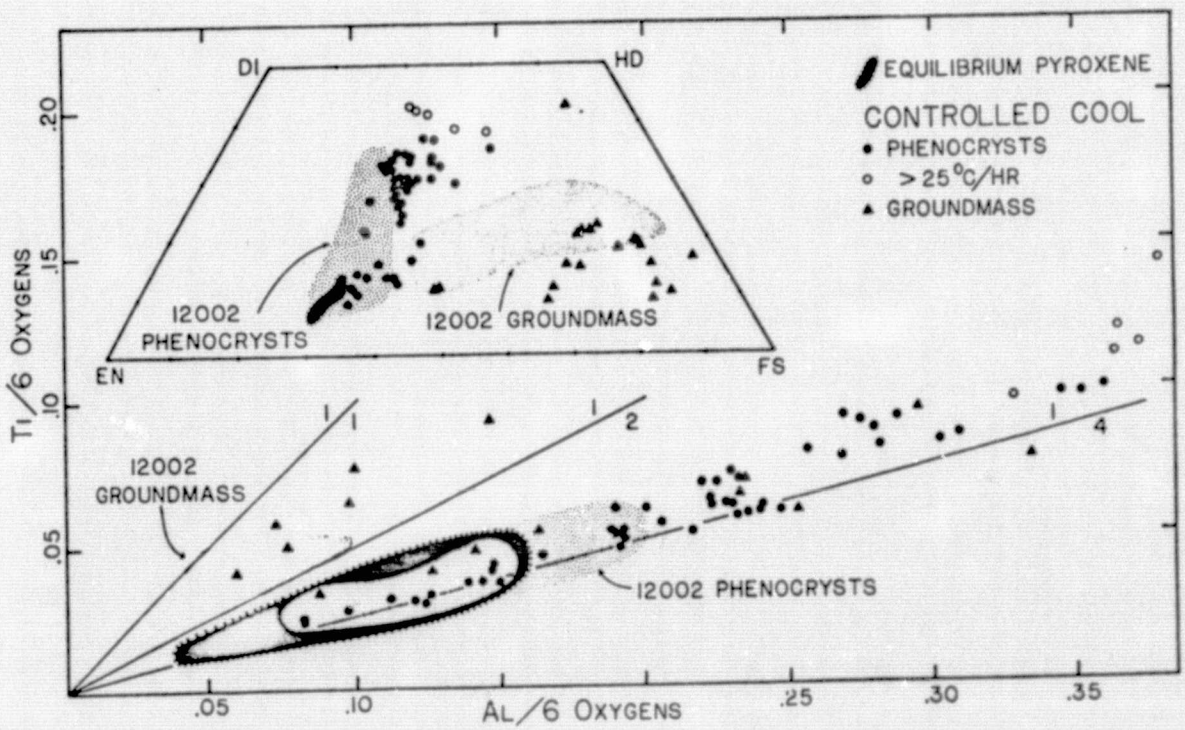

Walker et al. 12002
FIGURE 6 REVISED VERSION

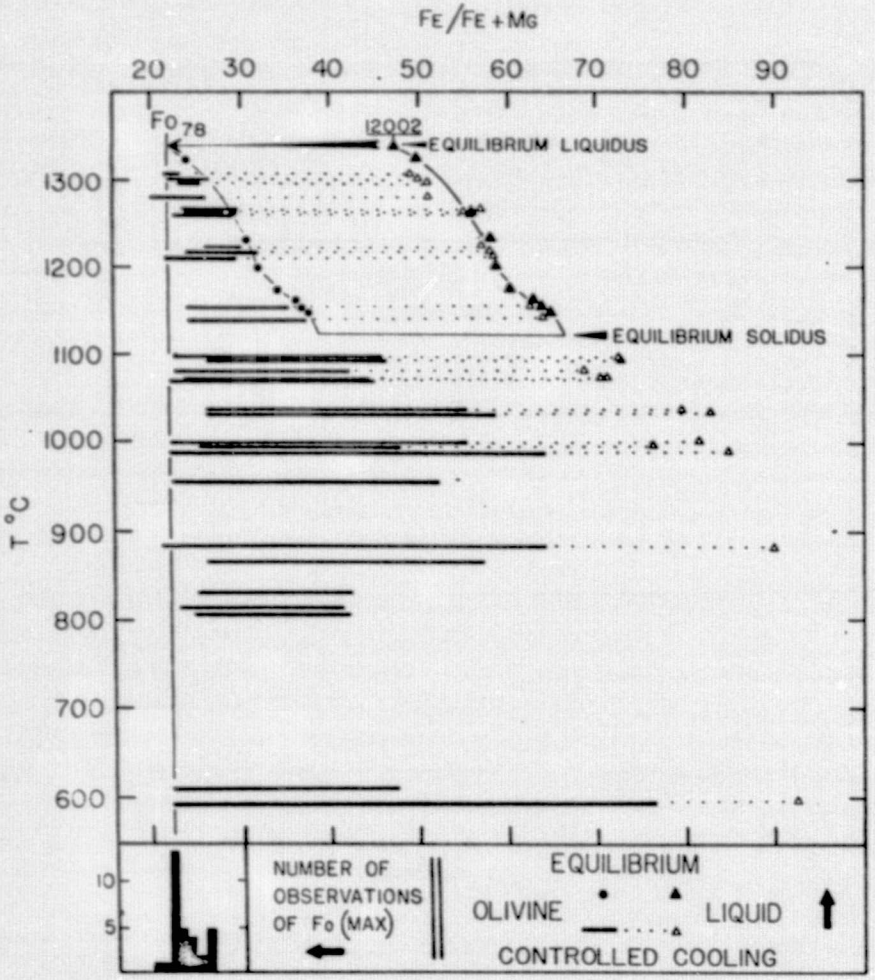

Walker et al. 12002
FIGURE 7 REVISED VERSION

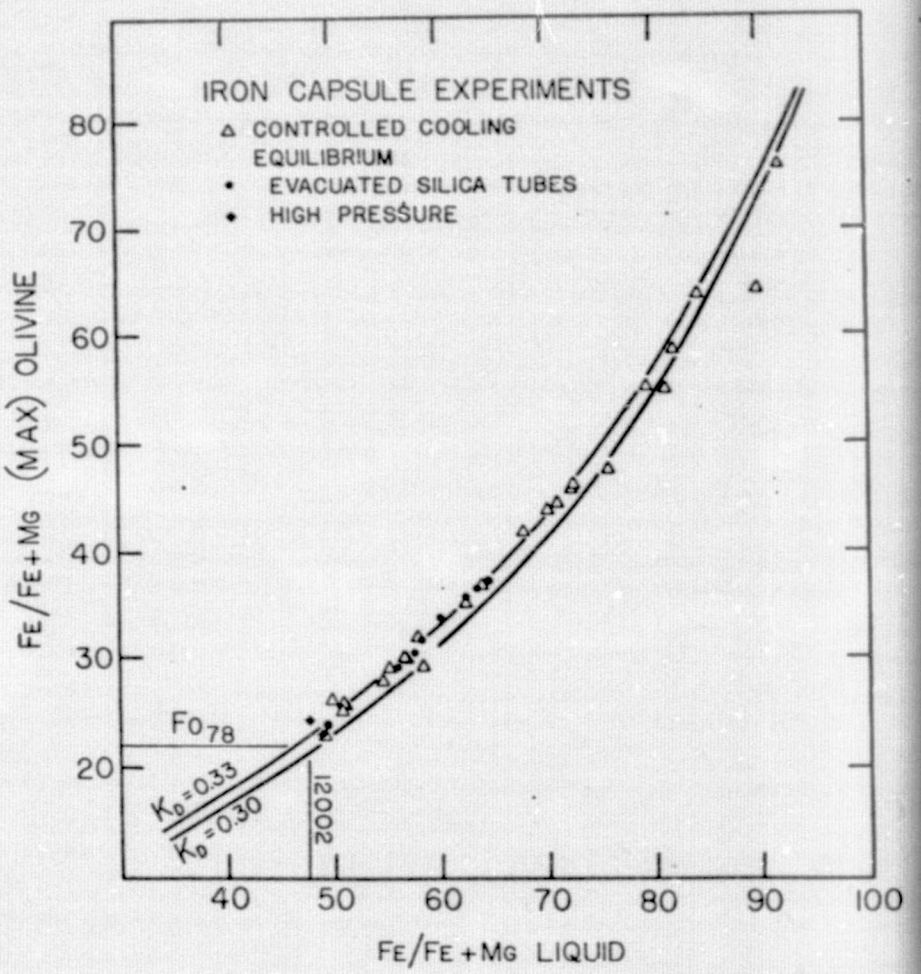

Walker et al. 12002
FIGURE 8 REVISED VERSION

Walker et al. 12002
- FIGURE 9 REVISED VERSION

Walker et al. 12002
- FIGURE 10 REVISED VERSION

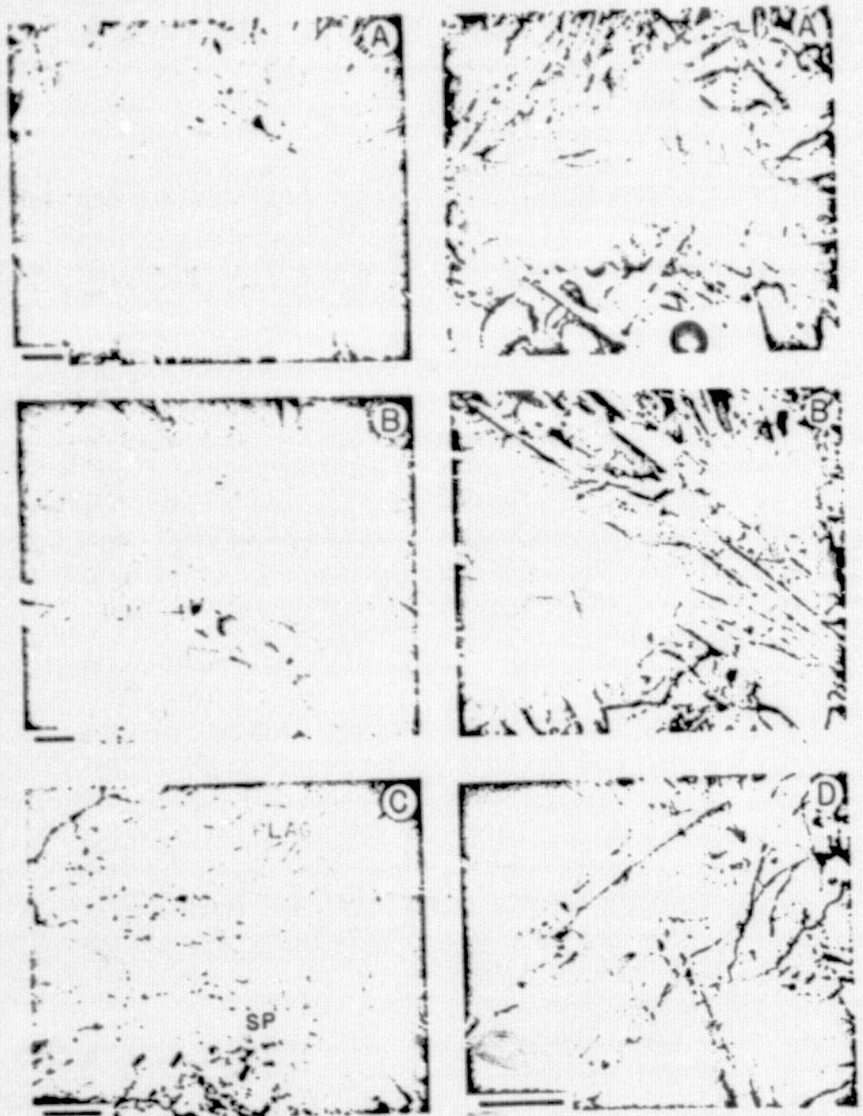

Walker et al. 12002
FIGURE 11 REVISED VERSION

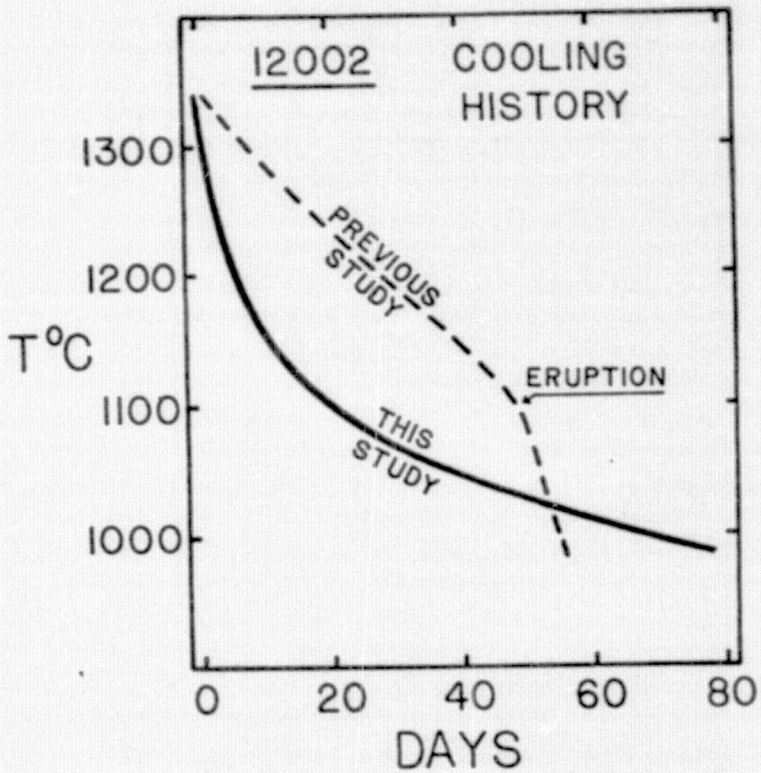

Walker et al. 12002
FIGURE 12 REVISED VERSION